EXPERIMENTAL INVESTIGATION OF THE BEHAVIOR OF THE STEEL REINFORCED HIGH DENSITY POLYETHYLENE AND CORRUGATED METAL PIPE

by

SAFA SADAT MASAJEDIAN

Presented to the Faculty of the Graduate School of

The University of Texas at Arlington in Partial Fulfillment

of the Requirements

for the Degree of

MASTER OF SCIENCE IN CIVIL ENGINEERING

THE UNIVERSITY OF TEXAS AT ARLINGTON

May 2011

Dedicated to my mother who taught me the value of unconditional love

ACKNOWLEDGEMENTS

I would like to express my sincere gratitude to my merciful God for blessing me with wonderful family, professional and supportive professor and many more things who gave them to me which I cannot count them one by one.

I would like to gratefully express my appreciation towards to my thesis supervisor Professor Abolmaali, for his invaluable supports and assistance through this study. I am heartily thankful to him, whose encouragement, guidance and support from the initial to the final level enabled me to develop an understanding of the subject. I am also grateful to him for careful reading and minute criticism of this thesis.

My gratitude goes to all Civil Engineering Lab, Hanson Pipe & Precast's representatives , and American Concrete Pipe Association Standards for their professional and technical suppor ts. In addition I wish to thank all friends in particular Mr. Joe Lundy, Mr. Josh Beakley, Dr. Tri Le, Dr. Anupong Kararam, Mr. S. M. Ashfaqul Hoq, for their supportive friendship and help.

I wish to express my gratitude to my family specially my parents and my siblings for their solid support and understanding. To whom, I am greatly indebted.

Last but not least, I want to offer my regards and blessings to all of those who supported me in any respect during the completion of the project. My appreciations always stay with them.

May 13, 2011

ABSTRACT

EXPERIMENTAL INVESTIGATION OF THE BEHAVIOR OF THE
STEEL REINFORCED HIGH DENSITY POLYETHYLENE
AND CORRUGATED METAL
PIPE

Safa Sadat Masajedian M.S

The University of Texas at Arlington, 2011

Supervising Professor: Ali Abolmaali

Steel reinforced high density polyethylene pipes are gaining popularity these days because of their good performance and advantages of them in comparison to the other pipe materials. By inverting the steel ribs vertically in to the HDPE materials, strength of steel and flexibility and light weight of HDPE materials have been combined. However due the limited study in this area, the failure modes and design parameters are not classified.

This study investigates the behavior and failure modes of SR-HDPE pipes under the simulated soil load and compares the results with the data obtained from the test on corrugated metal pipe under the identical test scenario. Full-scale experimental tests were conducted with soil boxes in order to determine if the steel ribs in SR-HDPE act continuously throughout the pipe structure. Local and global deformations of the pipe were monitored with displacement transducers and strain gauges, respectively. Strain gauges were placed at two sections of the

pipe. Each section contained six strain gauges at the crown, springline, and invert. Displacement transducers were installed in two sections along the pipe (middle and 12 in.(31 cm) from the end). Each section was capable of monitoring the vertical deflection and the horizontal deflection was measured at mid section. The load was applied through a hydraulic cylinder, and a rigid concrete slab. The data from these sensors were recorded and reported to identify the response of the pipes with regard to strength and serviceability. Three different pipe sizes (24 in. (61 cm), 36 in. (91 cm), and 48 in. (122 cm)) were tested in this situation and three different concrete slabs were casted whose dimensions were fixed by the pipe length which was 4 ft. (122 cm) and pipe and its width varied based on internal diameter.

The results showed that the CMP pipe has higher stiffness and load carrying capacity. Also CMP exhibited more ductility before the failure. The governing failure mode of the SR-HDPE pipe tested was lateral buckling of the ribs along the horizontal axis of the pipe at crown and springlines. This was due to the premature buckling of the HDPE material supporting the steel ribs, thus, causing discontinuous steel action. This study shows that the behavior ofr the SR-HDPE is different than the CMP pipe. By inspecting the pipe after reloading and removing from the soil box, three failure lines (crease) for 24 in. (61 cm) SR-HDPE and four failure lines for 36 in. (91 cm), and 48 in. (122 cm) SR-HDPE which is explained by the higher hoop capacity of the 24 in. (61 cm) SR-HDPE pipe in comparison with other pipe sizes. However CMP pipes exhibited a continuous hoop type buckling and smooth plastic hinge.

TABLE OF CONTENTS

LIST OF ILLUSTRATIONS

Figure Page

LIST OF TABLES

Table Page

CHAPTER 1

INTRODUCTION

1.1 Overview

Corrugated steel reinforced high-density polyethylene (SR-HDPE) and corrugated metal pipes are getting popularity for use as buried underground conduits for transportation gravity-flow applications. SR-HDPE pipe is a HDPE pipe with vertical steel ribs inserted into a plastic profile. In this way, the strength of steel pipes and behavior of HDPE material have been combined (ACPI 2009). Using HDPE gives the pipe advantages of high-density polyethylene material such as lighter in weight, more flexible in deformation behavior, cost efficiency and chemical resistance in comparison to other types of pipes such as concrete and corrugated metal pipes. Flexibility of the pipe results in more load transmission from the pipe to the soil of the surrounding pipe during the loading, at the same time, high flexibility of the HDPE causes large deformation in this type of pipe which is not desirable (Farshad 2006). Due to the lighter weight of the SR-HDPE, installation will be easier and less labor will be used, therefore, there is a reduction in construction time, which makes them more economical. Beside easier installation and high resistance to corrosion and erosion, due to its lower Manning's coefficient (major losses), and its shape, SR-HDPE is more hydraulically efficient, and has minor losses compared to CMP, which is an advantage of SR-HDPE pipe in compare to CMP pipe (David J. Keatley 2009). The aforementioned reasons make SR-HDPE more popular these days. The only problem with these types of pipe is lack of study in this area, and the exact behavior of the SR-HDPE pipes is not clear and classified for the designer. Meanwhile, more research is required to be performed to demonstrate the properties and behavior of this type of pipes in order to have a safe and reliable design. The results of the experimental study on the SR-HDPE pipes and CMP pipes under the same situation will be presented in this thesis.

1.2 Literature Review

1.2.1 HDPE Material and HDPE Pipe

Corrugated high-density polyethylene (HDPE), which according to AASHTO specification, is in flexible pipe category, is increasingly used as a structural material, because of its good performance and good properties. For example, because of the relatively low stiffness of polyethylene in trenchless methods, the required installation force has been reduced. On the other hand, its chemical nature makes it applicable for corrosive environments, and having adequate strength allows using it as buried underground conduits for road way and highway gravity-flow applications, and also sewer, gas, and water lines. In these applications, the pipes must support soil overburden, groundwater, and loads applied at the ground surface.

The flexible pipe design and installation need to meet the American Association of State Highway and Transportation Officials (AASHTO) requirements and Department of Transportation (DOT) design practice. The AASHTO designs of buried thermoplastic and metal pipes are generally based on the factored thrust and pipe wall resistance.

Recently, pipeline installation is based on underground pulling pipe through horizontal boreholes, and to minimize pulling loads, low stiffness of a pipe and PE is desirable for this installation method.

1.2.1.1 History of HDPE and HDPE Pipe

At the very end of the 18th century, German chemist Hans von Pechmann while working with a form of methane in ether found a precipitate which in 1900, German chemists Eugen Bamberger and Friedrich Tschirner identified this compound as polymethylene. An American chemist at E.I. du Pont de Nemours & Company Inc., Carl Shipp Marvel, obtained a high-density residue by having a large amount of pressure applied to ethylene, in 1930. British chemists, Eric Fawcett and Reginald Gibson created a solid form of polyethylene by working with ethylene at high pressures in 1935. Its industrial preliminary application was in insulating radar cable during Second World War. Karl Ziegler from the Max Planck Institute and Erhard Holzkamp created high-

density polyethylene (HDPE) in 1953. Sarkes and Smith (1983) pointed out that the use of plastic pipes began in the gas industry in 1955. For this successful invention, Ziegler achieved the Nobel Prize for Chemistry in 1963 (Lester H. Gabriel). Since then plastic pipes have been used as a piping material. In the early 1970s, plastic pipes started being used in highway drainage applications. At this time, HDPE drainage pipes are installed more frequently than all other plastic pipe combination. In the past thirty years, HDPE pipes have also been used as a protection layer for cables in segmental bridges, encasing steel strands and concrete to prevent corrosion. PE pipes have become popular for their combination of strength, attributes of toughness, flexibility, corrosion resistance, non-conducting electrical properties, and lightweight. Based on AASHTO specification, plastic pipes are classified under thermoplastic pipes (HDPE, PVC, and ABS) (Lester H. Gabriel 2003).

1.2.1.2 Chemical and Mechanical Property

HDPE is a polymer composed of carbon and hydrogen atoms and formed by applying heat and pressure to the ethylene (Figure 1.1). The carbon chain may vary from 500,000 to 1,000,000 carbon unit. The more carbon unit in the molecular chain causes the greater molecular weight. Many of the mechanical and chemical property of the end product are directly contributed to the molecular weight. The HDPE molecular structure shown below has two dimensions; however, in reality the HDPE molecule is in three dimensions. It has side chains branching off the main chain, and the density, flexibility, elongation, tensile strength, hardness, brittle, and most of the mechanical properties of the HDPE are dependent on the number, size and type of these side chains (Lester H. Gabriel 2003).

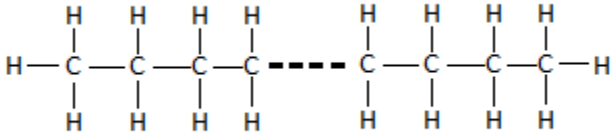

Figure 1.1 Two-dimensional HDPE molecular chains

High density polyethylene (HDPE) is a type of linear polyethylene which according to ASTM D883 has density range from 0.941 to 0.965 g/cc. HDPE showing high strength and modulus; which makes it suitable and apt for use in the manufacture of plastic pipes. According to AASHTO LRFD polyethylene pipe shall meet the requirement of AASHTO M 249, or ASTM F 714 or F 897.

Table 1.1 Corrugated HDPE Pipe Properties According to ASTM D 3350 Based on AASHTO M 294 Specification

Property	Test Method	Biology (%)	Education (%)
Density	ASTM D 1505	3	>0.945-0.950 (g/cc)
Melt index	ASTM D 1238	4	<0.15 (g/10 min.)
Flexural Modulus	ASTM D 790	5	110,000 - <160,000 psi
Tensile strength	ASTM D 638 Type IV	4	3000 -<3500 psi
SCGR*	ASTM D 1693 or F 1436	0	Unspecified
HDB**	ASTM D 2837	0	Unspecified
Carbon black	ASTM D 1603	C	>2%

Two stage of loading assumed for the pipe; short-term longitudinal stresses due to pulling forces, and long-term loading due to the live and dead loads. During the first step, because of the flexibly of the SR-HDPE and HDPE pipes, they need less force to install and this is another advantage of them compare to other type of pipes. Variable hoop stresses due to the internal and external pressures, which came with attrition of the outer surface of the pipe by the backfill material and also during the installation can result in slow crack growth and untimely failure. Adequate long-term strength and performance of the PE pipes are probably the major concerns in design and construction; however, no adequate predictive models exist that can link slow crack growth in real pipes with environmental stress crack resistance (ESCR) determined using standard laboratory tests. Creep of polymers is another issue which is related to their long-term strength and to ESCR. It also best represents the time-dependent nature of the behavior of

polymeric structures (e.g. pipes) subject to complex load history. Polyethylene shows time-dependent constitutive behavior which is also dependent on the applied stress level resulting in nonlinear stress–strain relationships. The creep behavior of semi-crystalline polymers depends, among other factors, on the level of loading and it has been experimentally observed that under lower levels of loading the behavior is characterized by initial creep which decays with time (see Fig. 1.2), and hence the viscoelastic behavior becomes elastic with time.

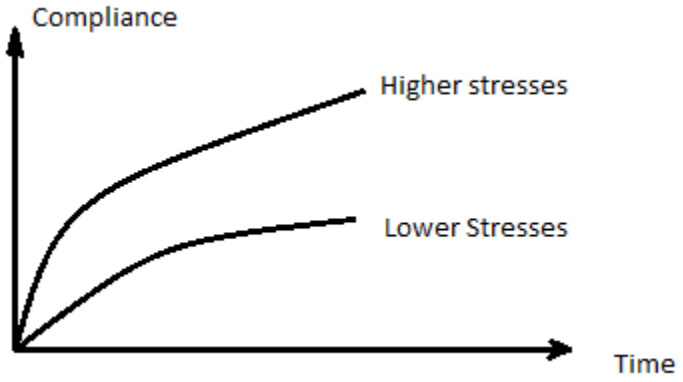

Figure 1.2 Typical Creep Compliance Curve for the PE Materials Due to Low and High Level of Stress

This type of behavior can be well modeled using the multi-Kelvin approach with properly chosen relaxation times. In creep tests under higher loads (for PE material these loads would be larger than 10 MPa), the behavior changes and strains continue to grow under these higher loads. The creep compliance does not approach an asymptotic value but grows continuously with time (P. Krishnaswamy, M.E. Tuttle, and A.F. Emery (1992)). According to results shown by them, to ignore the effect of the creep, the fast rate loading has been used in this study.

1.2.1.3 Backfill and Cover

One of the important factors for the current design method of buried thermoplastic and metal pipes is the vertical soil pressure at the pipe crown. When the flexible pipes are buried under shallow depths, the vertical crown pressure is mainly influenced by the live load effect.

Soil arching and soil pressure around the pipe caused by vertical settlement ratio between the pipe and soil column play vital roles in the pressure distribution on the pipes. A downward shear force appears on the sides of the soil column above the pipe resulting from the compressibility of the columns of soil adjacent to the rigid pipe. This effect is called negative soil arching since the load on the pipe is increased, becoming greater than the weight of the soil column above the pipe. When a flexible pipe is installed, the soil column above the pipe is more compressive. The load on the pipe is now less than the weight of the soil column above the pipe and we have positive soil arching (Sayed, G.A., Bahkt, B., & Jaeger, L.G. (1994)).

To find the performance and behavior of the HDPE pipe, as will be shown in this thesis, the type of backfill plays an important role. Daoud S. Al-Abri, and Yahia E-A. Mohamedzein in 2010 investigated the behavior of the plastic pipe buried in dune sand backfill. The study shows that these parameters have a large influential effect on the performance of thermoplastic pipes. For example, all the pipe responses (e.g. change in vertical diameter, thrust and bending moment) increase with the increase in relative density of soil and the increase in soil cover. The study considers different factors that affect the pipe-performance such as relative density (dense, medium dense and loose dune sand soil), pipe material (i.e. HDPE, PVC) and soil cover on the performance of plastic pipes installed in dune sand. However, it has been shown that the effect of pipe material is not as significant. There is a slight difference in percentage in vertical diameter for PVC and HDPE pipes, although the modulus of elasticity of PVC is larger than that of HDPE. The main conclusion of this study is that medium-dense to dense-dune sand can be used as a backfill material for thermoplastic plastic pipes. The predicted changes in vertical diameter using these backfills are much less than the typical specified value of 5%.

Teruhisa Masada and Shad M. Sargand (2004) illustrated that the flexible pipe installed in CLSM experienced less influence of loading than the same pipe installed in conventional soil backfill, as long as the stresses induced by the external loading do not exceed the strength of the CLSM.

Soil backfill quality, pipe geometrical and material properties, pipe installation condition, and loading configuration are also other important factors that govern the soil pressure distribution over the buried flexible pipes (Madasamy Arockiasamy Omar Chaallal and Terdkiat Limpeteeprakarn, 2007) Literature review conducted on buried flexible pipes subjected to live load application indicates that a minimum soil cover over the pipe crown appears to be the most important parameter on pipe-soil system responses. Watkins and Reeve (1982) performed field tests on corrugated polyethylene pipes, with pipe diameters ranging from 15 in. (38.1 cm) to 24 in. (64 cm). The test pipes were subjected to the concentrated wheel load, and it was found that a soil cover of 1 ft. over the pipe crown appeared to provide adequate protection against an excessive pipe deflection. Lohnes et al (1997) performed the field test on the HDPE pipes with a soil cover of 2 ft. (64 cm). It has been shown that the loading plate with a contact area of 12 in. (31 cm) by 12 in. (31 cm) punched into the soil when the bearing capacity of the soil backfill exceeded. This led to a stress increase at the pipe crown and anticipated failure of the pipe with a reversal of curvature (local wall bending). Most pipe failures occurred at vertical pipe deflections between 1.9 and 2.9% (Conard et al. 1998). There is very limited information on the pipe-soil system behavior with a soil cover of less than 2 ft. (64 cm) and without a pavement structure, especially for pipes with a nominal diameter equal to or greater than 36 in. (91 cm) Full-scale field tests were carried out at the Florida Department of Transportation (FDOT) during December 2001 to May 2002 (Arockiasamy Omar Chaallal; and Terdkiat Limpeteeprakarn 2007). The field test was conducted to investigate the behavior of buried thermoplastic and metal flexible pipes under the application of static concentrated wheel loads including a dynamic load allowance factor. They have shown when an additional soil cover of 6 in. (15.2 cm) is applied, the vertical soil pressure, at the pipe crown, of the larger HDPE pipe reduces 2 to 3 times in comparison to those of the smaller HDPE pipes in diameter.

According to AASHTO LRFD bedding and backfill material shall comply with AASHTO M145, A-1, A-2-4, A-2-5, or A-3. And the minimum cover and structural backfill shall be followed by 30.5.4-5.

To design the pipe, the pipe wall resistance must be greater than the factored thrust to guarantee safety of the structure. Two important factors for determination of the factored thrust are vertical soil pressure at the pipe crown level and pipe outside diameter. The other two important factors are the vertical pipe deflections during installation and applied live load. The AASHTO specified deflection limit of 5% which is adequate for the installation. However, a vertical deflection limits to 2% for the HDPE pipes in the construction phase for road way and highway applications.

Because of the increasingly use of high density polyethylene (HDPE) in transportation applications, there is more concern about their long-term properties. Thus, Y. G. Hsuan in 2005 published a paper to initiate the long-term properties of corrugated HDPE pipes. He evaluated the stress crack resistance (SCR) part of a project. To evaluate the SCR in this study he showed that the junction and longitudinal profiles of the corrugated HDPE pipes is most affected by stress cracking. In general the accepted current design life of such pipe is 50-years. Essentially, the material properties for the HDPE resin are provided in the AASHTO M294 specification, which in the last revision the stress crack resistance (SCR) of the resin was the main evaluation factor.

1.2.1.4 Deflection of Thermoplastic Pipe

Two types of deflection will be discussed in the following: peaking up behavior during installation and pipe deflection during the different loading conditions.

Most thermoplastic pipes show peaking deflection during the installation process. Teruhisa Masada and Shad M. Sargand in 2005 have indicated a minor peaking behavior exhibited by the pipe according to the field test on HDPE pipes with CLSM-CDF backfill. As long as this kind of deflection is so small in comparison to the other type of deflection of flexible pipe, it has been received little attention, although it has been known that flexible pipe deformed to a shape similar

to a vertical ellipse during the initial backfilling (McGrath et al. 1999). The peaking up deflection continues until the backfill of the pipe reaches the crown level. By increasing the soil height above the crown level, pipe will deform in the opposite direction to change the pipe shape to the horizontal ellipse. Teruhisa Masada and Shad M. Sargand in 2005 have shown that peaking deflections can help to minimizing the long-term deflections of these pipes. AASHTO specification has limited the deflection of the pipe after 30 days following completion of installation to 5 %.

1.2.2 Corrugated Metal Pipe

Corrugated metal pipe (CMP) culverts have been commonly used for many years especially in place of small bridges for small and medium-sized streams and for the first time have been used in 1931 (Sayed, G.A., Bahkt, B., & Jaeger, L.G. (1994). Since that time, lots of improvements have been made on corrugated metal plate pipes such as larger diameters, material property, and irregular shapes and because of that, the popularity of them has increased dramatically. Another reason for them to become popular has come from design. In the past thirty years, it was not common to use the pipes in deep-fill installations. These days because of new technology, it is no longer difficult to reach a depth of seventy five feet or more for deep-burial installations. These types of pipes are prefabricated bent plates which bolted together at their joints. The CPM pipes mostly design based on The American Association of State Highway and Transportation Officials AASHTO 2010, and State Departments of Transportation design requirements which has adapted the supplementary guidelines of the National Corrugated Steel Pipe Association NCSPA. Referring to the current design methods, culverts are generally designed as a structural shell elements therefore, no moment will consider in the design procedures, and assume that the wall trusts are proportional to deflections. Selig and Calabrese in 1975 by conducting the field tests on a full-scale elliptical corrugated steel culvert with a span length of 8.2 m, and by evaluating the influence of dead and live loads during the construction have showed that the deflections and stresses in the culvert are primarily controlled by the dead weight of backfill material over the crown.

According to AASHTO specification corrugated metal culvert is considered in flexible pipe category, and the soil-load carrying capacity derives from its flexibility. Three failure modes are assumed for the corrugated metal; yielding of the wall, buckling of the wall, and failure of the seams. Leonards and Juang in 1985 mentioned that the pipes shape is not too asymmetrical and the soil backfill has good support characteristics, because of the unsupported condition of the pipe during and before construction and the non-uniform loading imposed by the placement of the backfill soil layers during installation and due to its flexibility, there is a possibility of local yielding in the conduit wall. They also stated that in the absence of buckling, yielding in the pipe walls can result in a favorable redistribution of soil pressures, thus it can permit the pipe to support the overburden loads more efficiently. Therefore, buckling of buried metal pipes has been shown to be an important failure mode. Elastic buckling is not expected mode of failure if the pipe surrounded by the backfill which is well compacted. Duncan has shown that with good backfill, the buckling load is greater than the seam strength even for quiet flexible pipes. Thus, for structures backfilled with good quality soil it sounds to be sufficient to design against seam compression and wall crushing and there is no need to consider the buckling capacity of the pipe (Duncan, J.M. (1979)). The longitudinal seams, contrary the circumferential seams, of corrugated metal pipes in general have to transmit thrusts between plate segments. Because of that the compressive strength of the metal and the bolted seams must be sufficient to resist the axial forces in the structure to keep it from the occurring of seam failure.

Corrugated steel pipe has a life of 10 years to 35 years (Rinker material). The metallic materials can change this life time and make it shorter or longer. There are three common coatings for these types of pipes: zinc coated steel, aluminum coated steel, and aluminum-zinc coated steel. AASHTO specification has requirement in M 218, Table 1 for base metal composition for galvanized corrugated metal pipe which needs to be followed; however the base metal is the same for all metallic coatings. The usual length fabricated of the corrugated steel pipe is 20ft. (50.8 cm) and 24 ft. (61cm) lengths.

Corrugated metal pipe and pipe-arches commonly meet the requirements of AASHTO M 36 or ASTM A 929. Bolts, nuts, and washers used with coupling bands must be galvanized and followed the AASHTO M 232 (ASTM A 153) or AASHTO M 298 (ASTM B 695) Class 50 (Rinker material).

For the first time, finite element analysis of metal conduits characterization was demonstrated by Leonards, Juang, and Stetkar (1985) using Culvert Analysis and Design (CANDE) computer program, they also checked different soil's effect, and different soil pipe interface condition, sequence of soil layers, and monitoring the analysis in real experiments.

Later, soil response was represented in Duncan-Chang model in the soil-pipe system which is recommended for routine studies of soil pipe interaction. Soil-pipe interface effects on pipe response were considered. Their demonstration, using finite element analysis indicated the importance of the sequence in placement of soil layers. Their investigations were made based on applying favorable and unfavorable maximum bending moments in shallow cover pipes.

They concluded the importance of soil sequential modeling as closely as possible to actual construction to obtain reasonable comparisons between anticipated and observed performance of buried conduit.

Finite element studies were continued by Sharma and Hardcastle (1993) using the CANDE program on the evaluation of a rib reinforced, low profile, and long span steel arch culvert. The non-linear elastic modulus was chosen for soil modeling to demonstrate a better simulation of the expected behavior of the culvert and supporting soils. The sub-soil profile was developed from data collected from soil borings at the site.

The deformations computed by CANDE were smaller than the maximum observed values, while the relative deformations with respect to the footing elevation were predicted within reasonable accuracy.

The importance of backfilling with good quality was studied in paper by Katona and Akl (1985).Their work was consecrated to the analysis and characterization of buried culverts with

slotted joints. They stated well compacted soil around the culvert results in dominating the flexural stiffness of the culvert by the stiffness of the enveloping soil mass. However, circumferential stiffness of the corrugated metal culverts tends to dominate the corresponding soil stiffness. Thus, the culvert tends to attract circumferential thrust loading (i.e., negative arching) limiting the allowable burial depth. By allowing a predetermined amount of joint slippage through the use of slotted bolt holes the circumferential stiffness will be reduced. As the culvert circumferentially contracts from joint slippage, the surrounding soil envelope is forced in to a compression arch, which in turn carries a greater portion of additional loading (i.e., positive soil arching). Consequently, deeper burial depths can be achieved.

The finite element program CANDE was used to evaluate the corrugated metal culverts with slotted bolt holes. Finite element analyses were performed using interface elements from frictionless to fully bonded. The fully bonded condition induced a larger net thrust into the slotted and un-slotted pipe. It was found that the predicted response of horizontal elongation and vertical flattening correlated well with the experimental trends.

Another study of long span culverts using finite element method was done by Katona (1978).Two finite element programs were used; Automatic Dynamic Incremental Nonlinear Analysis (ADINA) and CANDE. The two programs were used in contrast of large versus small deformation theory. ADINA uses large deformation theory while CANDE uses small deformation theory. Katona stated small deformation theory and infinitesimal stress-strain laws may be used for analyzing long span systems if the percentage of crown deflection remains within practical limits. The effects of modeling the structure monolithically versus an incremented structure sequence also were considered in Katona's works. Katona concluded incremented construction techniques should be used over the monolithic technique, because monolithic system was not able to track the trajectory of deformations such as maximum peaking, nor it was able to consider compaction loads, however, the incremental solution showed peaking behavior similar to what is seen in the field.

It was observed that by increasing the compaction pressure, maximum peaking increases substantially. It was found that maximum peaking and maximum flattening occur almost in inverse proportion to soil stiffness.

Chang, Espinoza and Selig (1980) compared finite element predictions from CANDE to the field measurements of a buried corrugated steel arch. During construction, measurements were made for bending and thrust stresses in steel, deflections of the culvert, backfill stresses, and backfill strains.

Three soil models, linear elastic, overburden dependent, and the extended Hardin's model, were used in the finite element analyses. Field data showed a substantial amount of circumferential shortening during the placement of the backfill, especially when the height of the backfill was below the crown of the culvert.

Neglecting the effect of compaction during backfilling and slip occurring at the bolted seams permits a circumferential shortening of the structure shell, caused major discrepancies between the measured and predicted behavior of construction before the backfill was above the crown. The limitations of the stress-strain model assumed for the soil according to Chang, Espinoza and Selig were other reasons of discrepancies. The behavior predicted by the finite element method was founded a good agreement with measured changes after the backfill was above the crown. However, they stated that the proper values for the soil modulus must be used and the bolted seam compressibility must be represented.

Based on aforementioned discussions, it is concluded that the CMP pipes are not able to bear much loading by itself due to its high flexibility, nevertheless, by combining with a good quality backfill the combination of pipe and backfill can carry an acceptable amount of load. The backfill of the CMP pipes plays two significant roles when the gravity loads results in lateral deformation of the pipe, it is generating the lateral pressure against the pipe: First, provide lateral support for the pipe, and secondly, carrying the load from the pipe (Andrew Moreland 2004).

In the work done by Kjartanson, Heilers, Lohnes and Klaiber in 2007, the backfill foreslope has a significant effect on uplift response, backfill stiffness and strength, and CMP longitudinal stiffness properties for field tests. As expected, less resistance was mobilized as the depth of cover along the foreslope decreased. Moreover, the analyses indicate that the backfill soil cohesion and stiffness properties have the most significant effect on the uplift resistance; the magnitude of uplift resistance mobilized was less sensitive to the soil friction angle and the properties of the soil/CMP interface, and all these together indicate the most important parameters of the soil-structure interaction.

1.3 Goals and Scope

Although, many studies have been conducted on HDPE and CMP pipes over years the number of reported studies on buried SR-HDPE are limited. The main objective of this study is to investigate the behavior and compare the failure modes of steel reinforced high-density polyethylene (SR-HDPE) and corrugated metal pipe (CMP) under live load with regard to stress and serviceability. Indeed, this study will determine if the steel ribs in SR-HDPE act continuously throughout the pipe structure though the lateral support provided by the HDPE materials. If SR-HDPE is compared with the CMP pipes, then the above has to hold and to be true.

To achieve this objective, full scale experimental tests will be conducted in which soil boxes will to incorporate SR-HDPE and corrugated metal pipe of identical sizes under identical conditions. Load-deflection plots and strain gauge reading will assist in identifying the global and local behavior of each pipe material. The CMP and SR-HDPE‘s test results with regard to strength and serviceability will be compared.

CHAPTER 2

EXPERIMENTAL TEST STUDY

2.1 Introduction

An experimental testing program was undertaken to investigate the performance of the steel reinforced high density polyethylene pipes and effects of the steel ribs. In order to achieve these goals, a series of tests were performed on three different pipes with internal diameters of (24 in.(61 cm), 36in.(91 cm), and 48 in.(122 cm)), and two different backfill materials (ASTM C-33, and ¾ in. gravel). Span length was kept constant at 48 in. (122 cm) for all pipe materials, since plane strain elasticity is applicable to analysis and design of underground linear structures. The pipe length is arbitrary. A concrete culvert has been used as a soil box whose dimension changes with the pipe diameter. Uniform load has been applied to the pipe through a rigid concrete slab.

Two experimental testing facilities at UT Arlington have been used for this testing program. The instrumentation, in general, consisted of: three displacement transducers, load cell, strain gauges, earth pressure cell, and data acquisition system. For each pipe twelve strain gauges and three transducer displacement sensor have been used to identify the stress- strain and load-deflection relationships.

All the pipes were loaded uniformly in 2 kip. (8.9 KN) intervals until failure. Each test was performed with the assistance of a minimum of three researchers to scribing each event of test. The load-deflection plots and detailed report on stress-strain relation, load-deflection, and discussion of the failure mode are reported.

2.2 Instrumentation

2.2.1 Load Cell

The load cells, used in this study, were standard 450 Ω (single) full-bridge axial units with 200 kip and 500 kip capacities with a tolerance of 0.15% of the full-scale. (Figure 2.1) The load cell was placed on top of the rigid concrete slab and the load was applied through it.

2.2.2 Strain Gauge

Local deformations of the pipes were recorded with the general purpose uniaxial gauges (Figure 2.2). To investigate hoop deformation of the pipes, preliminary gauging configuration was chosen. The strain gauges have a constantan 350 Ω grid with a polyimide encapsulation and large-area copper soldering tabs. Strain gauge installation consists of different aspects, and due to its sensitivity, requires a great deal of care. Since the most important part of the strain gauges' installation is the surface preparation, to have an accurate data reading, special care was taken to this part. After preparation of the surface, using the special adhesive, strain gauges were installed on the surface. Each gauge was soldered using standard three-conductor lead wire connections. Due to significant concerns in strain gauges' installation, and substantial impacts during the test setup and testing, strain gauge and connections were protected with a special M-COAT J-3 compound to maximize the survival. Lead wires were fed to an internal face of the pipe where they would be protected from the impact of backfill, moreover, to have an extra protection; epoxy was applied to them which is shown in Figure 2.2(b).

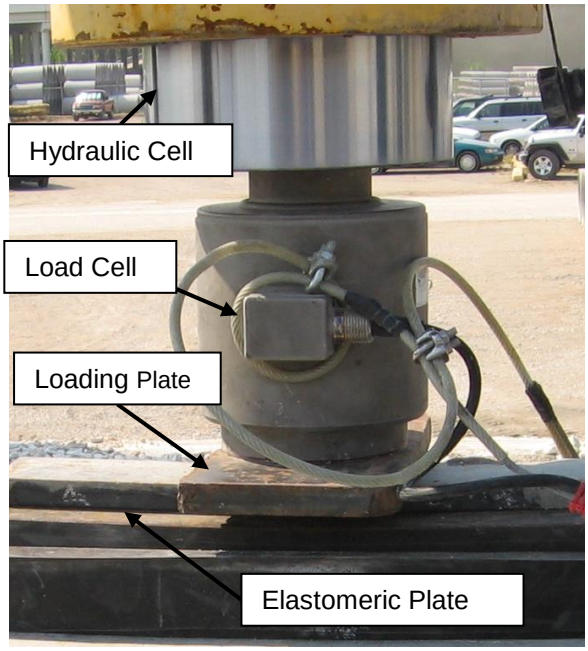

(a)

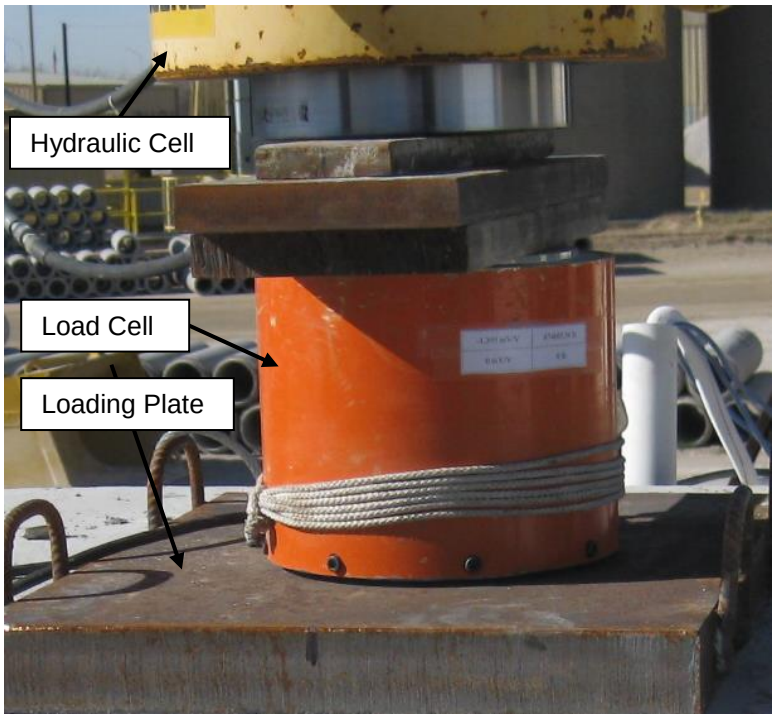

(b)

Figure 2.1 Detail of Load Cell and plate assembly (a) 200 kip Load Cell. (b) 600 kip Load Cell

(a)

(b)

(c)

Figure 2.2 Strain Gauge (a) Strain Gauge Property; (b) Strain Gauge and Connector wire; (c) Epoxy Used for Protection of the Strain Gauge

Special connections were used to connect lead wires to the data acquisition system which is indicated in Figure 2.5. The strain gauge locations were at mid-span, and 12 in. (31 cm) apart from the end of the pipe, at spring line, crown and bottom of the pipe.

2.2.3 Displacement Transducer

One 20 in. and two 10 in. full scale range Displacement Transducer (DT) (Fig 2.3) were used to measure the relative displacement of the inside face of the pipe at the middle and end section of the pipe.

Figure 2.3 Displacement transducers

2.2.4 Earth Pressure Cell

The earth pressure cell used in this study was 4800 earth pressure model. The earth pressure measures the vertical stress applied to the flat plate. On these series of tests, earth pressures were installed horizontally, and were utilized to measure the vertical pressure applied to the pipe (Figure 2.4). Also to ensure that the applied pressure to the buried pipe is uniformed, the measurements of induced pressure on the pipe, deformation of the pipe's cross sections, and failure behavior were considered. The induced pressure was measured by earth pressure cells all acquired information was processed via data acquisition methods.

2.2.5 Data Acquisition Unit

The aforementioned strain gauges, displacement transducers, earth pressure cell, and load cell were connected to a signal processing and data acquisition unit. The strain gauges were directly wired into the individual quarter-bridge completion networks (model Omega BCM-1), and these were in turn connected directly to the data acquisition board—which was capable of providing the required excitation voltage.

The data acquisition unit was an InstruNet model INET-100HC from Omega Engineering. This was a high-performance, high-precision computer-based acquisition system with the ability to interface directly to the most standard sensors. The HC version features high-current output capability, which was employed to power the strain bridges and ratio metric sensors. In order to use this software, the first step is defining sensors where the type of sensor, calibration values for each one and excitation voltage was defined. In the next step, each channel was be assigned to an appropriate sensor. Thereafter, by defining the scan session and number of reported data per second, programming was done. The software allows the user to directly monitor each channel in terms of the specific sensor used; this is particularly helpful when the non-linear quarter-bridge strain gauge outputs are under processing. The other advantages of this system is simplicity in defining the calibration value of the sensor by providing only two points, automatic nulling of strain channels, engineering unit conversion, availability of input voltage ranges, and realtime visualization and acquisition of input channels during the data processing.

In this study, two Data Acquisition Units were used because of the number of the strain gauges and displacement transducers (DT) and load cell. The Data Acquisition Unit is shown in Figure 2.5.

Figure 2.4 Earth Pressure Cell

Figure 2.5 Data acquisition unit

2.3 Specimen Preparation

2.3.2 Specimen Preparation of Type I

The pipe preparation process composed of strain gauging and installation of transducer displacement sensor. For the first try, the pipe was cut into 12 in. (31 cm) length and after removing the polyethylene from the steel rib, the strain gauges were installed in three different locations at the mid span (spring line, crown and bottom of the pipe). In order to have an accurate data two strain gauges were installed at the both side of the steel ribs. And to avoid reading the strain causes by the bending of the ribs itself the strain gauges were installed at the neutral axis of the ribs. At this time as long as the pipe did not contact to the soil, just M-Coating was applied to the strain gauges. For this pipe two displacement transducers were used: one for the vertical deflection reading and the other one for the horizontal one (Figure 2.6-2.7).

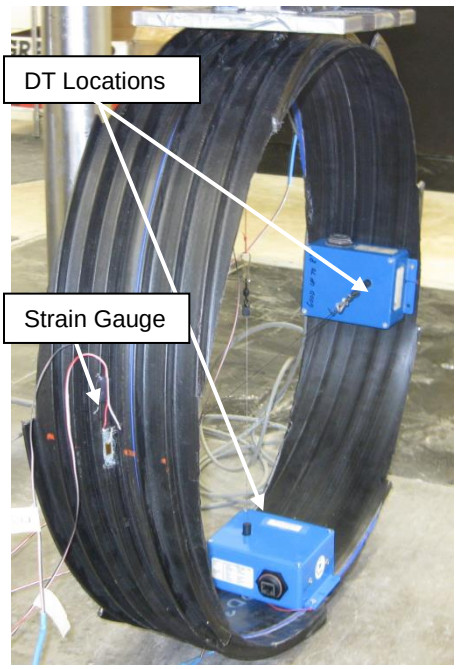

Figure 2.6 Positions of Displacement Transducers and Strain Gauges

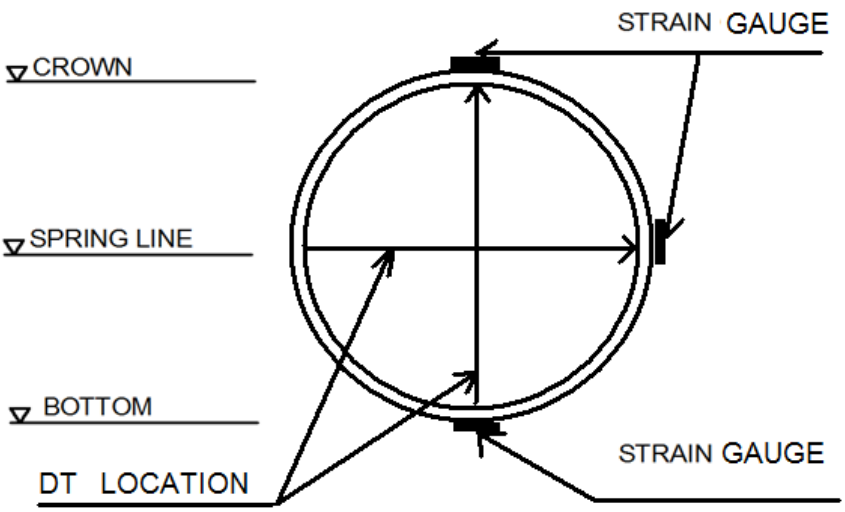

(a)

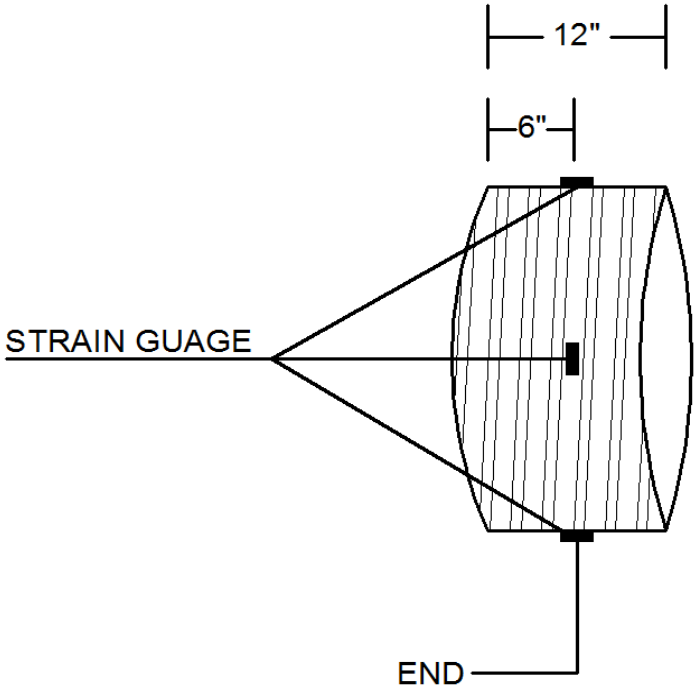

(b)

Figure 2.7 Strain Gauge and LT Location for Test Type I (a) Section View; (b) Side View

2.3.2 Specimen preparation of Type II

To prepare the specimens, the SR-HDPE pipes and CMP pipes were cut into 48 in. (122 cm) length. The strain gauges were installed in two sections of the pipe: one at the 12 in. (31 cm) from the end edge, and the other was placed at the middle of the span. At each section, six of them were used at three locations (crown, spring line, and bottom of the pipe) and both sides of the ribs. For the test Type II since the pipe is in direct contact with soil, epoxy was used to protect them from the impact loads and stone crush and erosion from the soil during test setup and testing procedure.

To install the strain gauge, after removing the polyethylene from the SR-HDPE pipe and proper surface preparation, the strain gauges were fixed by using adhesive recommended by the strain gauge manufacturer which in this case is M-Coat A; then, they were cured under the recommended pressure for proper adhesion (M bond 200 adhesive). Thereafter, the lead wires were soldered to the strain gauges and consequently, the strain gauges as well as the lead wires connection, were properly protected with epoxy to withstand the pressure. This also prevented pipe from erosion of the soil during the test setup and testing process. To protect the wires, PVC pipe were used to bring out the wires from the pipe and soil box. All positions the attached strain gauges are illustrated in Figure 2.8.

Two displacement transducers were used to monitor the vertical deflection of the pipe during the test: one located at the mid span, the other one 12 in. (31 cm) from the end edge of the sample, to validate whether the load is applying uniformly or not, by comparison the value of the each one. Another displacement transducer was installed at the mid span horizontally, to record the horizontal expansion of the pipe (Figure 2.8).

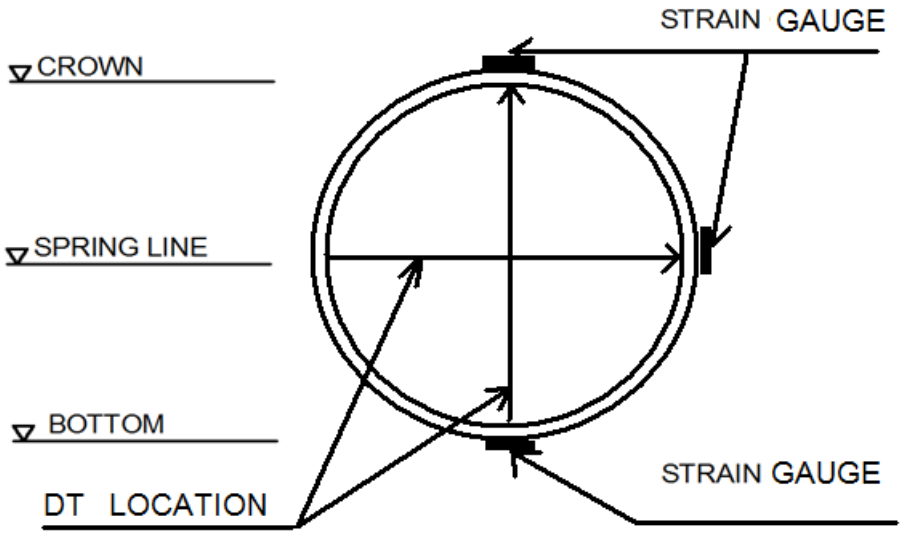

(a)

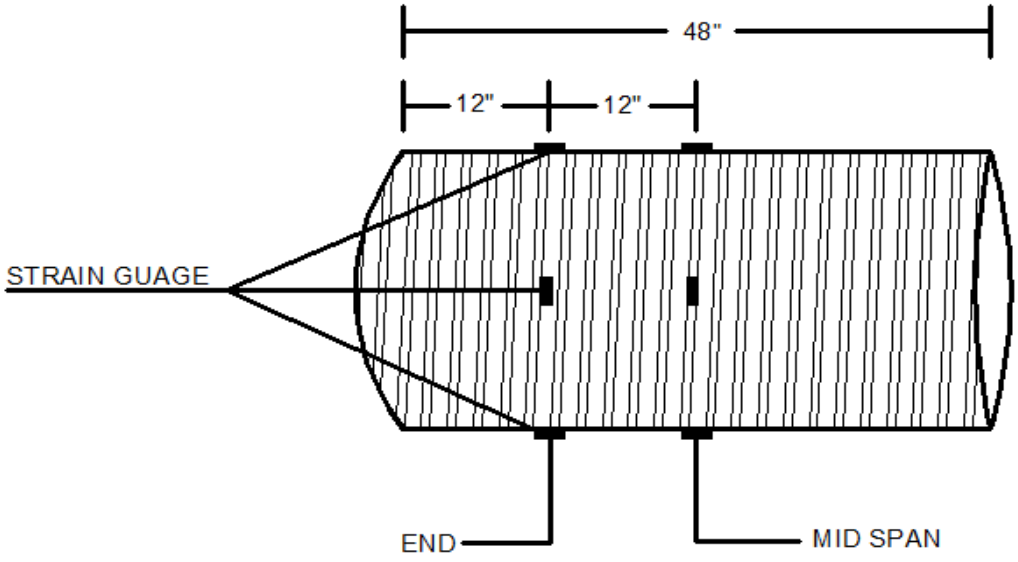

(b)

Figure 2.8 Strain Gauge and DT Location for Test Type II (a) Section View; (b) Side View

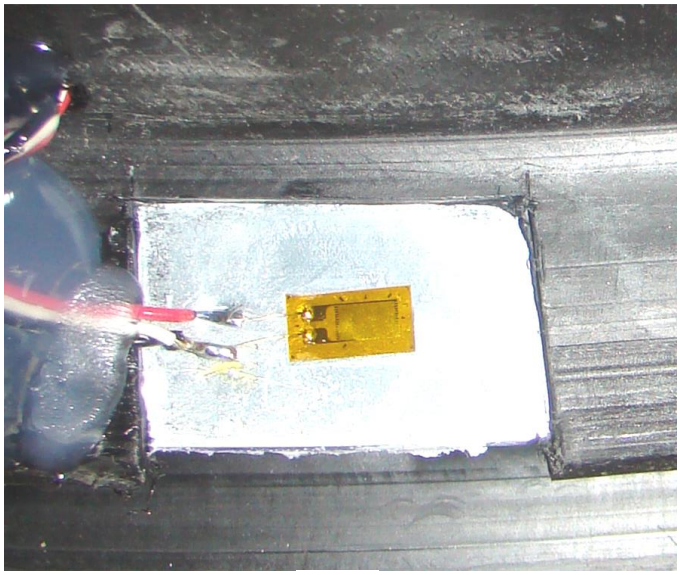

(a)

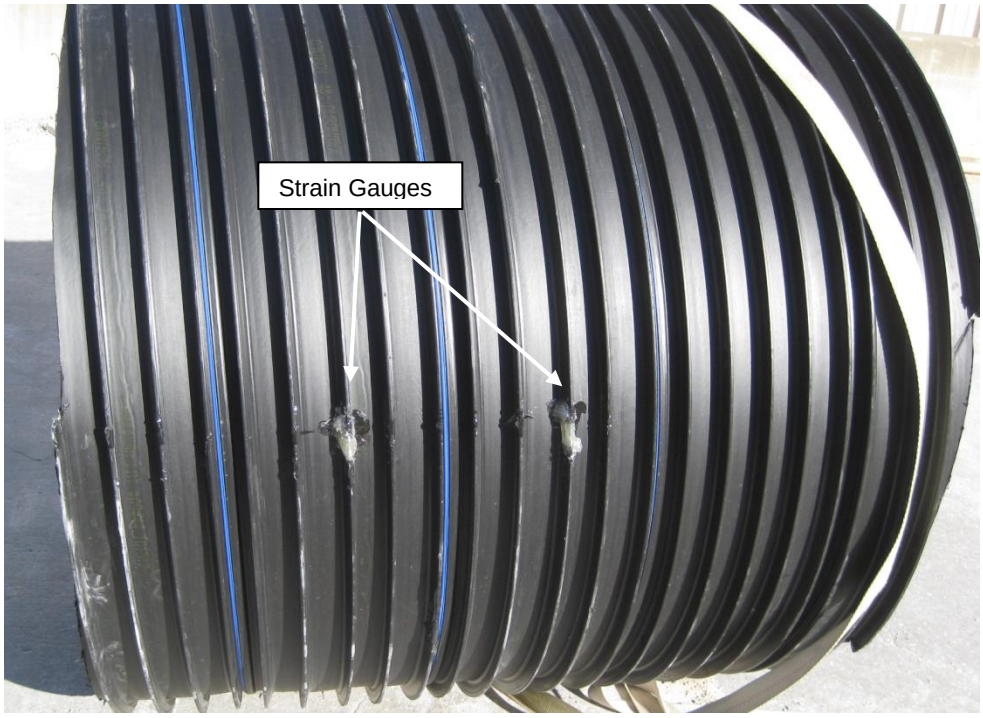

(b)

Figure 2.9 Strain Gauge Locations on SR-HDPE: (a) Location on the Rib; (b) Location on the Pipe.

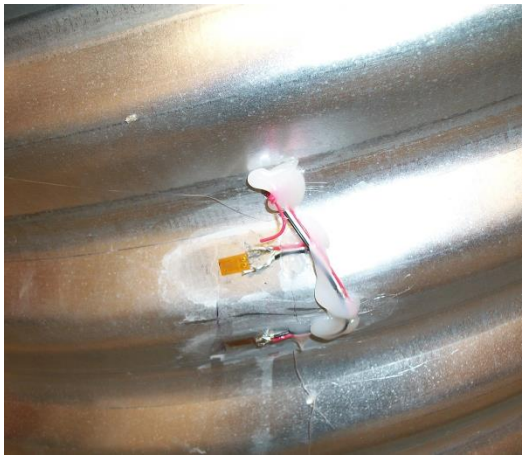

(a)

(b)

Figure 2.10 Strain Gauge Locations on CMP pipe: (a) Location on the Rib; (b) Location on the Pipe

(a)

(b)

Figure 2.11 Displacement Transducers Locations in the Pipe. (a) SR-HDPE pipe. (b) CMP pipe

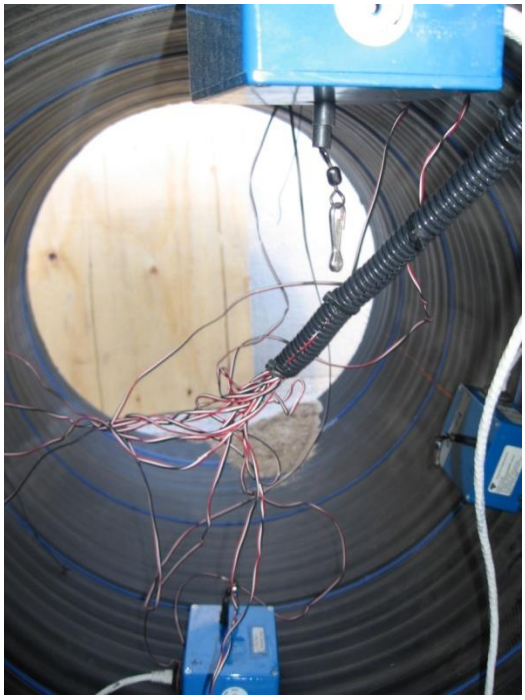

Figure 2.12 View of Pipe From Inside

The load from the hydraulic cylinder was acted through the concrete slab. The pressure is calculated by dividing the load to the projected area calculated by multiplying the pipe's diameter by its length. Based on the aforementioned definition and given there are three different types of pipe's diameter, three different slab were casted. Since by increasing pipe diameter, its load carrying capacity increases, the slab for each pipe diameter was designed and produced accordingly. This was done to avoid slab's punching shear during the testing. Slabs' dimensions and required reinforcement are illustrated in Figure 2.13-2.15.

For the soil box preparation, a concrete slab was added to the end of the concrete culvert. Two different culvert sizes were used in this study, one for 24 in. (61 cm) pipe diameter [6 ft.x6 ft. joint length 6 ft.(182.8 cm x 182.9 cm x 182.9 cm)] and another for 36 in. (91 cm) and 48 in. (122 cm) pipe diameters [6ft.x6ft. joint length 7ft. (182.9 cm x 182.9 cm x 213.4 cm)].

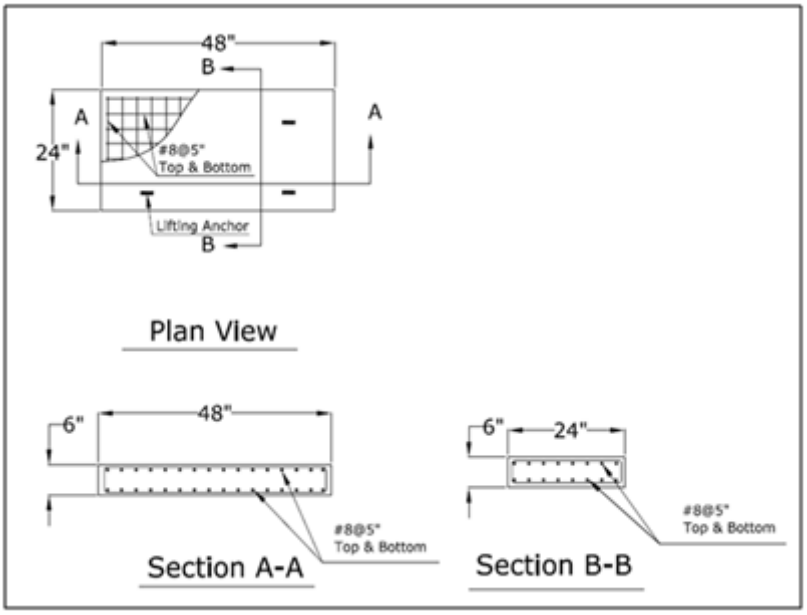

Figure 2.13 Slab Layout for 24in. (61 cm) Pipe

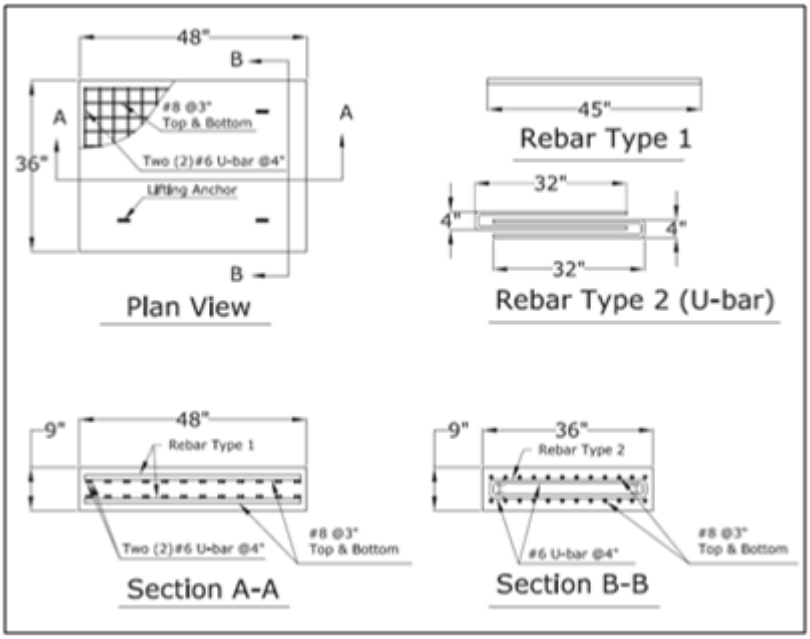

Figure 2.14 Slab Layout for 36 in. (91 cm) Pipe

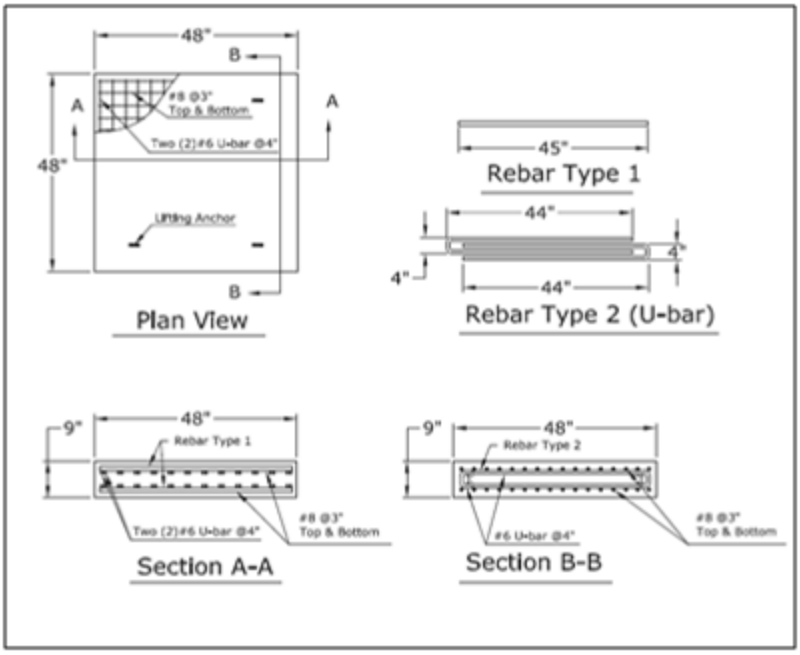

Figure 2.15 Slab Layout for 48 in. (122 cm) Pipe

2.4 Test Setup and Testing Procedure

2.4.1 Test Setup for Test Type I

In this type of test prepared specimen was directly placed under the Tensile-Compression Machine (TCM) with 400 kip (1779 KN) capacity to apply tension and compression forces. Point load was applied through the crown level of the pipe (Figure 2.16). The data for the strain gauges reading, displacement transducers, and load cell were monitored by data acquisition system. Since there was no lateral support for the pipe, pipe twisted during the testing procedure, and this was the reason to continue this study with soil box.

(a) (b)

Figure 2.16 SR-HDPE Pipes Under Tensile-Compression Machine (a) During the Testing. (b) Before Testing

2.4.2 Testing Frame

The testing frame at Hanson has a concrete reinforcement floor in 21 ft x 14 ft x 2 ft (6.4 m x 4.27 m x 0.61 m), and its steel frame consists of four W12x87 steel columns with the span of 16 ft (48.8 m). The frame was fixed to the reaction frame through 16 - 2 in. diameter bolts (Figure 2.17).

Figure 2.17 Testing

2.4.3 Test Setup and Testing Procedure of Type II

The configuration of the soil box and position of the pipe inside that, are illustrated in Figure 2.18-20. Based on the AASHTO specifications (Table 12.6.6.3-1) minimum of the soil cover is required to be 12 in. (31 cm), however, due to the limitation of the facilities and the height of the testing frame, different depths of soil cover were utilized. This is justified since both CMP and SR-HDPE pipes were tested under identical conditions.

Two different types of backfill were used during the execution of these series of tests. (ASTM C-33 and ¾ in. gravel)

Table 2.1 Minimum Soil Cover (Table 12.6.6.3-1 AASHTO Specification)

Type	Condition	Minimum Cover
Corrugated Metal Pipe	-	S/8 ≥ 12.0 in.
Spiral Rib Metal Pipe	Steel Conduit	S/4 ≥ 12.0 in.
	Aluminum Conduit where S ≤48.0 in.	S/2 ≥ 12.0 in.
	Aluminum Conduit where S ≥48.0 in.	S/2.75 ≥ 24.0 in.
Structural Plate Pipe Structures	-	S/8 ≥ 12.0 in.
Long-Span Structural Plate Pipe Structures	-	Refer to Table 12.8.3.1.1-1
Structural Plate Box Structures	-	1.4 ft. as specified in Article 12.9.1
Reinforced Concrete Pipe	Unpaved areas and under flexible pavement	Bc/8 or B'c /8, whichever is greater,≥12.0 in.
	Compacted granular fill under rigid pavement	9.0 in.
Thermoplastic Pipe	-	*ID*/8≥12.0 in.

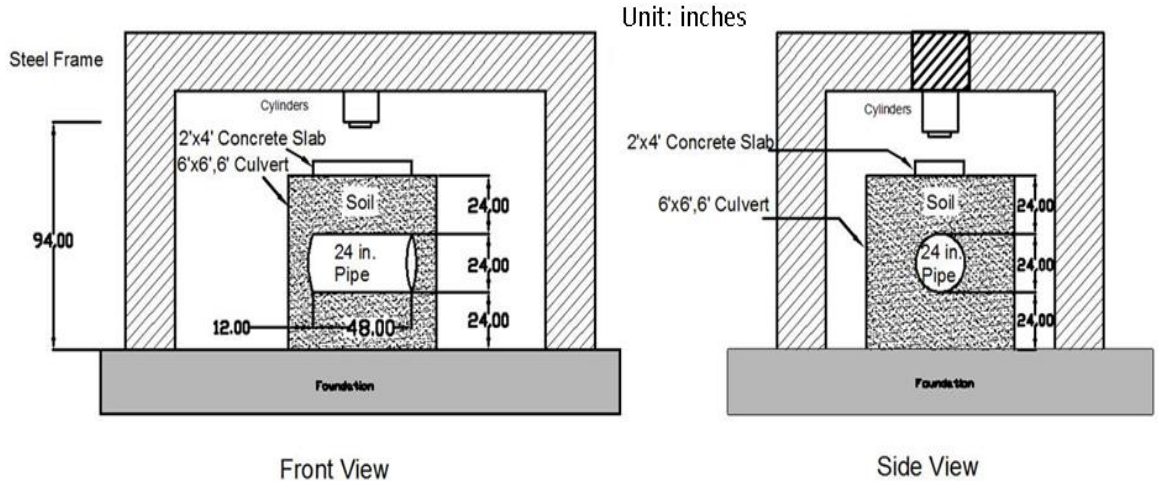

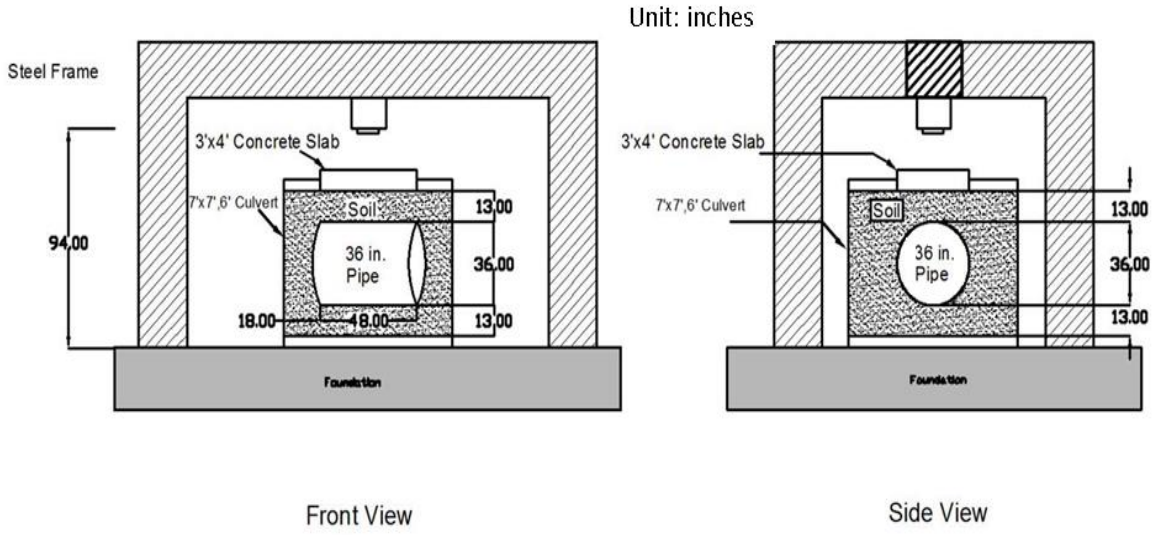

Figure 2.18 Test Descriptions (24 in. (61 cm) pipe)

Figure 2.19 Test Descriptions (36 in. (91 cm) pipe)

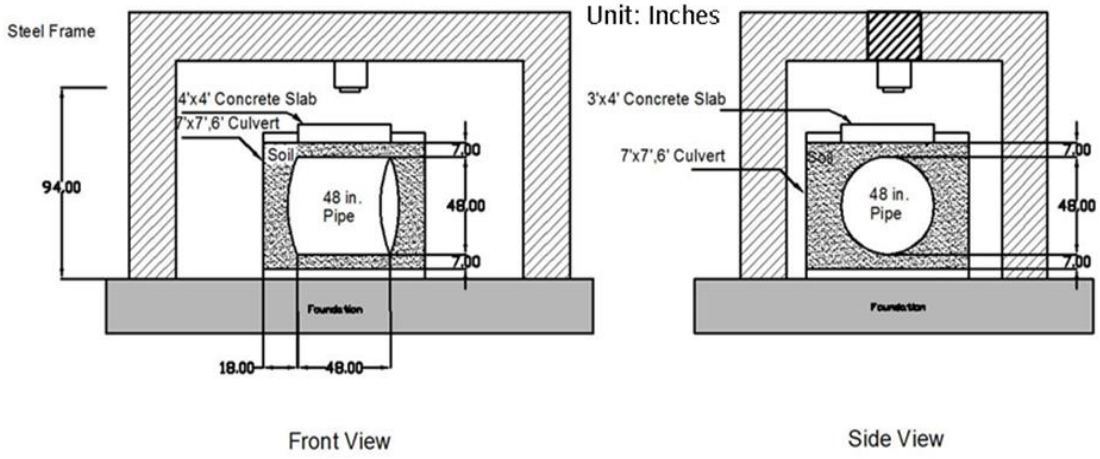

Figure 2.20 Test Description (48 in. (122 cm) pipe)

2.4.3.1 Testing with ASTM C-33 Sand

The ASTM C-33 sand was used to test the 24 in. (61 cm) SR-HDPE and CMP pipes. Both 24 in. (61 cm) CMP pipe and SR-HDPE pipe were tested under the same situation in terms of bedding and soil cover depth with same backfill material as will be described in the following. Specimens were instrumented at CELB Lab were delivered to the Hanson for the test setup and testing. After soil box preparation, the bedding layer which was 2 ft. (61 cm) and filled and compacted in 6 in. (15.2 cm) increments with ASTM C-33 sand (Figure 2.21),. The bedding was compacted to 90% of Standard Proctor Density, measured by nuclear gauge as shown in 2.24-25.

Figure 2.21 Filling the Box at 6 increments

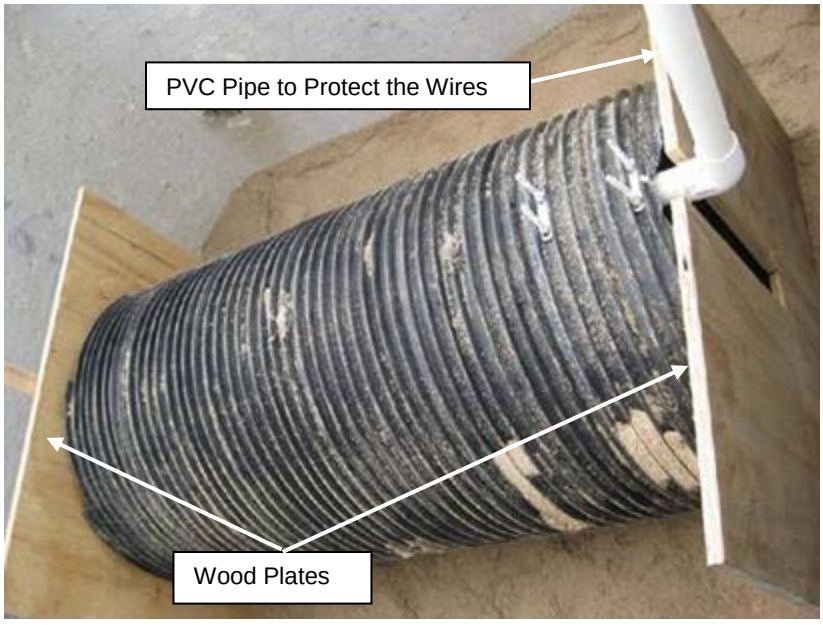

Figure 2.22 Pipe Position in the Box

Figure 2.23 Pipe position in the Box

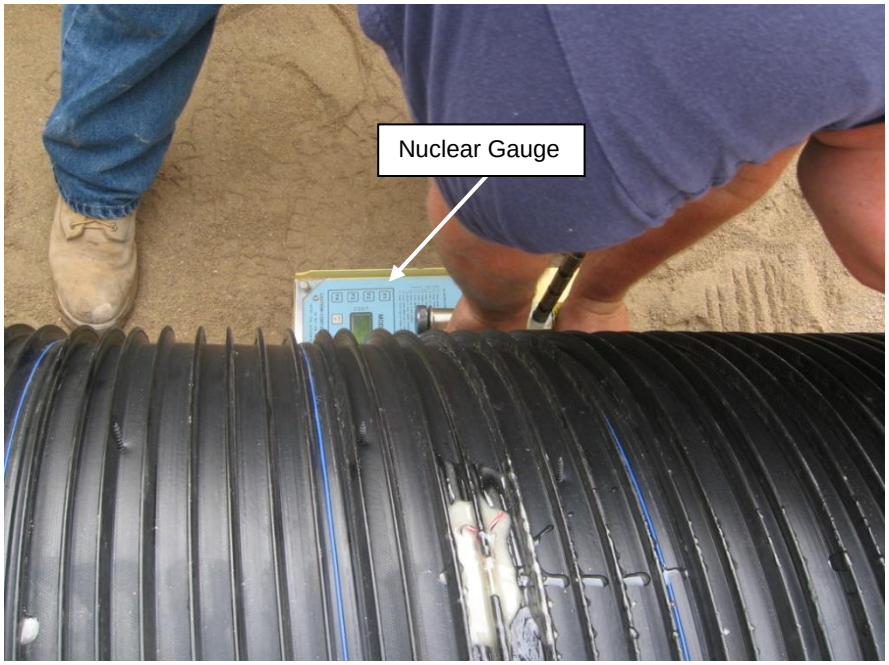

Figure 2.24 Nuclear Gauge to Verify the Bedding Compaction Level

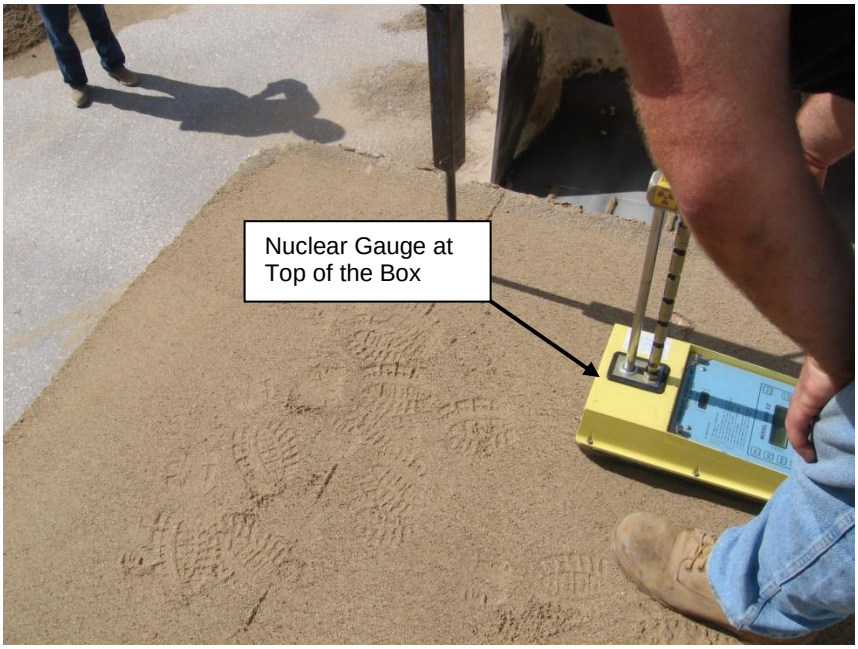

Figure 2.25 Nuclear Gauge to Verify the Top Compaction Level

Upon placing the bedding materials, each test pipe was placed in the box. With placing two wood plates at the ends to prevent soil from entering into the pipe, as indicated in Figure 2.21-2.23.

The box was filled in the same way up to the pipe's crown level. At the crown level, two pressure cells were installed, one at the mid span of the pipe, and the other at the end section of pipe to check the uniformity of the applied load.

The filling procedure was continued up to the edge of the soil box, thereafter, the rigid concrete slab was placed exactly on top of the pipe (Figure 2.26). The box was then delivered to the reaction frame for the test execution (Figure 2.16 and 2.27).

Figure 2.26 Concrete Slab Position on Top of the Soil Box

Figure 2.27 Load Cell Position on Top of the Concrete Slab

Figure 2.28 Data Acquisition System and InstruNet Soft Ware

After placing the pipe under the testing frame all the sensors were connected to the data acquisition system (Figure 2.28). Then the load cell was placed on the top of the slab (Figure 2.27). Load was applied to the pipe in 2 kip (8.9 KN) increments until failure of the test pipe specimen (Figure 2.29). After finishing the test, pipe was removed from the box for more failure inspection.

Figure 2.29 During the Test

2.4.3.2 Testing Procedure for ¾ in. Gravel

The procedure for this type of test follows exactly the same pattern as the previous one except, here the depth of bedding and also the soil cover are variable for different pipe diameters as shown in Figure 2.17-19 and also no compaction was required for the backfill.

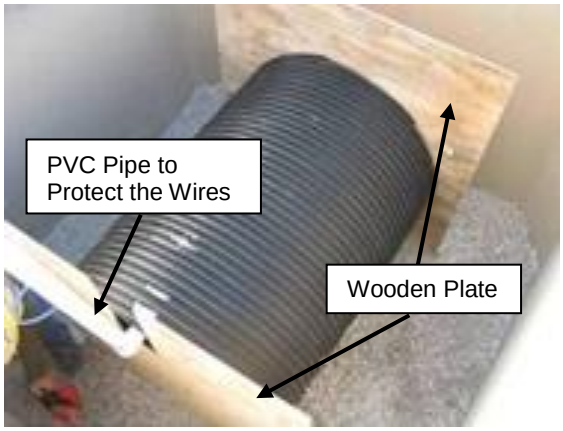

Figure 2.30 Pipe Position inside the Box

Figure 2.31 Filing the Box with ¾ in. Gravel

Figure 2.32 Filing the Pipe up to Crown Level

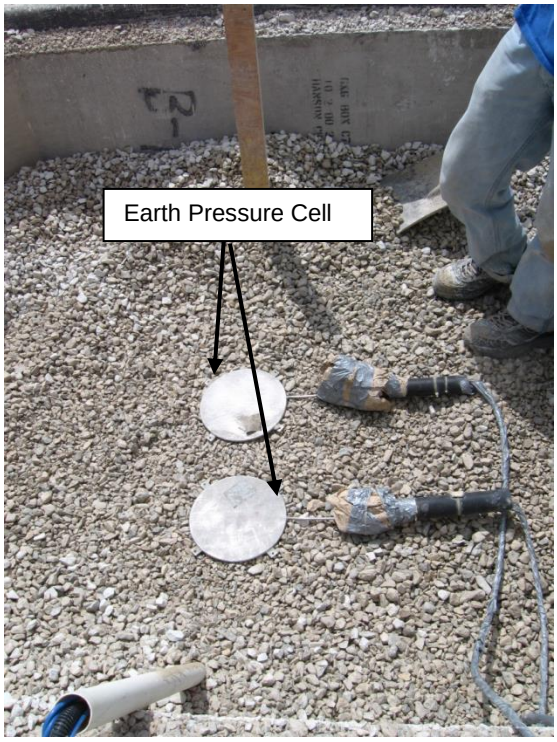

Figure 2.33 Position of Earth Pressure Cell

Figure 2.34 Slab Position on Top of the Box

Figure 2.35 Concrete Slab and Load Cell Position under the Testing Frame

Figure 2.36 Pipe under the Testing

CHAPTER 3

EXPERIMENTAL TEST RESULTS

3.1 Introduction

After performing all the experimental tests, the soil pressure distribution and the pipe deflection profile have been measured for two different types of pipes (CMP and SR-HDPE), and the obtained results was collected and compared to each other. Thereafter, related deflections to each type of pipes were illustrated and consequently, different failure modes were indentified.

The pipes were loaded in 2 kip (8.9 KN) increments until failure and after taking no more loads the unloading process started. The results were divided in two categories: first to compare pipes with same diameter and different type of backfill, secondly to compare pipes with different internal diameter.

The results obtained from the experiment and the deformed pipes show the behavior and failure modes of each pipe.

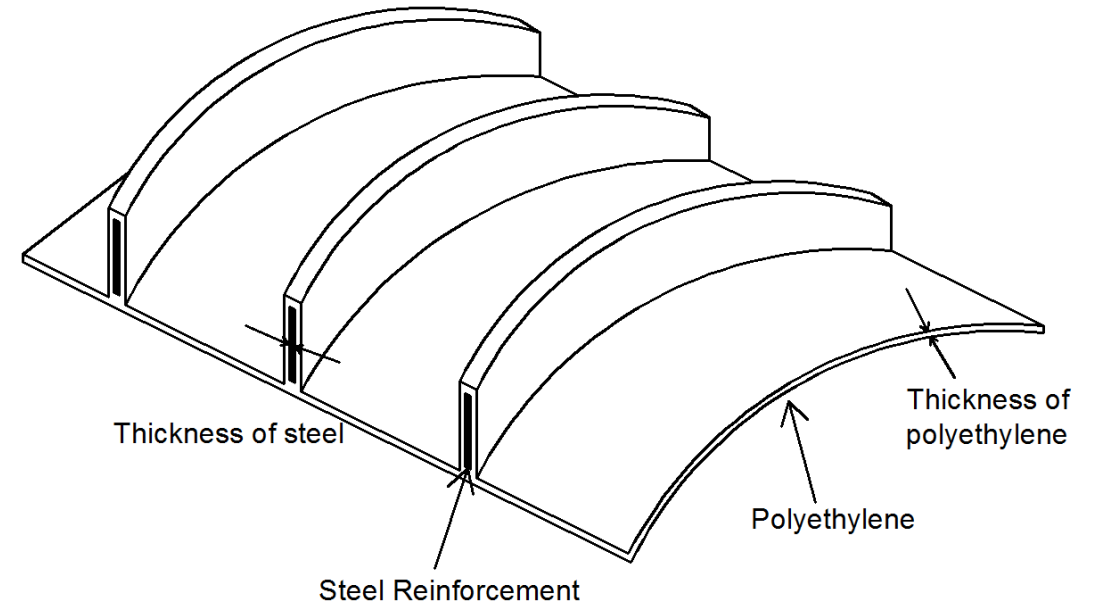

(a)

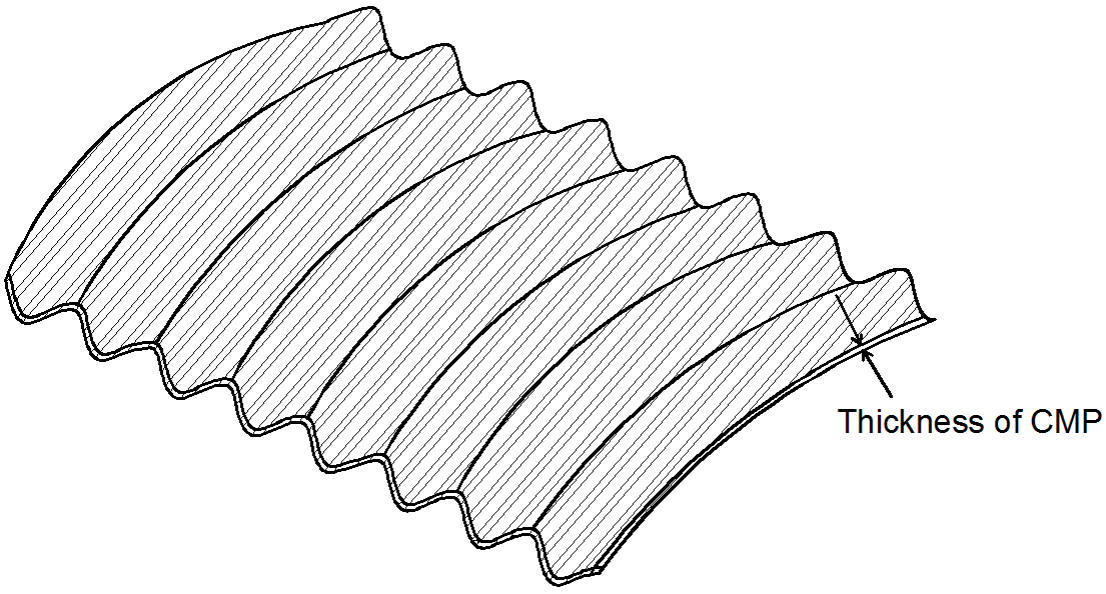

(b)

Figure 3.1 (a) SR-HDPE; (b) CMP

3.2 Thickness

Considering the goal of this study which is comparison of the behavior of the SR-HDPE and CMP pips relative thickness of the pipe which is the ration of the thickness of the pipe to the internal diameter is of the important factors in the pipe behavior, which is indicative of pipe's load carrying capacity. To have a better and more reliable understanding and reliable the results obtained from strain gauges and transducers sensors having this ration is beneficial. This factor has been calculated and the related values are tabulated in the Table3.1-2.

As shown in Figure 3.1 and 3.2 SR-HDPE pipes consist of two part; polyethylene and steel reinforcement. The value of the equivalent thickness of the steel ribs is presented in Table 3.2.

Table 3.1 Corrugated Metal Pipe Thickness

Pipe internal diameter	Equal thickness (in.)	T/D
24 in. (61 cm)	0.067 in. (0.2 cm)	0.001458
36 in.(91 cm)	0.096 in. (0.2 cm)	0.002667
48 in.(122 cm)	0.07in. (0.2 cm)	0.002792

Table 3.2 Steel Reinforced High Density Polyethylene Thickness

Pipe internal diameter	Thickness		Equivalent thickness	T/D
	Polyethylene	Steel rib		
24 in. (61 cm)	0.11 (0.3 cm)	0.56 in.(1.4 cm)	1.141552	0.047565
36 in.(91 cm)	0.12(0.3 cm)	0.89 in.(2.3 cm)	0.969718	0.026937
48 in.(122 cm)	0.17 (0.4 cm)	1.27 in.(1.27 cm)	0.70804	0.014751

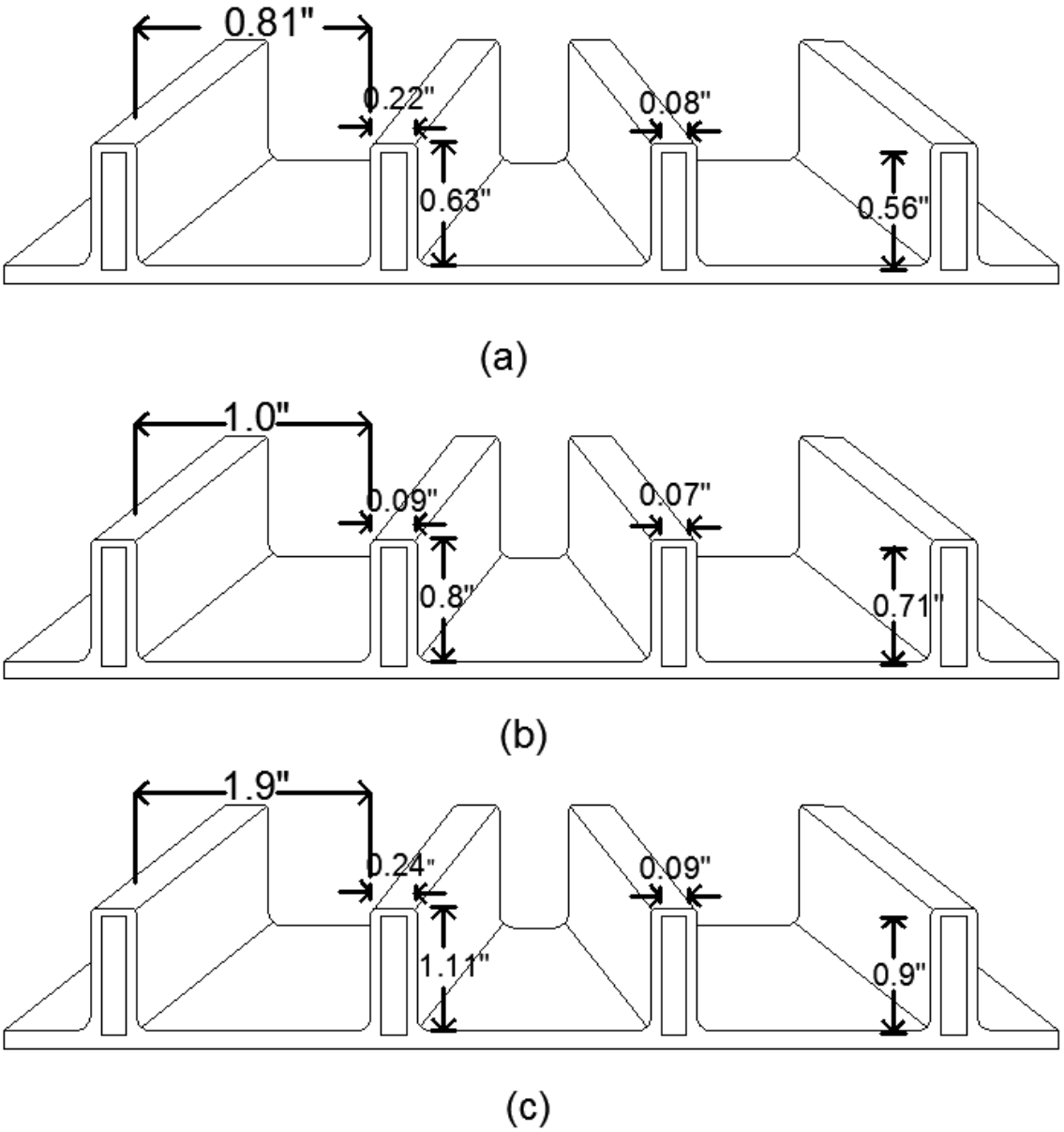

Figure 3.2 SR-HDPE Dimensions. (a) 24 in.(61 cm) Pipe. (b) 36 in.(91 cm) Pipe. (c) 48 in. (122 cm) Pipe.

3.3 Experimental Results

As it is mentioned in Chapter II, totally, twelve strain gauges and three transducer sensors were used for each specimen in order to maintain the purpose of the study. Positions of the sensors are illustrated in Figure 3.2 and 3.3.

At the end, thirteen tests have been performed, which were composed of three sets of pipe diameter of 24 in.(61 cm), 36 in(91 cm)., and 48 in.(122 cm), two types of pipe (SR-HDPE, and CMP), with two types of backfill (ASTM C-33, and ¾ in. gravel) as shown in Table 3.3.

The test results include pressure-deflection and pressure-strain plots which are illustrated in the following. Pressure as shown in (3.1) is defined as the ration of applied load to the area which is equal to the pipe diameter multiplied by pipe's length (4 feet (122 cm) for all specimens).

$$\Pr essure(ksi) = \frac{Load}{Diameter \times length} \tag{3.1}$$

Table 3.3 Test Matrix

Pipe internal diameter	Soil type	Number of testing specimens	
		SR-HDPE	CMP
24 in. (61 cm)	ASTM C-33	3	2
	¾ in Gravel	2	2
36 in.(91 cm)	¾ in Gravel	1	1
48 in.(122 cm)	¾ in Gravel	1	N/A

To investigate the behavior of the pipe, the targeted locations at the crown, invert, and springline were monitored at the middle-span and end span of the pipe with Vishay Scanners. The following nomenclatures were used to identify each test specimen:

- For strain gauges:

AAA_BB_CCC_DD_E_FF_GGG

Where:

AAA – Type of the pipe, composed of,

CMP – Corrugated metal pipe.

SRH – Steel reinforced high density polyethylene.

BB – Internal diameter of the pipe.

CCC – Positions of the strain gauge on the pipe wall for each cross-section, composed of

CRN – Crown.

SPL– Springline.

BOT – Invert.

DD – Positions with respect to the span of the pipeline (see Figure 2.5(a)), composed of

MS – Middle section of the pipe.

ES – End section of the pipe.

E– Position respect to the ribs of the pipe, composed of

1 – Strain gauge close to the end section of the pipe.

2 – Strain gauge close to the middle section of the pipe.

F– Number of tests.

GGG– Type of the backfill, composed of,

AST– ASTM C-33.

GRV– ¾ in. gravel.

HH– Level of the compaction of the backfill is only applicable for the ASTM C-33.

For instances;

CMP_24_BOT_MS_ 1_05_GRV defines the corrugated metal 24 in. pipe strain gauge located at bottom , middle span of pipe, position number one, test number five, with ¾ in. gravel as backfill.

CMP_36_CRN_ES_ 2_11_AST_98 defines the steel reinforcement high density polyethylene 36 in. pipe, strain gauge located at CRN, end span of pipe, position number two, test number eleven, with ASTM C-33 as backfill and 98% proctor.

CMP__ 48_SPL_MS_ 1_08_GRV defines the corrugated metal 48 in. pipe strain gauge located at springline , middle span of pipe, position number one, test number eight, with ¾ in. gravel as backfill.

- For linear transducer sensors:

AAA_BB_DD_F_CCC_GGG

Where AAA, BB, DD, F, and GGG terms are the same as for strain gauges (as charted earlier) and CCC defined as the position of the displacement transducer with respect to the pipe section, and it is composed of:

VER – Linear transducer placed vertically to monitor the vertical deflection of the pipe.

HOR – Linear transducer placed horizontally to monitor the horizontal deflection of the pipe.

For instances;

SRH_24_ES_ 3_VER_AST_97 defines the 24 in. diameter SR-HDPE pipe sensor located vertically at end section , test number three, with ASTM C-33 as backfill and 97% proctor.

As mentioned in a previously , to fully understand the behavior of the pipes and to have a reliable comparison between the two types of pipes, strain gauges and linear transducers were installed on the specimen and their locations have been illustrated in the Figure 3.5-6.

Figure 3.5 shows that three linear transducers were utilized for each pipe. Two of them were located vertically to monitor the vertical deformation of the pipe and the other one was utilized to monitor the horizontal deformation of the pipe.

Locations of the installed strain gauges have been illustrated in Figure 3.6. Twelve strain gauges were used to monitor the required deformations at two different sections: mid span and end span, which each of them consisted of three locations: crown (top), springline (side), and invert (bottom).

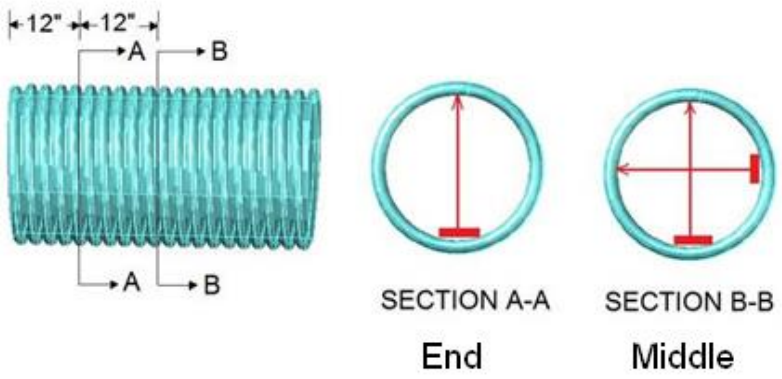

Figure 3.5 Location of Displacement Transducers

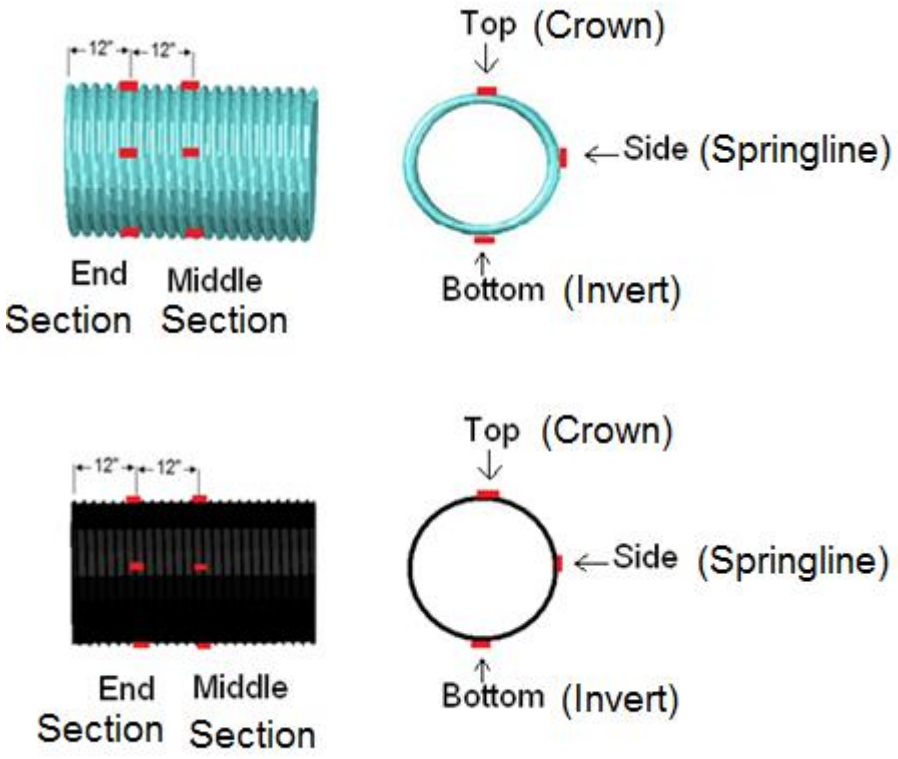

(a)

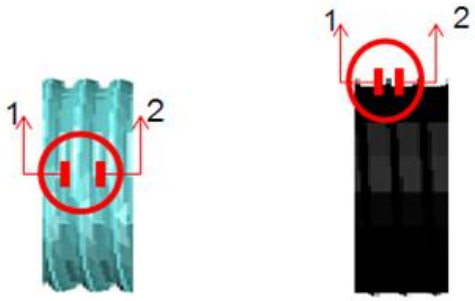

(b)

Figure 3.6 Strain Gauges Location. (a) Position on the Pipe. (b) Position on the Rib.

Table 3.4 Experimental Test Results of 24in.(61 cm) Pipe Diameter (Strain Gauges Reading)

#	Pipe type	Pipe size	Backfill	Strain gauge location	Strain	Pressure (ksi)	Pressure (M Pa)
1	SR-HDPE	24 in. (61 cm)	ASTM C-33	SRH_24_CRN_MS_ 1_1_AST_96.4	-1399.75	0.0929	0.6407
				SRH_24_CRN_MS_ 2_1_AST_96.4	-6446.31		
				SRH_24_CRN_ES_ 1_1_AST_96.4	-7071.78		
				SRH_24_CRN_ES_ 2_1_AST_96.4	-6369.1		
				SRH_24_SPR_MS_ 1_1_AST_96.4	788.332		
				SRH_24_SPR_MS_ 2_1_AST_96.4	788.332		
				SRH_24_SPR_ES_ 1_1_AST_96.4	986.876		
				SRH_24_SPR_ES_ 2_1_AST_96.4	432.745		
				SRH_24_BOT_MS_ 1_1_AST_96.4	-1685.21		
				SRH_24_BOT_MS_ 2_1_AST_96.4	-2112.56		
				SRH_24_BOT_ES_ 1_1_AST_96.4	-		
				SRH_24_BOT_ES_ 2_1_AST_96.4	-2969.56		
2	CMP	24 in. (61 cm)	ASTM C-33	CMP_24_CRN_MS_ 1_2_AST_97.3	-6164.73	0.0414	0.2851
				CMP_24_CRN_MS_ 2_2_AST_97.3	-7341.96		
				CMP_24_CRN_ES_ 1_2_AST_97.3	-5813.08		
				CMP_24_CRN_ES_ 2_2_AST_97.3	-		
				CMP_24_SPR_MS_ 1_2_AST_97.3	798.884		
				CMP_24_SPR_MS_ 2_2_AST_97.3	1081.95		
				CMP_24_SPR_ES_ 1_2_AST_97.3	1791.17		
				CMP_24_SPR_ES_ 2_2_AST_97.3	147.555		
				CMP_24_BOT_MS_ 1_2_AST_97.3	-1347.66		
				CMP_24_BOT_MS_ 2_2_AST_97.3	-872.15		
				CMP_24_BOT_ES_ 1_2_AST_97.3	-820.325		
				CMP_24_BOT_ES_ 2_2_AST_97.3	594.128		
3	SR-HDPE	24 in. (61 cm)	ASTM C-33	SRH_24_CRN_MS_ 1_3_AST_96.4	-9007.05	0.1359	0.9368
				SRH_24_CRN_MS_ 2_3_AST_96.4	-6625.47		
				SRH_24_CRN_ES_ 1_3_AST_96.4	-6792.51		
				SRH_24_CRN_ES_ 2_3_AST_96.4	-6355.03		
				SRH_24_SPR_MS_ 1_3_AST_96.4	3155.17		
				SRH_24_SPR_MS_ 2_3_AST_96.4	7838.57		
				SRH_24_SPR_ES_ 1_3_AST_96.4	3235.11		
				SRH_24_SPR_ES_ 2_3_AST_96.4	5160.38		
				SRH_24_BOT_MS_ 1_3_AST_96.4			
				SRH_24_BOT_MS_ 2_3_AST_96.4	-872.15		
				SRH_24_BOT_ES_ 1_3_AST_96.4	-820.325		
				SRH_24_BOT_ES_ 2_3_AST_96.4	594.128		
4	CMP	24 in. (61 cm)	ASTM C-33	CMP_24_CRN_MS_ 1_4_AST_97.6	-5835.08	0.0385	0.2655
				CMP_24_CRN_MS_ 2_4_AST_97.6	-4799.84		
				CMP_24_CRN_ES_ 1_4_AST_97.6	-2816.89		
				CMP_24_CRN_ES_ 2_4_AST_97.6	-7136.7		
				CMP_24_SPR_MS_ 1_4_AST_97.6	-753.322		
				CMP_24_SPR_MS_ 2_4_AST_97.6	-229.437		
				CMP_24_SPR_ES_ 1_4_AST_97.6	-517.968		
				CMP_24_SPR_ES_ 2_4_AST_97.6	-141.994		
				CMP_24_BOT_MS_ 1_4_AST_97.6	-1538.81		
				CMP_24_BOT_MS_ 2_4_AST_97.6	-998.217		
				CMP_24_BOT_ES_ 1_4_AST_97.6	-393.05		
				CMP_24_BOT_ES_ 2_4_AST_97.6	-1299.68		

Table 3.4 Continued

5	SR-HDPE	24 in. (61 cm)	ASTM C-33	SRH_24_CRN_MS_ 1_5_AST_95.67	-4187.23	0.0538	0.3709
				SRH_24_CRN_MS_ 2_5_AST_95.67	-4197.65		
				SRH_24_CRN_ES_ 1_5_AST_95.67	-3466.63		
				SRH_24_CRN_ES_ 2_5_AST_95.67	-1164.38		
				SRH_24_SPR_MS_ 1_5_AST_95.67	3155.17		
				SRH_24_SPR_MS_ 2_5_AST_95.67	7838.57		
				SRH_24_SPR_ES_ 1_5_AST_95.67	3235.11		
				SRH_24_SPR_ES_ 2_5_AST_95.67	5160.38		
				SRH_24_BOT_MS_ 1_5_AST_95.67	-1164.38		
				SRH_24_BOT_MS_ 2_5_AST_95.67	-1539.61		
				SRH_24_BOT_ES_ 1_5_AST_95.67	-1022.85		
				SRH_24_BOT_ES_ 2_5_AST_95.67	-956.578		
6	CMP	24 in. (61 cm)	3/4 in. gravel	CMP_24_CRN_MS_ 1_6_GRV	-	0.133684	0.92172
				CMP_24_CRN_MS_ 2_6_GRV	-12336.6		
				CMP_24_CRN_ES_ 1_6_GRV	-7058.42		
				CMP_24_CRN_ES_ 2_6_GRV	-7058.42		
				CMP_24_SPR_MS_ 1_6_GRV	-932.034		
				CMP_24_SPR_MS_ 2_6_GRV	-810.976		
				CMP_24_SPR_ES_ 1_6_GRV	-244.719		
				CMP_24_SPR_ES_ 2_6_GRV	-311.349		
				CMP_24_BOT_MS_ 1_6_GRV	-152.423		
				CMP_24_BOT_MS_ 2_6_GRV	-152.423		
				CMP_24_BOT_ES_ 1_6_GRV	-273.847		
				CMP_24_BOT_ES_ 2_6_GRV	-275.053		
7	SR-HDPE	24 in. (61 cm)	3/4 in. gravel	SRH_24_CRN_MS_ 1_7_GRV	-3902.29	0.1004	0.6920
				SRH_24_CRN_MS_ 2_7_GRV	-3716.43		
				SRH_24_CRN_ES_ 1_7_GRV	-5126.42		
				SRH_24_CRN_ES_ 2_7_GRV	-6263.67		
				SRH_24_SPR_MS_ 1_7_GRV	-742.716		
				SRH_24_SPR_MS_ 2_7_GRV	-607.3		
				SRH_24_SPR_ES_ 1_7_GRV	-802.741		
				SRH_24_SPR_ES_ 2_7_GRV	-698.994		
				SRH_24_BOT_MS_ 1_7_GRV	-769.745		
				SRH_24_BOT_MS_ 2_7_GRV	-365.389		
				SRH_24_BOT_ES_ 1_7_GRV	-309.631		
				SRH_24_BOT_ES_ 2_7_GRV	-324.631		
8	CMP	24 in. (61 cm)	3/4 in. gravel	CMP_24_CRN_MS_ 1_8_GRV	-13808.7	0.1523	1.0498
				CMP_24_CRN_MS_ 2_8_GRV	-12587.7		
				CMP_24_CRN_ES_ 1_8_GRV	-		
				CMP_24_CRN_ES_ 2_8_GRV	-530.138		
				CMP_24_SPR_MS_ 1_8_GRV	-742.716		
				CMP_24_SPR_MS_ 2_8_GRV	-742.716		
				CMP_24_SPR_ES_ 1_8_GRV	-		
				CMP_24_SPR_ES_ 2_8_GRV	-948.766		
				CMP_24_BOT_MS_ 1_8_GRV	-265.538		
				CMP_24_BOT_MS_ 2_8_GRV	-466.882		
				CMP_24_BOT_ES_ 1_8_GRV	-278.451		
				CMP_24_BOT_ES_ 2_8_GRV	-262.358		

Table 3.4 Continued

9	SR-HDPE	24 in. (61 cm)	3/4 in. gravel	SRH_24_CRN_MS_ 1_9_GRV	-2673.22	0.1291	0.8899
				SRH_24_CRN_MS_ 2_9_GRV	-3404.52		
				SRH_24_CRN_ES_ 1_9_GRV	-3779.37		
				SRH_24_CRN_ES_ 2_9_GRV	-2142.59		
				SRH_24_SPR_MS_ 1_9_GRV	-674.73		
				SRH_24_SPR_MS_ 2_9_GRV	-1043.3		
				SRH_24_SPR_ES_ 1_9_GRV	3.49434		
				SRH_24_SPR_ES_ 2_9_GRV	-211.513		
				SRH_24_BOT_MS_ 1_9_GRV	-1191.19		
				SRH_24_BOT_MS_ 2_9_GRV	-20.0615		
				SRH_24_BOT_ES_ 1_9_GRV	-34.0614		
				SRH_24_BOT_ES_ 2_9_GRV	-211.513		

Table 3.5 Experimental Test Results of the 24 in. (61 cm) Pipe Diameter (Displacement Transducers Reading)

#	Pipe type	Pipe size	Backfill	Linear trancducer sensor location	Deflection	Pressure (ksi)	Pressure (ksi)
1	SR-HDPE	24 in. (61 cm)	ASTM C-33	SRH_24_MS_ 1_VER_AST_96.4	-2.8228	0.0929	0.6407
				SRH_24_ES_ 1_VER_AST_96.4	-3.2856		
				SRH_24_MS_ 1_HOR_AST_96.4	-3.8412		
2	CMP	24 in. (61 cm)	ASTM C-33	CMP_24_MS_ 2_VER_AST_97.3	-5.92417	0.0414	0.2851
				CMP_24_ES_ 2_VER_AST_97.3	-6.13873		
				CMP_24_MS_ 2_HOR_AST_97.3	3.338422		
3	SR-HDPE	24 in. (61 cm)	ASTM C-33	SRH_24_MS_ 3_VER_AST_96.4	-5.92417	0.1359	0.9368
				SRH_24_ES_ 3_VER_AST_96.4	-6.13873		
				SRH_24_MS_ 3_HOR_AST_96.4	3.338422		
4	CMP	24 in. (61 cm)	ASTM C-33	CMP_24_MS_ 4_VER_AST_97.6	-1.1435	0.0385	0.2655
				CMP_24_ES_ 4_VER_AST_97.6	-1.033		
				CMP_24_MS_ 4_HOR_AST_97.6	0.32575		
5	SR-HDPE	24 in. (61 cm)	ASTM C-33	SRH_24_MS_ 5_VER_AST_95.67	-3.10975	0.0538	0.3709
				SRH_24_ES_ 5_VER_AST_95.67	-2.84976		
				SRH_24_MS_ 5_HOR_AST_95.67	1.264353		
6	CMP	24 in. (61 cm)	3/4 in. gravel	CMP_24_MS_ 6_VER_GRV	-4.71511	0.133684	0.92172
				CMP_24_ES_ 6_VER_GRV	-3.59102		
				CMP_24_MS_ 6_HOR_GRV	1.833477		
7	SR-HDPE	24 in. (61 cm)	3/4 in. gravel	SRH_24_MS_ 7_VER_GRV	-6.83708	0.1004	0.6920
				SRH_24_ES_ 7_VER_GRV	-7.24346		
				SRH_24_MS_ 7_HOR_GRV	1.217893		
8	CMP	24 in. (61 cm)	3/4 in. gravel	CMP_24_MS_ 8_VER_GRV	-4.75465	0.1523	1.0498
				CMP_24_ES_ 8_VER_GRV	-4.56455		
				CMP_24_MS_ 8_HOR_GRV	1.795314		
9	SR-HDPE	24 in. (61 cm)	3/4 in. gravel	SRH_24_MS_ 9_VER_GRV	-3.87204	0.1291	0.8899
				SRH_24_ES_ 9_VER_GRV	-3.73742		
				SRH_24_MS_ 9_HOR_GRV	1.352293		

Table 3.6 Experimental Test Results of 36 in. (91 cm) Pipe Diameter (Strain Gauges Reading)

#	Pipe type	Pipe size	Backfill	Strain gauge location	Strain	Pressure (ksi)	Pressure (M Pa)
1	SR-HDPE	36 in. (91.4 cm)	3/4 in. gravel	SRH_36_CRN_MS_ 1_1_GRV	-1624	0.07017	0.48383
				SRH_36_CRN_MS_ 2_1_GRV	-1726.7		
				SRH_36_CRN_ES_ 1_1_GRV	-2547.9		
				SRH_36_CRN_ES_ 2_1_GRV	-2637.9		
				SRH_36_SPR_MS_ 1_1_GRV	-		
				SRH_36_SPR_MS_ 2_1_GRV	-		
				SRH_36_SPR_ES_ 1_1_GRV	-		
				SRH_36_SPR_ES_ 2_1_GRV	-		
				SRH_36_BOT_MS_ 1_1_GRV	-841.75		
				SRH_36_BOT_MS_ 2_1_GRV	-860.05		
				SRH_36_BOT_ES_ 1_1_GRV	-768.55		
				SRH_36_BOT_ES_ 2_1_GRV	-878.35		
2	CMP	36 in. (91.4 cm)	3/4 in. gravel	CMP_36_CRN_MS_ 1_2_GRV	-5721.8	0.0872	0.6015
				CMP_36_CRN_MS_ 2_2_GRV	-6003.7		
				CMP_36_CRN_ES_ 1_2_GRV	-5627.9		
				CMP_36_CRN_ES_ 2_2_GRV	-5431.9		
				CMP_36_SPR_MS_ 1_2_GRV	-3633.5		
				CMP_36_SPR_MS_ 2_2_GRV	-2614.4		
				CMP_36_SPR_ES_ 1_2_GRV	-866.98		
				CMP_36_SPR_ES_ 2_2_GRV	-436.25		
				CMP_36_BOT_MS_ 1_2_GRV	-464.98		
				CMP_36_BOT_MS_ 2_2_GRV	-475.93		
				CMP_36_BOT_ES_ 1_2_GRV	-486.89		
				CMP_36_BOT_ES_ 2_2_GRV	-481.44		

Table 3.7 Experimental Test Results of the 36 in. (91 cm) Pipe Diameter (Displacement Transducers Reading)

#	Pipe type	Pipe size	Backfill	Linear trancducer sensor location	Deflection	Pressure (ksi)	Pressure (M Pa)
1	SR-HDPE	36 in. (91.4 cm)	3/4 in. gravel	SRH_36_MS_1_VER_GRV	-2.62932	0.0702	0.4838
				SRH_36_ES_1_VER_GRV	-2.51708		
				SRH_36_MS_1_HOR_GRV	1.69244		
2	CMP	36 in. (91.4 cm)	3/4 in. gravel	CMP_36_MS_2_VER_GRV	-4.4913	0.0872	0.6015
				CMP_36_ES_2_VER_GRV	-4.36089		
				CMP_36_MS_2_HOR_GRV	1.499967		

Table 3.8 Experimental Test Results of 48 in. (122 cm) Pipe Diameter (Strain Gauges Reading)

#	Pipe type	Pipe size	Backfill	Strain gauge location	Strain	Pressure (ksi)	Pressure (M Pa)
1	SR-HDPE	48 in. (121.9 cm)	3/4 in. gravel	SRH_48_CRN_MS_ 1_1_GRV	-202.672	0.0549	0.3788
				SRH_48_CRN_MS_ 2_1_GRV	-1334.7		
				SRH_48_CRN_ES_ 1_1_GRV	-1097.38		
				SRH_48_CRN_ES_ 2_1_GRV	-768.685		
				SRH_48_SPR_MS_ 1_1_GRV	-1247.91		
				SRH_48_SPR_MS_ 2_1_GRV	-914.23		
				SRH_48_SPR_ES_ 1_1_GRV	-1081.07		
				SRH_48_SPR_ES_ 2_1_GRV	-1081.07		
				SRH_48_BOT_MS_ 1_1_GRV	-197.412		
				SRH_48_BOT_MS_ 2_1_GRV	-189.819		
				SRH_48_BOT_ES_ 1_1_GRV	-205.004		
				SRH_48_BOT_ES_ 2_1_GRV	-197.412		

Table 3.9 Experimental Test Results of the 48 in. (122 cm) Pipe Diameter (Displacement Transducers Reading)

#	Pipe type	Pipe size	Backfill	Linear trancducer sensor location	Deflection	Pressure (ksi)	Pressure (M Pa)
1	SR-HDPE	48 in. (121.9 cm)	3/4 in. gravel	SRH_48_MS_1_V_GRV	-2.63353	0.0549	0.3788
				SRH_48_ES_1_V_GRV	-2.4764		
				SRH_48_MS_1_H_GRV	1.42362		

The deformation results were which measured by the strain gauges and linear transducers sensors attached to each pipe have been presented in table 3.4-9. Tables 3.4, 3.6, and 3.8 are reflecting the information obtained from strain gauges, and tables 3.5, 3.7, and 3.9 indicate the results gained from linear transducer sensors based on maximum yield load of the pipe.

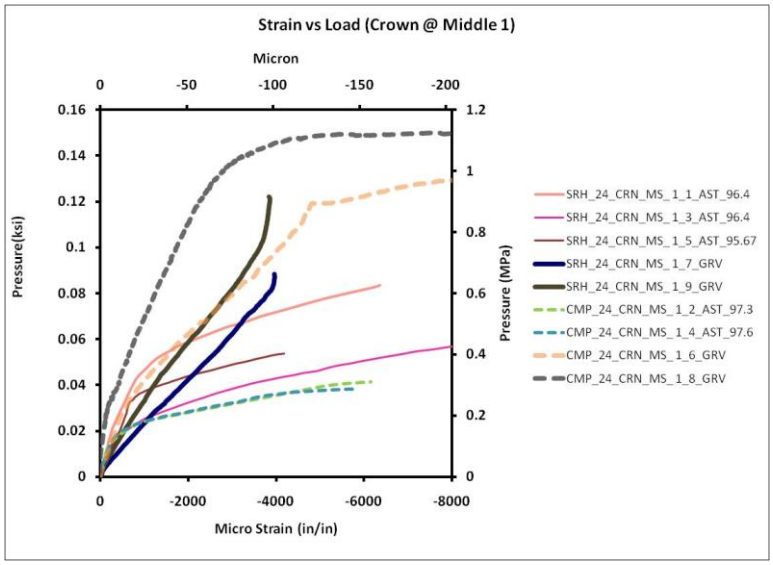

Figure 3.7 Pressure vs. Strain at the Crown-Middle Section of the 24 in. (61 cm) Pipe Position 1

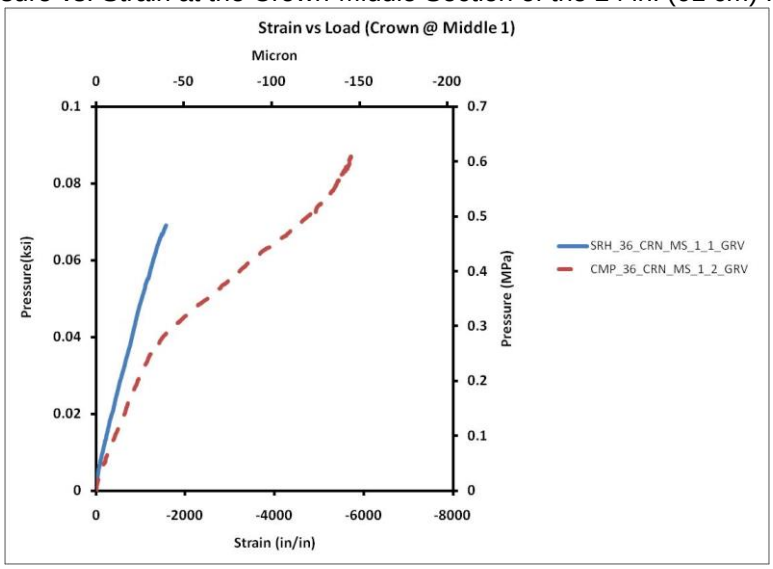

.

Figure 3.8 Pressure vs. Strain at the Crown-Middle Section of the 36 in. (91 cm) Pipe Position1.

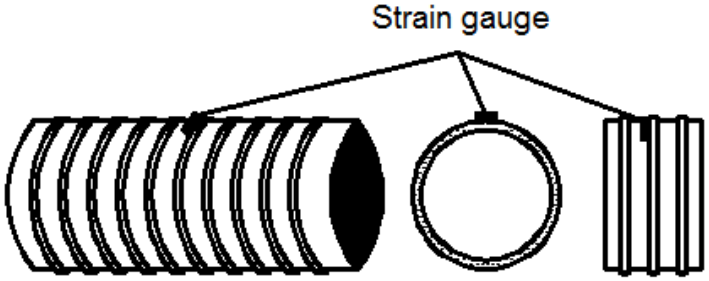

Figure 3.9 Strain Gauge Location of the Figure 3.7-10

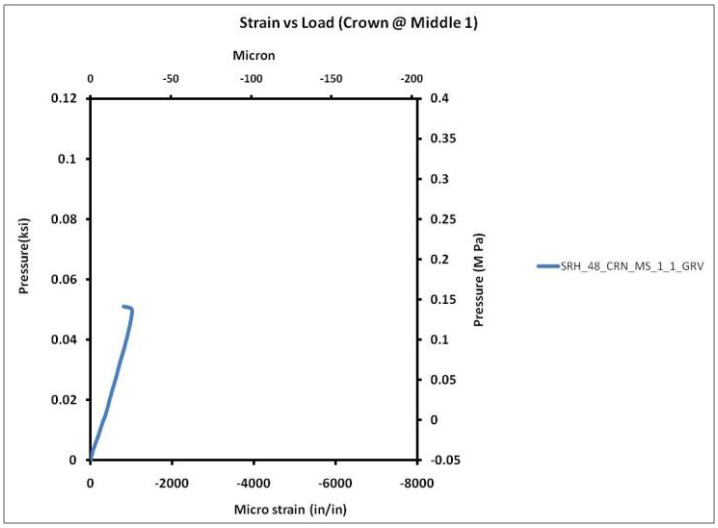

Figure 3.10 Pressure vs. Strain at the Crown-Middle Section of the 48in.(122 cm)Pipe Position 1.

Based on the data from tables 3.4-5 and referring to Figures 3.7, 3.10, and 3.14, SR-HDPE pipes withstand more loads, using ASTM C-33 as backfill, in comparison to the CMP pipes. However, using ¾ in. gravel as backfill increases the capacity of applied loads carried by both pipes, but in this case, this is CMP pipe which withstands more loads in compare to SR-HDPE pipe.

Based on recorded data, 24 in.(61 cm) pipes are stiffer than 36 in.(91 cm), and 36 in. (91 cm) pipes are stiffer than 48 in. (122 cm) pipes analogically. The reasons of the comparison stated before are the T/D ratio (Table 3.2) and also cover depth. The more T/D ratio is the more yield load will be carried by the pipe. As mentioned in table 3.2, 24 in. (61 cm) pipes have the highest T/D ratio among those three sizes of SR-HDPE pipes.

Recalling the information from chapter two, cover depth of 24 in. (61 cm), 36 in. (91 cm), and 48 in. (122 cm) pipes were 24 in. (61 cm), 12 in. (31 cm), and 6 in. (15.2 cm), respectfully. The less applied cover depth causes, more load to be transferred directly to the pipe; this means less load will be carried by the structure. For instance, in this case, less cover depth used for 48

in. pipe, resulted in a higher ratio of the applied to the carried load by the pipe in comparison to the 36 in. and 24 in. pipes which have more cover depth.

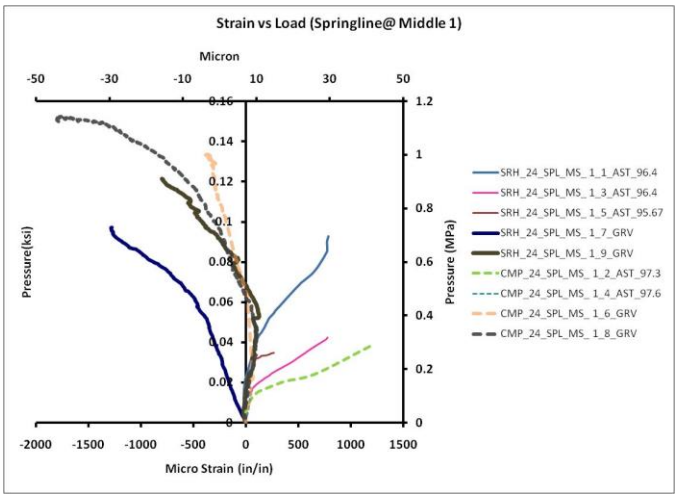

Figure 3.11 Pressure vs. Strain at the Springline-Middle Section of the 24 in.(61 cm)Pipe Position 1.

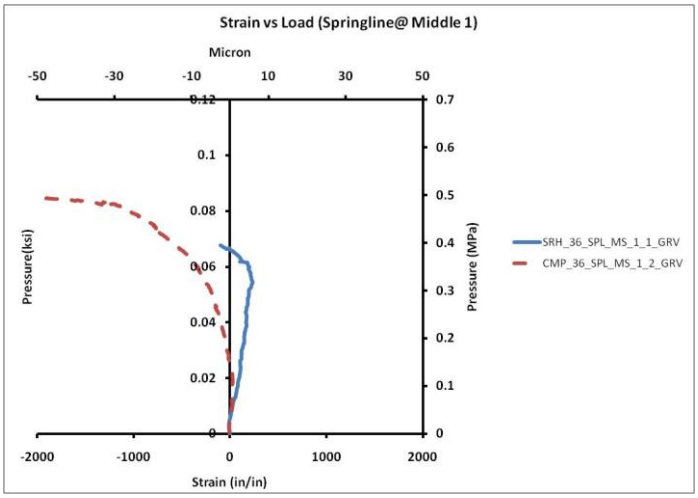

Figure 3.12 Pressure vs. strain at the Springline-Middle Section of the 36 in. (91 cm) Pipe Position 1.

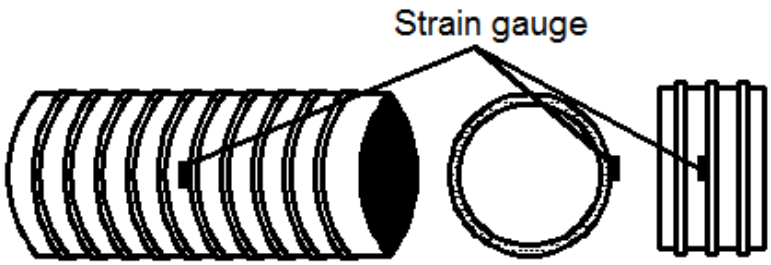

Figure 3.13 Strain Gauge Location of the Figure 3.11-14

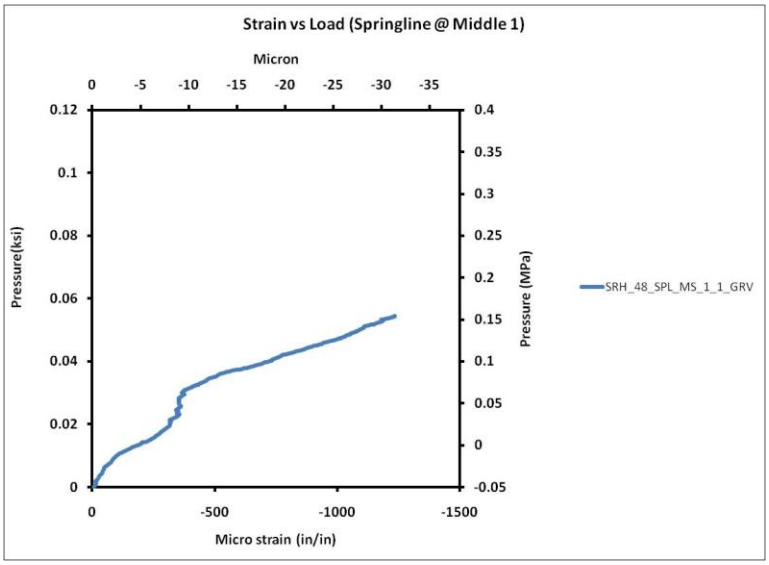

Figure 3.14 Pressure vs. Strain at the Springline-Middle Section of the 48 in.(122 cm) Pipe Position 1.

As shown in Figure 3.11-14, during the loading procedure, the pipe's wall in the springline zone has firstly been compressed due to the resistance force of the sidefill material. That prevents horizontally expansion of the pipes at springline. By increasing the applied load to the pipe, the load transferred from the pipe's wall to the soil exceeds than the transferred load to the pipe through the soil. Therefore, the pressure of the pipe's wall govern this load which results in pipe's expansion and tension stresses in the pipe's wall. However, by using ASTM C-33 as backfill, these tension stresses will be eliminated due to the soil compaction. In comparison to the other size of pipes, in 48 in. (122 cm) pipes, does not exist any compression stress due to less sidefill material which means the transferred pressure from the pipe's wall conquers to the transferred pressure from the sidefill.

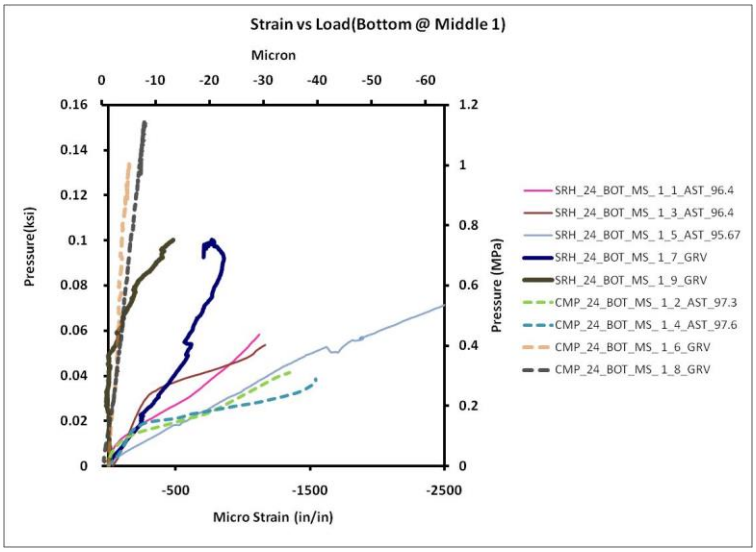

Figure 3.15 Pressure vs. Strain at the Bottom-Middle Section of the 24 in. (61 cm) Pipe Position 1.

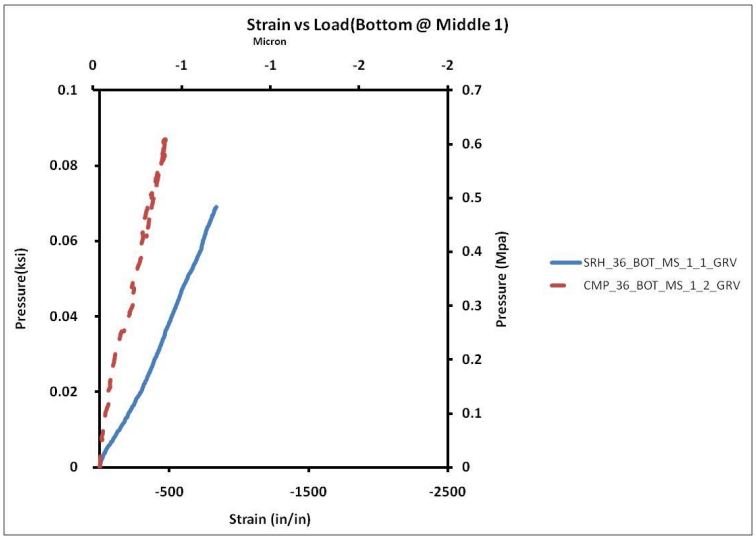

Figure 3.16 Pressure vs. Strain at the Bottom-Middle Section of the 36 in(91 cm)Pipe Position 1

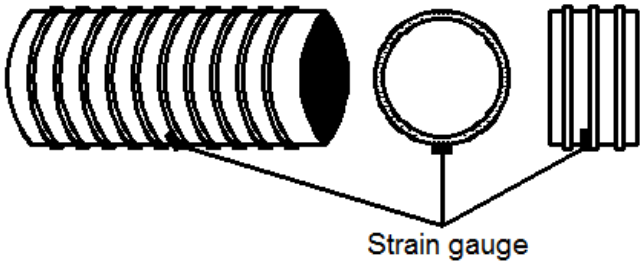

Figure 3.17 Strain Gauge Location of the Figure 3.16-18

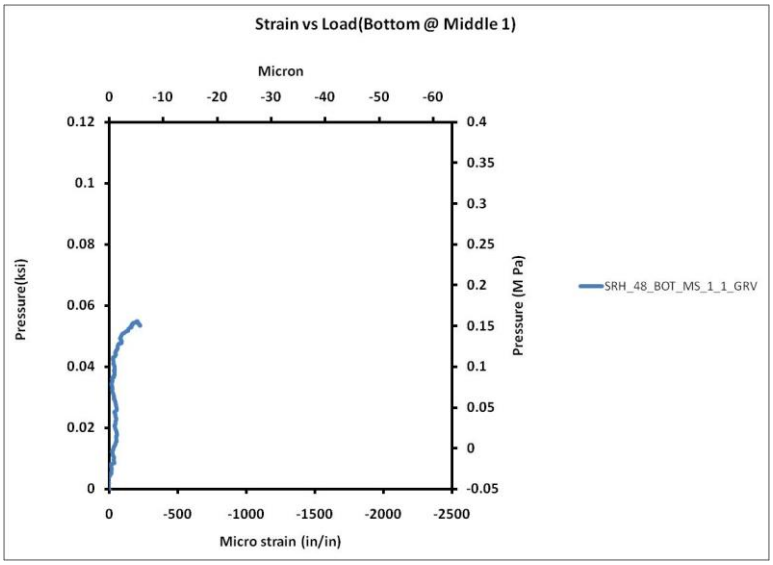

Figure 3.18 Pressure vs. Strain at the Bottom-Middle Section of the 48 in.(122 cm) Pipe Position 1.

The result obtained from strain gauges located at the invert of the pipes (Figure 3.15-18), indicates that the pipe's deformation was more distinguished at the crown (top), and springline (side), in comparison to the invert (bottom). Based on obtained information, the occurred tension at the invert (bottom) zone is too small in comparison to other two zones, crown (top), springline (side).

Based on these results, it can be concluded the major portion of the load has been carried by the upper side of the pipe and has been transferred to the backfill, therefore the lower part of the pipe has not been deformed as much as the related deformation of the top region.

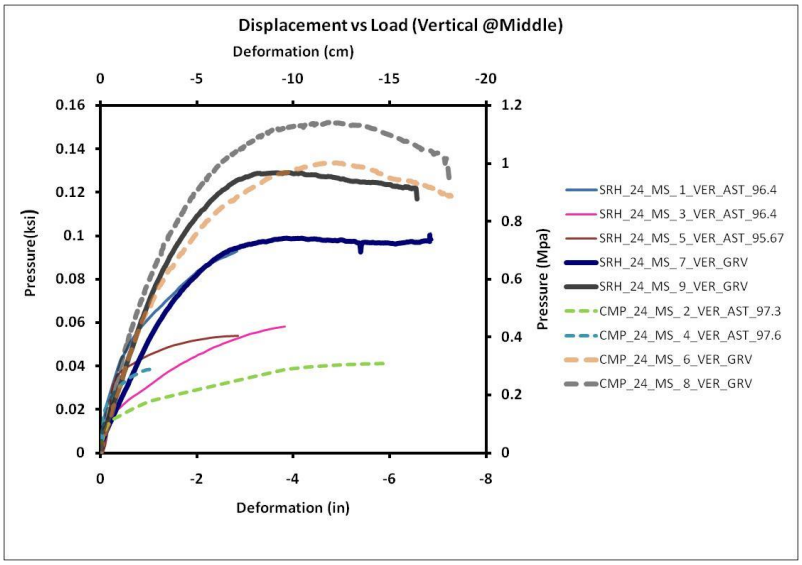

Figure 3.19 Pressure vs. Vertical Deformation at the Middle Section of the 24 in. (61 cm) Pipe.

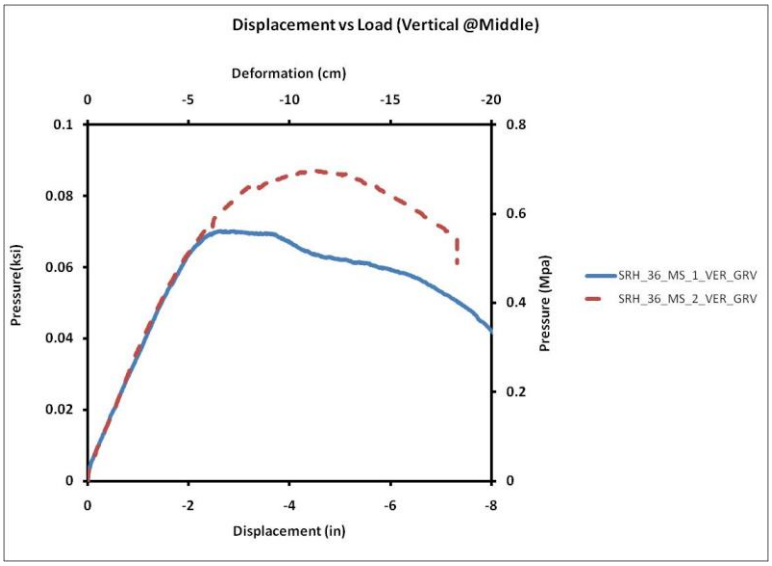

Figure 3.20 Pressure vs. Vertical Deformation at the Middle Section of the 36 in. (91 cm) Pipe.

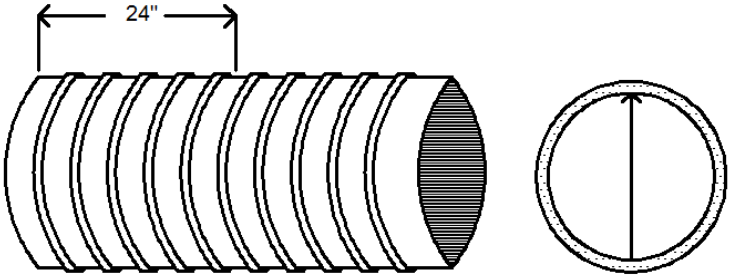

Figure 3.21 Displacement Transducer Location of the Figure 3.19-22

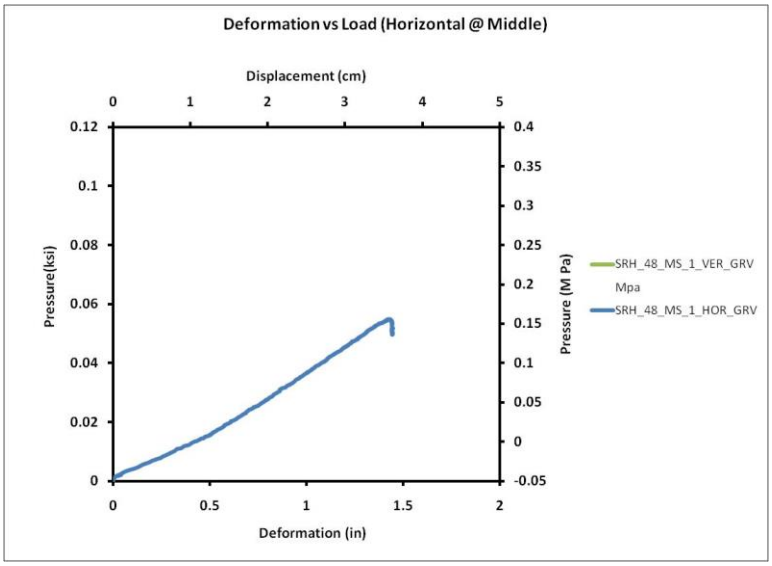

Figure 3.22 Pressure vs. Vertical Deformation at the Middle Section of the 48 in. (122 cm) Pipe.

The results of vertical deformation of the specimens, recorded by linear transducer sensors have been presented in Figure 3.19-22. It can be concluded the CMP pipes are stiffer and results show less deformation at the yield point compared to the SR-HDPE pipes. Flexibility at ribs support stage made of HDPE, and also the thin ribs, have been introduced as main reasons of the SR-HDPE pipes out of plane buckling.

During all experiments, to ensure having a uniform distributed load condition on the pipe, the load was applied through a rigid slab. Figure 3.19 shows the vertical deformation of the pipe versus applied pressure on the pipe. This Figure shows that the concrete slab fulfills all desired purposes of the rigid plate and also indicates the identical vertical deformation of the pipe at the end section and mid span. This means that the load has been applied uniformly through the whole span.

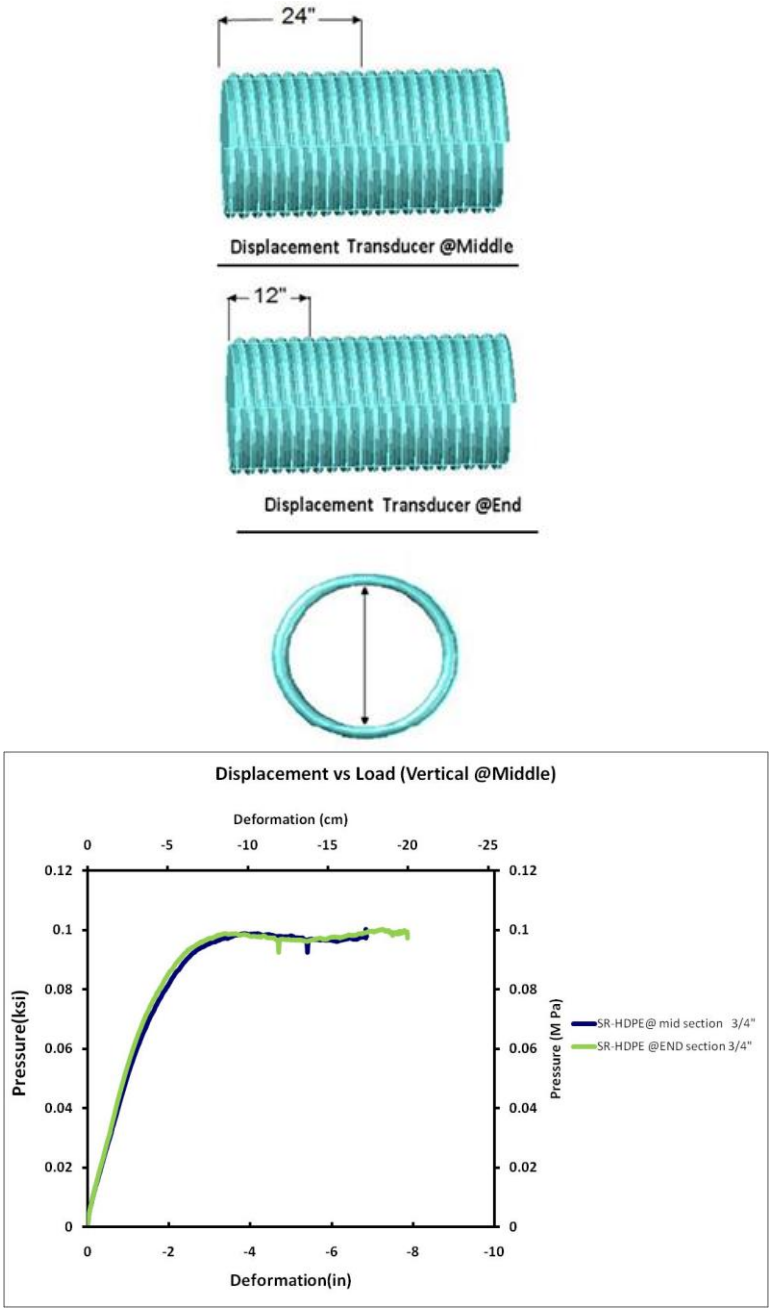

Figure 3.23 Comparison of Pressure vs. Vertical Deformation at the Middle and End Section of the 24 in. (61 cm) Pipe

.

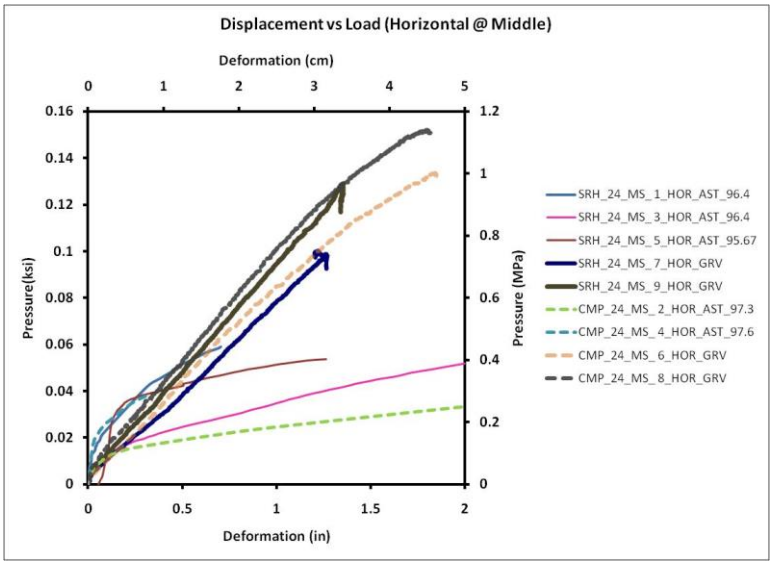

Figure 3.24 Pressure vs. Horizontal Deformation at the Middle Section of the 24 in. (61 cm) Pipe.

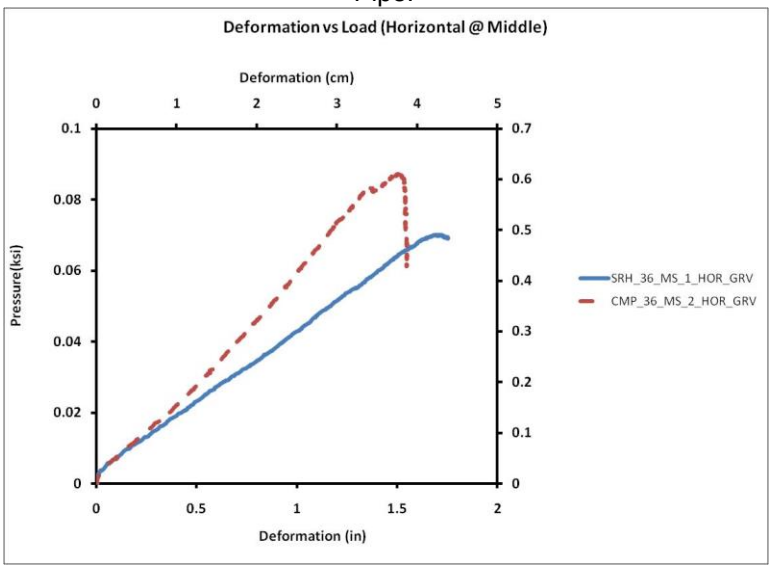

Figure 3.25 Pressure vs. Horizontal Deformation at the Middle Section of the 36 in.(91 cm) Pipe.

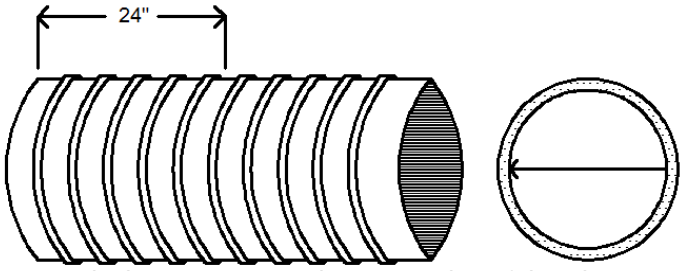

Figure 3.26 Displacement Transducer Location of the Figure 3.24-27

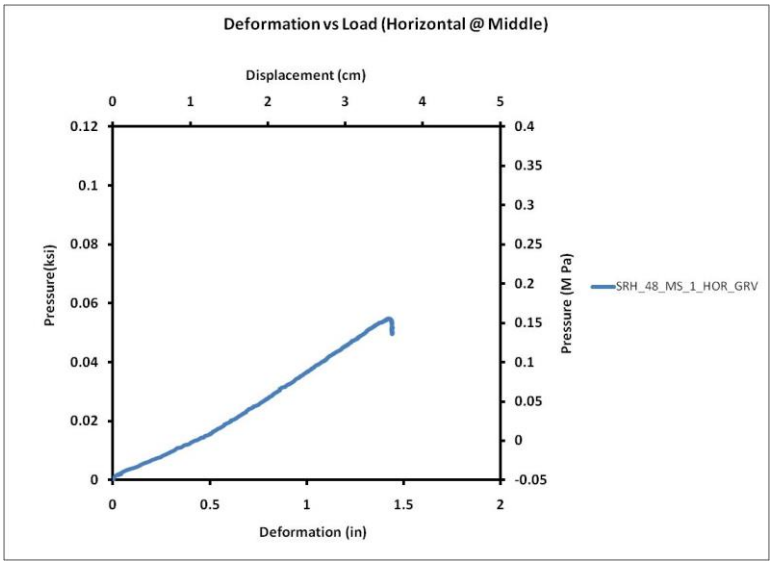

Figure 3.27 Pressure vs. Horizontal Deformation at the Middle Section of the 48 in.(122 cm) Pipe.

Figure 3.23 through 3.27 shows that with the exception of one case (when ASTM C-33 backfill was used), the CMP showed higher stiffness and load carrying capacity. It is particularly interesting given the ratio of the thickness to diameter was less for CMP when compare to SR-HDPE (see Table 3.1 and 3.2).

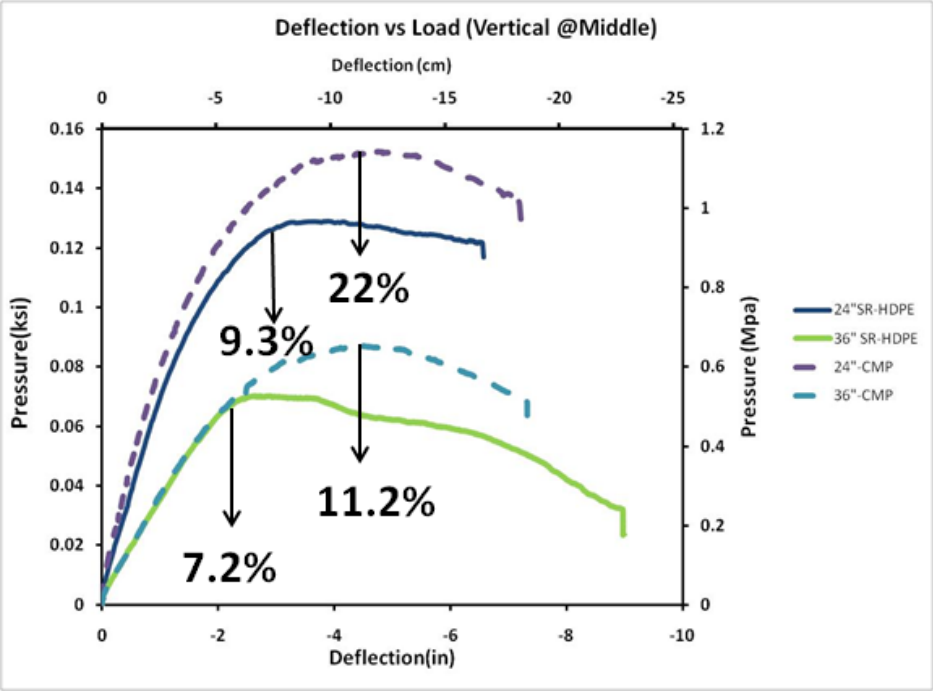

Figure 3.28 Percentile Deformations at Failure

Figure 3.28 shows the pressure-deflection plots for the representative tests of the 24 in. (61 cm), and 36 in. (91 cm) pipes. As shown in this figure, the CMP has more loads carrying capacity and exhibits more ductility before the initiation of failure. For example, 24 in. (61 cm) CMP undergoes 22% deformation while the 24 in. (61 cm) SR-HDPE experiences 9.3 % under identical test conditions. This is also true for 36 in. (91 cm) CMP and SR-HDPE pipes which undergo 11.2 % and 7.2 % of deflection, respectively.

3.4 Failure Modes

3.5.1 Failure Modes of 24 in. (61 cm) Pipe

After reloading and inspecting the 24 in. (61 cm) failed pipe, two different failure modes were identified for corrugated metal pipe and steel reinforced high density polyethylene pipe.

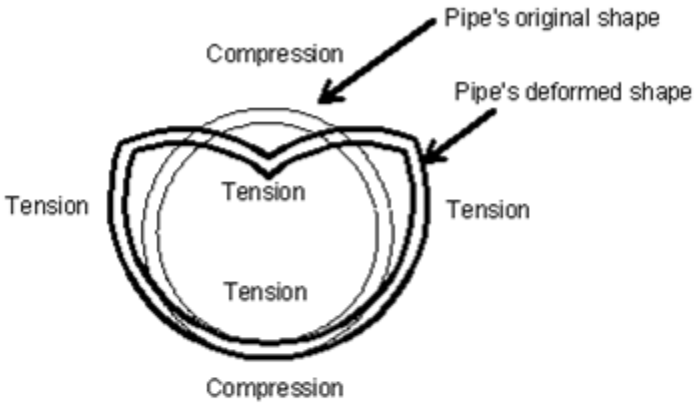

(a)

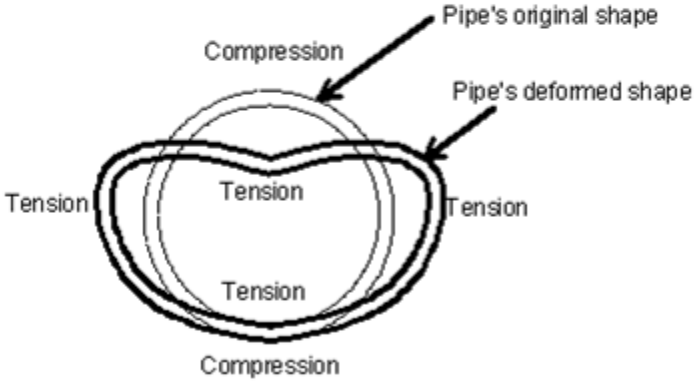

(b)

Figure 3.29 Failure Modes of 24 in. Pipes. (a) Failure Mode of SR-HDPE Pipe. (b) Failure Mode of CMP Pipe.

(a) (b)

Figure 3.30 SR-HDPE 24 in. Pipe after Testing. (a) Side View. (b) Top View

(a) (b)

Figure 3.31 CMP 24 in. Pipe after Testing. (a) Top View. (b) Side View

As shown in Figure 3.29-31, there are three failure lines for steel reinforced high density polyethylene pipe, while; there is one failure line for the corrugated metal pipe. The close up picture of failure regions of the SR-HDPE pipe, illustrated in Figure 3.32, indicates that the steel ribs have been buckled out of plane due to loss of lateral support from HDPE. For the corrugated metal pipe, the failure line is smooth and the pipe wall has not been buckled in a distinctive manner. Therefore, the supposed failure mode for the CMP pipe is the hoop failure. (Figure 3.31, and 3.33)

(a) (b)

Figure 3.32 Failure Lines of 24 in. SR-HDPE Pipes. (a) Springline. (b) Crown.

Based on the above observations, steel ribs in SR-HDPE transfer the load to the HDPE material which provides the lateral support to the steel ribs. Thus, HDPE material simultaneously with steel ribs resists the total applied load. Since the HDPE is a low modulus material, buckles first and discontinues supporting the steel ribs. Thus, steel ribs buckles. This continuous buckling along the crown and springlines forms these plastic hinges along the longitudinal axis of the pipe.

(a) (b)

Figure 3.33 Failure Lines of 24 in. (a) Springline. (b) Crown

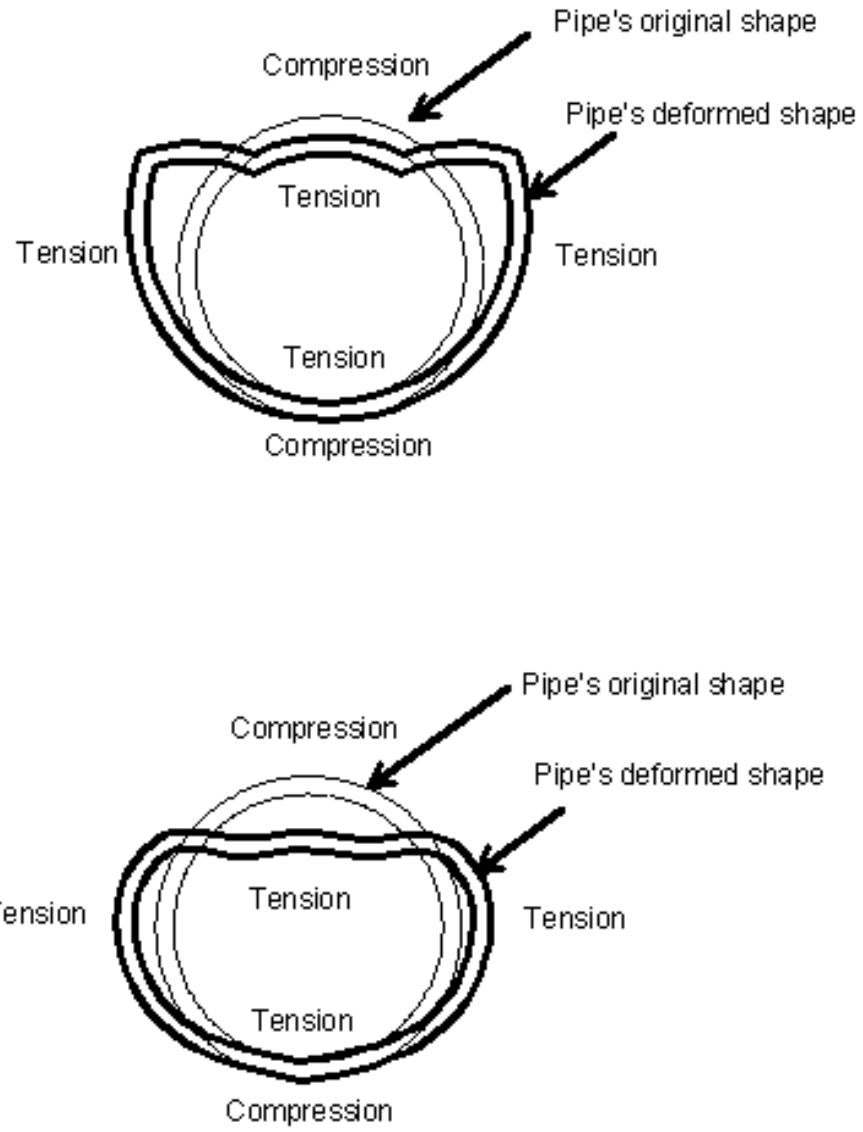

Figure 3.34 Failure Modes of 36 in. (91 cm), and 48 in. (122 cm) Pipes. (a) SR-HDPE Pipe. (b) CMP Pipe.

3.5.2 Failure Modes of 36 in. (91 cm), and 48 in. (122 cm) Pipe

Regardless of having three failure lines (plastic hinges) in 24 in. (61 cm) SR-HDPE pipe, four failure lines have been observed in 36 in. (91 cm) and 48 in. (122 cm) SR-HDPE pipes. Figure 3.34, illustrates the deformed shapes of 36 in. and 48 in. pipes. As perceived from Figure 3.30, the failure mode of CMP pipe is almost the same in all diameters.

(a) (b)

Figure 3.35 Failed 36 in. SR-HDPE Pipe. (a) Top View. (b) Side View.

(a) (b)

Figure 3.36 Failed 36 in. CMP Pipe. (a) Top View. (b) Side View.

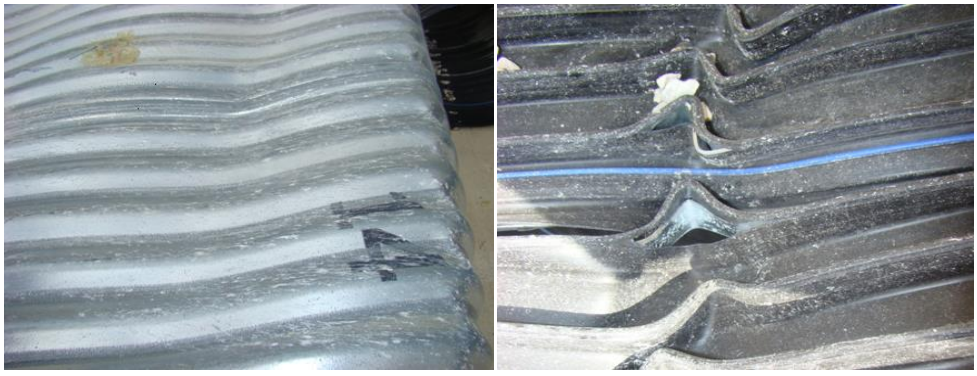

(a) (b)

Figure 3.37 CMP and SR-HDPE Pipes at Failure Lines. (a) CMP Pipe at Crown. (b) SR-HDPE Pipe at Crown

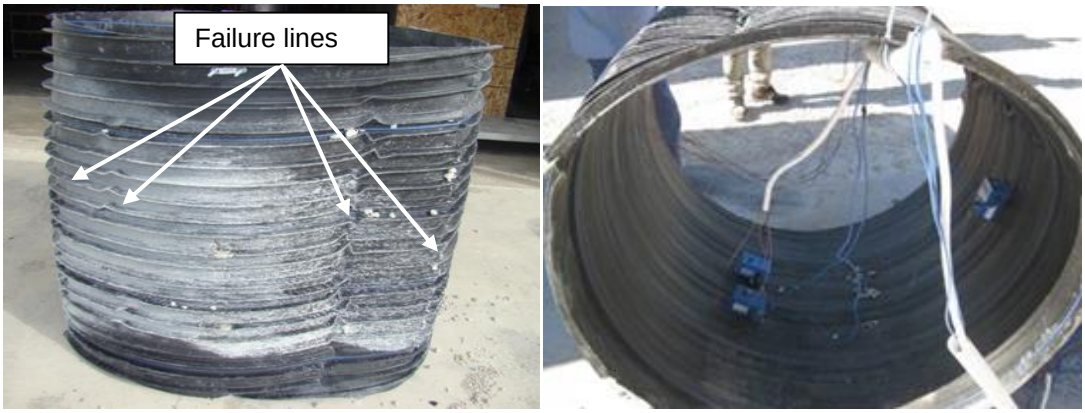

(a) (b)

Figure 3.38 Failed 48 in. SR-HDPE Pipe. (a) Top View. (b) Side View.

As recognized from Figures 3.35-38, the major deformation of the pipe is related to the region restricted between springline and crown, which leads us to the same conclusion which is that the load were carried by the top part of the pipe and after that were transferred to the backfill.

As shown in Figure 3.39 a weak point for SR-HDPE pipe at its joints was recognized. At these points the HDPE part was torn which is not suitable from the serviceability point of view. Also Figure 3.37(b) indicates that steel and HDPE material were separated from each other which are in contradiction with the concept of continuous steel action.

Figure 3.39 Tearing of HDPE Part at Joints

Figure 3.40 SR-HDPE 48 in. (122 cm) Pipe from Inside after Testing.

Figure 3.41 SR-HDPE Tested Pipes (Right: 24 in.(61 cm), Left: 48 in. (122 cm))

The failure lines of the 24 in. and 36 in. SR-HDPE pipes were illustrated in Figure 3.41. Also the failure of the HDPE material was shown in Figure 3.40 which has been taken from inside the failed pipe.

CHAPTER 4

SUMMARY, CONCLUSION, AND RECOMMENDATION

4.1 Summary

Through this study, experimental investigations of the behavior and the failure modes of steel reinforced high density polyethylene (SR-HDPE) pipes subjected to the simulated soil load have been demonstrated. The numerical comparisons between results of the corrugated metal pipe and SR-HDPE pipe in the identical in the same situation have been made. Three sizes of pipes (24 in.(61 m), 36 in. (91 cm), and 48 in. (122 cm)) and two types of backfill including: ASTM C-33 sand and ¾ in. gravel were considered to complete the study. The overall work consisting of the pipes' tests, buried in the soil box under certain applied load, have been studied.

At the beginning of the tests, a pipe specimen was set up in Tensile-Compression Machine (TCM), without any surrounding soil. In this situation test, TCM machine applied compressive point load to the specimens and pipe was fixed at the bottom. The length of specimen was 12 in. (31 cm) with the internal diameter of 24 in. (61 cm). The instruments of the test were consisted of strain gauges and linear variable displacement transducers to measure the strain and pipe's deformation. Due to the twisting of the pipe during the test, the actual capacity of the pipe could not be determined, therefore the other method has been considered for this study.

Thereafter, test installation of the pipe was performed. The concern of pipe's twisting in the previous stage caused to the study of pipes under soil pressure. The pipes were installed in the soil box which was a concrete culvert with the concrete slab at the end. The pipe specimens were equipped with the following instruments: strain gauges, linear variable displacement

transducers, and earth pressure cells. This was done because the test data were recorded during the test in help of data acquisition system. The investigation was made for lateral sides of pipe's crown, as well as the bottom of the pipe and the crown.

According to the real construction, compaction of the bedding, sidefill and the cover of the pipe were applied at 6 in. increment layers of backfill and the compaction of each level was tested with the Nuclear Soil Density Gauge. The pipes were loaded until failure at every two kip (8.9 KN) increments. Experimental test resulted in identifying vertical and horizontal deflections of the pipe, strains, and the failure modes of the pipes. Due to the failing of the pipe, the pipe was reloaded to investigate the failure modes.

The first experimental procedure was using the 24 in. (61 cm) CMP and SR-HDPE pipes with ASTM C-33 backfill. The results obtained from this stage indicate that the failure loads of the pipes are depended on the level of the compaction of the backfill. Thus this method cannot be used to compare the pipe materials. This concern led to the study of pipes with the ¾ in. gavel with no compaction as backfill for the test set up. To insure a constant distributed load on the pipe, load was applied through a rigid slab and to check the uniformity of the load, pressure cells were installed. The applied load steps were controlled by using the Data Acquisition Unit. For each pipe size, the results showed failure load, stress- strain curves, and failure modes corresponding to the load-deformation curves, so that the pipe's behaviors could be continuously investigated.

The minimum cover depth, based on AASHTO specifications, is 12 in. (31 cm) for these two types of pipes regarding to the internal diameter of the pipe. In this study, various cover depth has been applied for different pipe diameter due to the restriction in testing frame's height, and even less cover depths have been used for 36 in. (91 cm) and 48 in. (122 cm) pipes. However, since the main concern of this research was the comparison of SR-HDPE and CMP pipes, and whereas both kinds of pipes were investigated under the same condition, the cover depth factor was neglected.

4.2 Conclusion

The conclusion of this study has been proposed in the following forefront:

- The results of experimental tests and the Load- Deflection diagrams for SR-HDPE and CMP pipes under identical test condition show that the SR-HDPE pipes typically exhibited less stiffness when compared to the CMP pipes.
- In composite structures, all parts of composite structure are assumed to act together to withstand the applied load. In this case, it is assumed that HDPE material and steel ribs act together. However, the results of this study showed that the SR-HDPE buckles earlier than the steel ribs, and does not provide lateral support to the steel ribs. Thus, steel ribs will buckle which form multiple lines of plastic hinges along the pipe longitudinal axis. This study concludes that SR-HDPE does not experience continuous steel action.
- The level of the compaction has more significant effect in the behavior of the SR-HDPE pipe compared to the CMP pipe. The effect of compaction is predominant on the behavior of SR-HDPE pipes.
- CMP and SR-HDPE pipes exhibited different failure modes. The failure of SR-HDPE was governed by out of plane buckling of HDPE in between the steel ribs which caused the steel ribs to lose its lateral support. Consequently, steel ribs experienced lateral buckling. Thus, HDPE fails by out of plane buckling of the steel ribs which formed hinge (crease) along more than one-line. In 24 in. (61 cm) pipe diameter, three failure lines were formed: one of them was along the crown and two between the crown and springline. In 36in. (91 cm) and 48 in. (122 cm) pipe diameters there are four lines which steel ribs have been buckled. All four lines formed between crown and springline. CMP typically fails by continuous hoop type buckling. Also, smooth plastic hinge line was observed in some test specimens which were not similar in nature to those of SR-HDPE.
- CMP exhibited more deflection carrying capacity based on load-deflection plots than SR-HDPE pipes. The AASHTO specification limited this value to five percent of the pipe

diameter. The results indicated that this value for SR-HDPE pipes is closer to the minimum requirement of the AASHTO which needs to be considered in the design procedure.

4.3 Recommendation

Structural behavior and characteristics, as well as mechanical and material properties of CMP and SR-HDPE are shown to be different when subjected to simulated soil load. Thus, more research is required for development of informed design specifications and for strengthening structure, increasing performance, and reducing losses. However the SR-HDPE pipes in the flexible category, which have been shown in this study, but have different behavior in certain area in comparison to CMP pipes, so same specifications cannot be implemented for both.

APPENDIX A

EXPERIMENTAL PIPE TEST RESULTS

A.1 Results of 24 in. Pipe Diameter

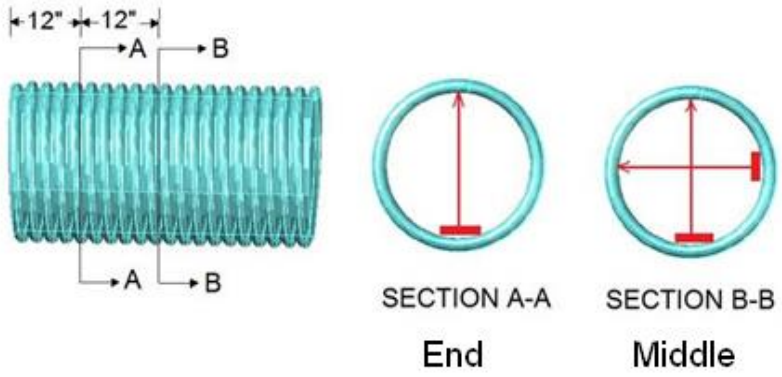

Figure A.1 Location of Displacement Transducer Sensors

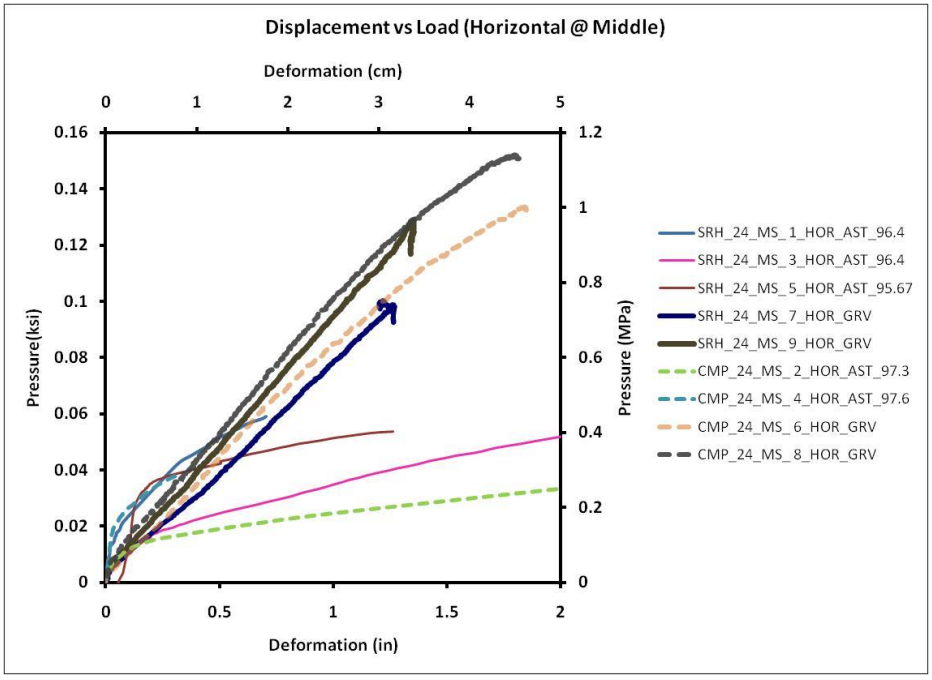

Figure A.2 Pressure vs. Horizontal Deformation at the Middle Section of the 24 in. Pipe.

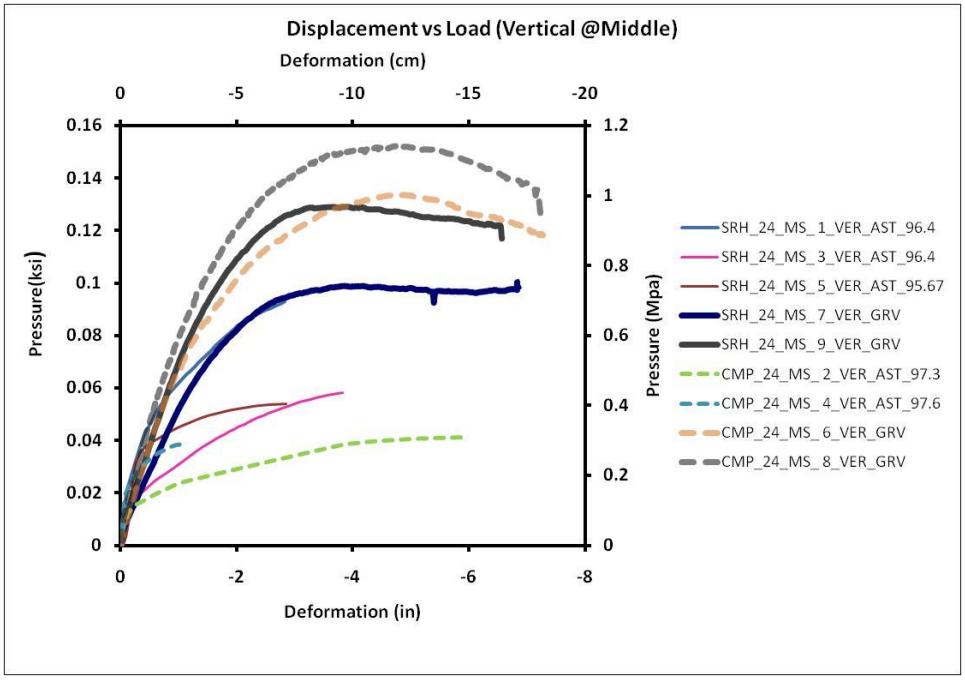

Figure A.3 Pressure vs. Vertical Deformation at the Middle Section of the 24 in. Pipe.

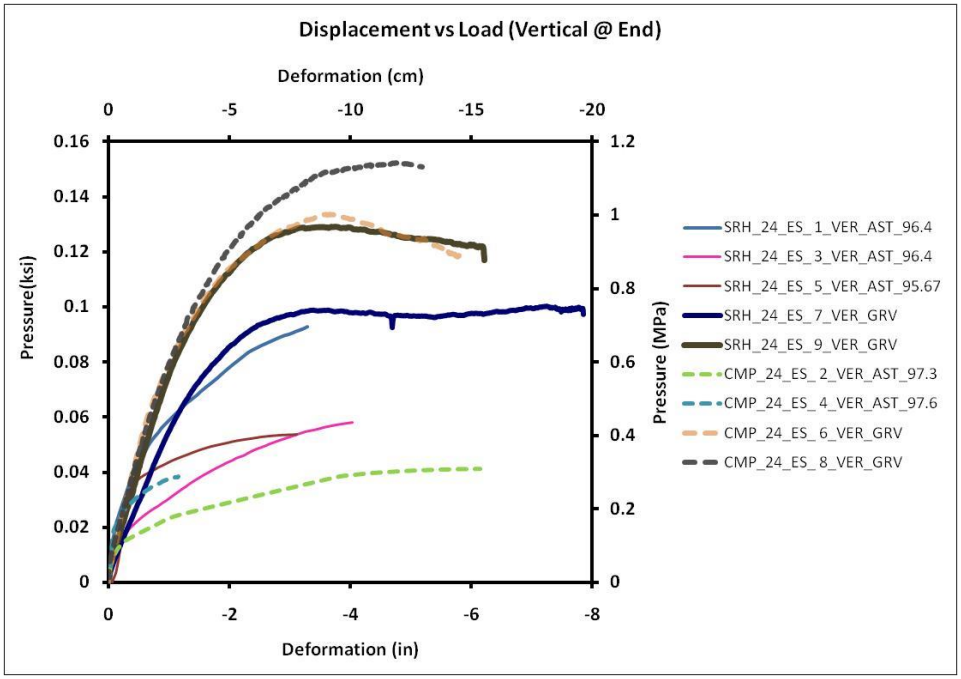

Figure A.4 Pressure vs. Vertical Deformation at the End Section of the 24 in. Pipe.

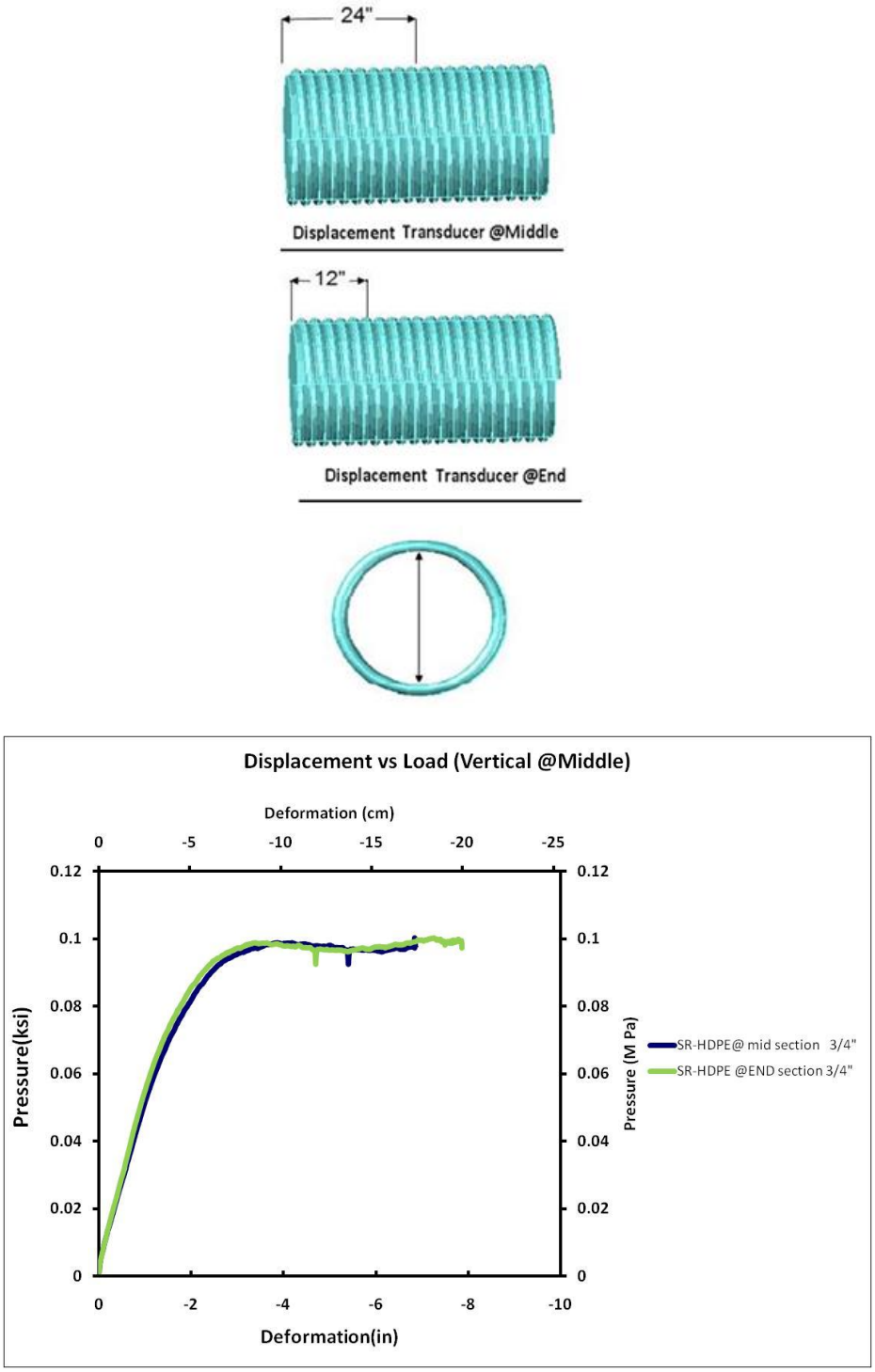

Figure A.5 Comparison of Pressure vs. Vertical Deformation at the Middle and End Sections of the 24 in. Pipe.

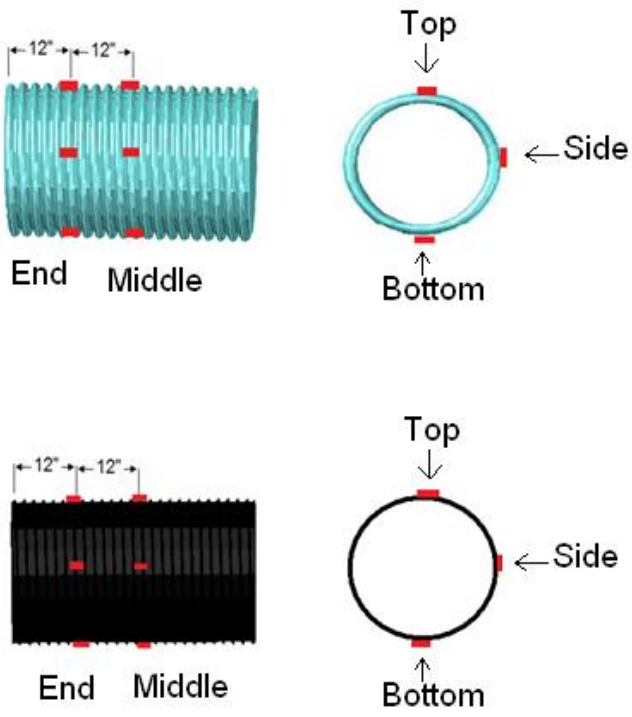

(a)

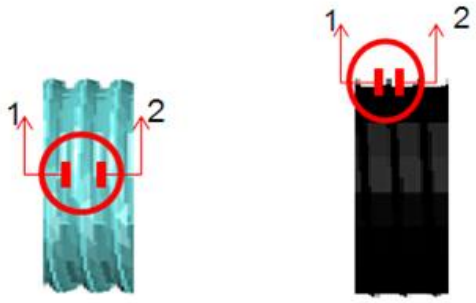

(b)

Figure A.6 Strain gauges location. (a) Position on the pipe. (b) Position in the rib.

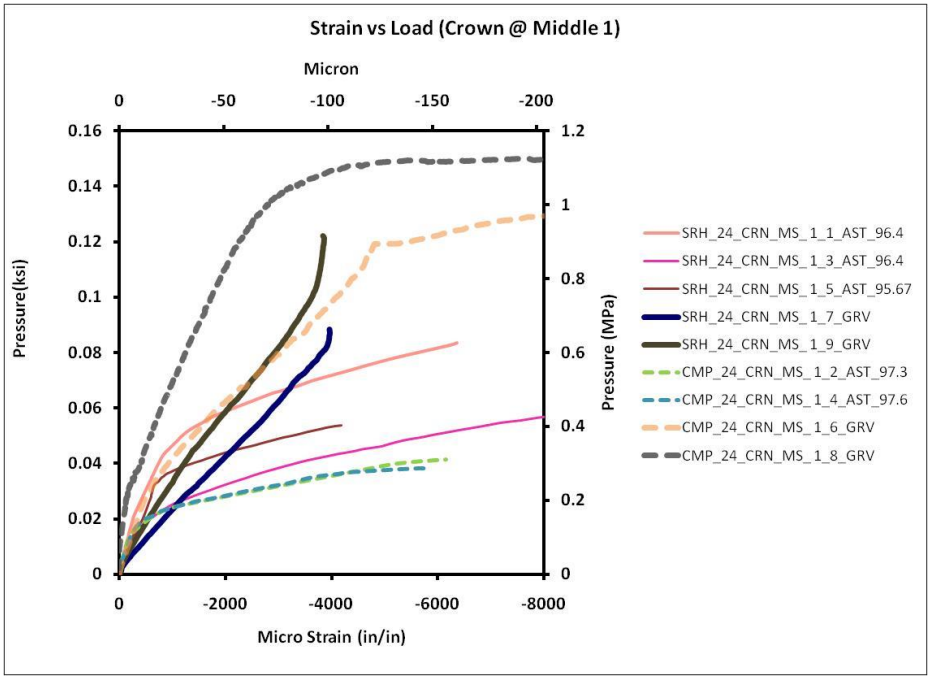

Figure A.7 Pressure vs. Strain at the Crown-Middle Section of the 24 in. Pipe Position 1.

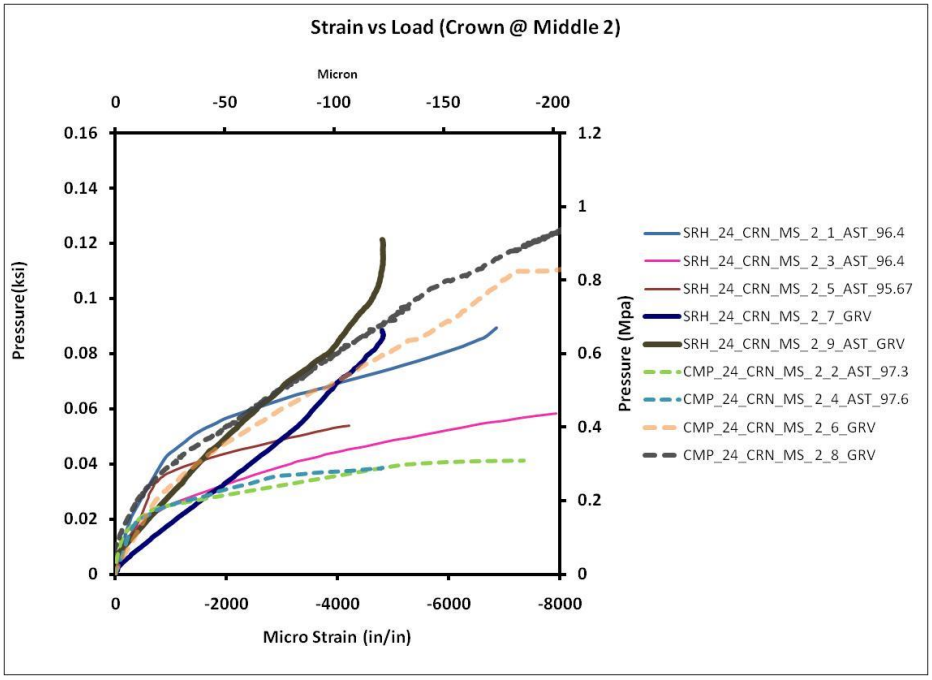

Figure A.8 Pressure vs. Strain at the Crown-Middle Section of the 24 in. Pipe Position 2.

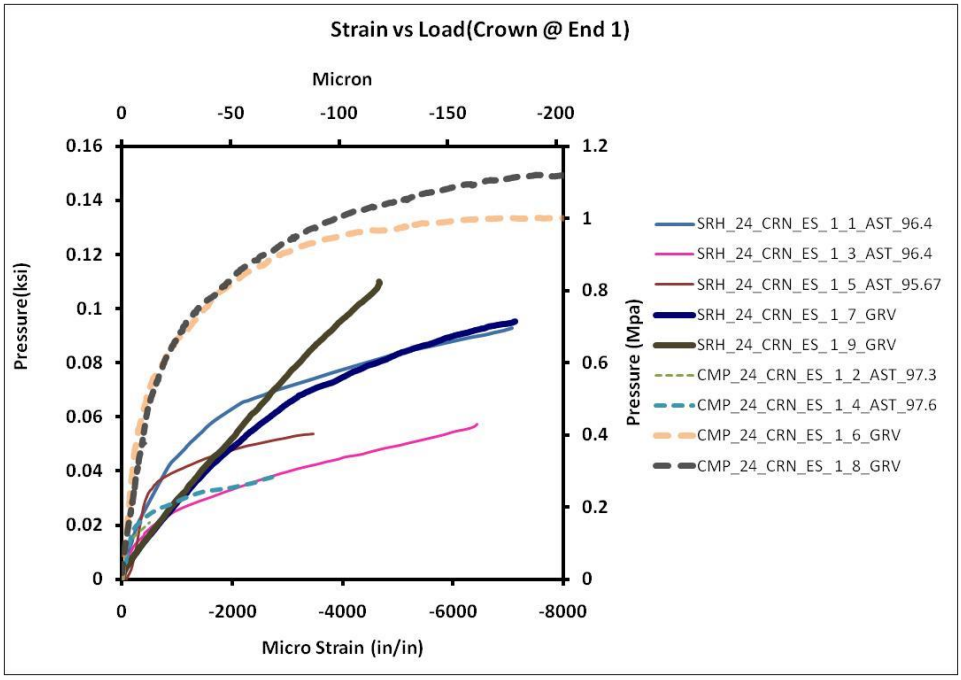

Figure A.9 Pressure vs. Strain at the Crown-End Section of the 24 in. Pipe Position 1.

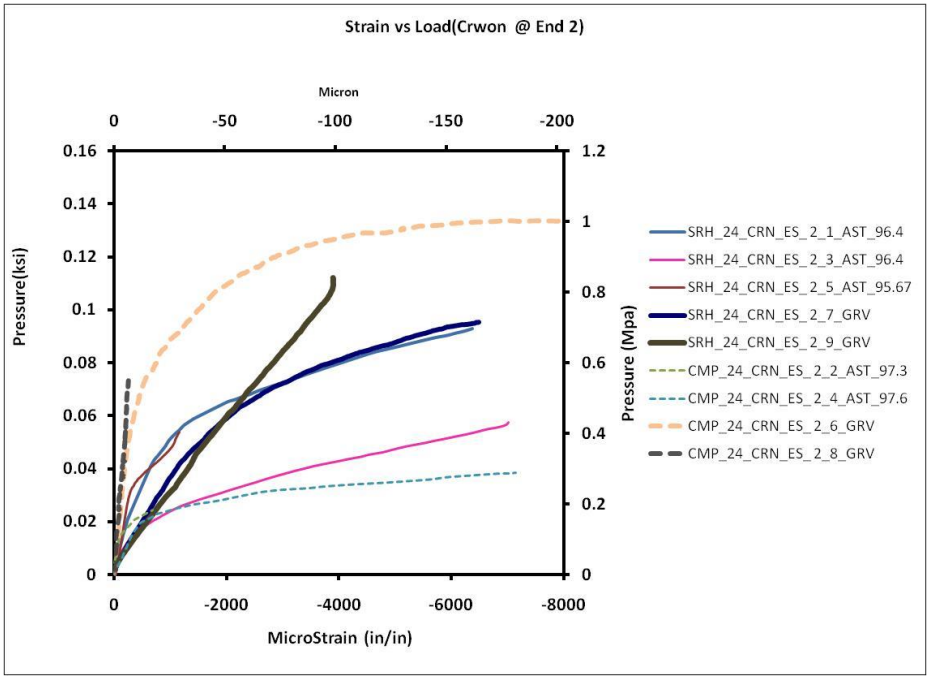

Figure A.10 Pressure vs. Strain at the Crown-End Section of the 24 in. Pipe Position 2.

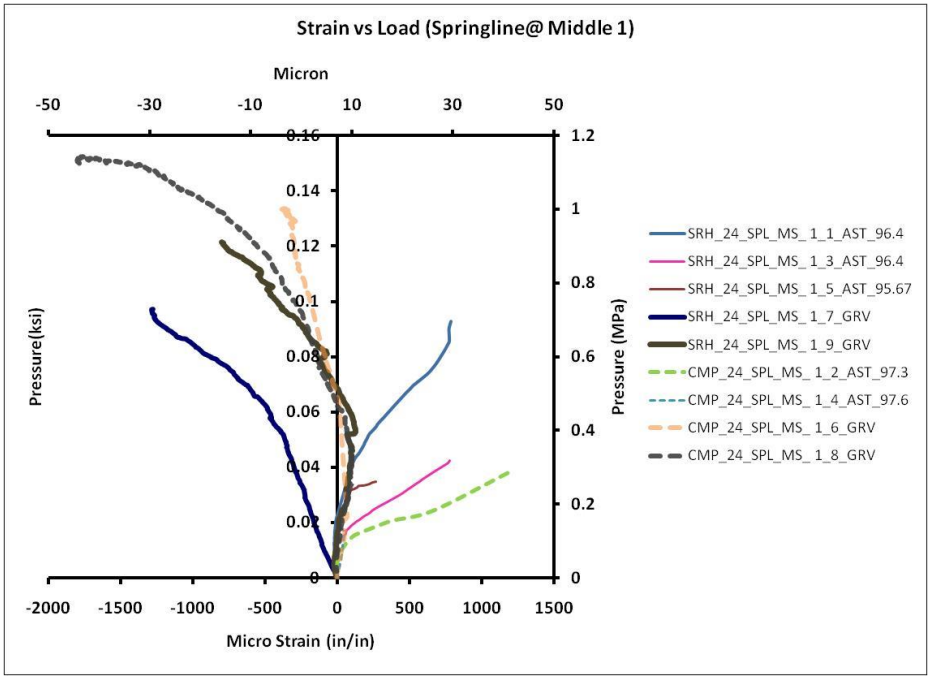

Figure A.11 Pressure vs. Strain at the Springline-Middle Section of the 24 in. Pipe Position 1.

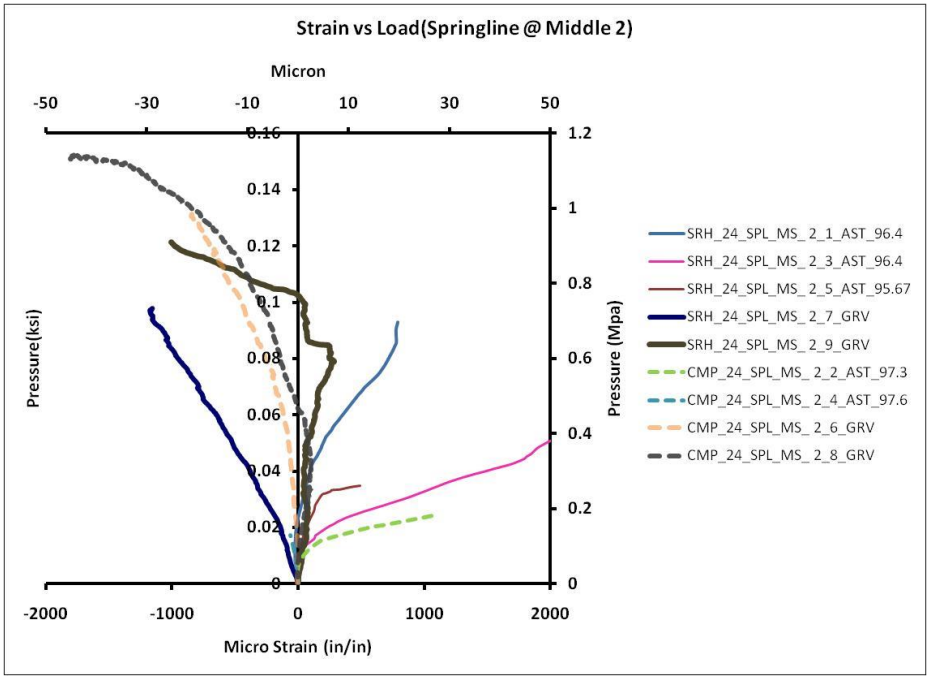

Figure A.12 Pressure vs. Strain at the Springline-Middle Section of the 24 in. Pipe Position 2.

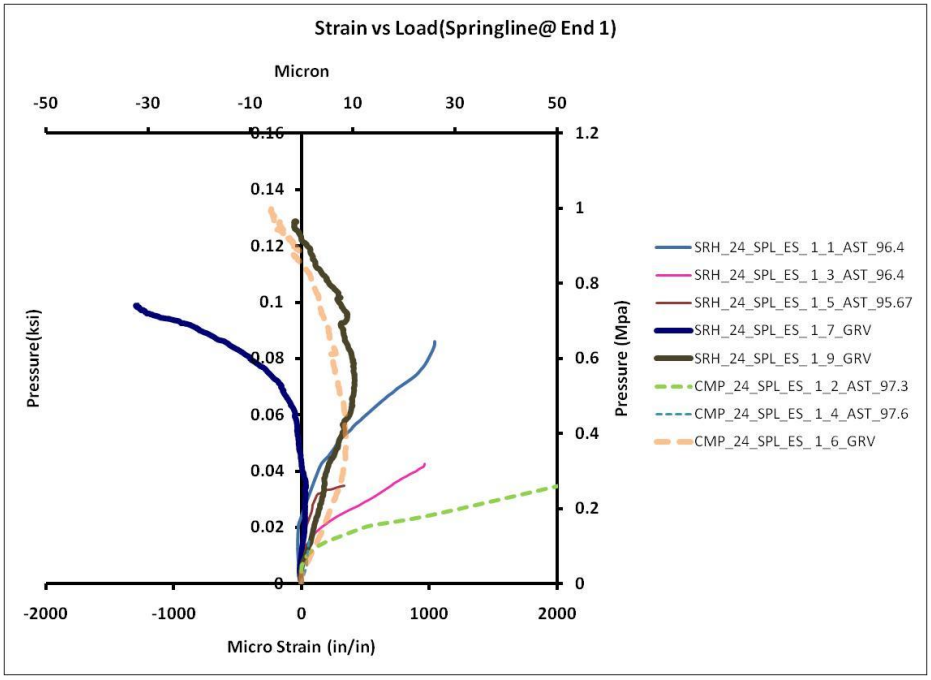

Figure A.13 Pressure vs. Strain at the Springline-End Section of the 24 in. Pipe Position 1.

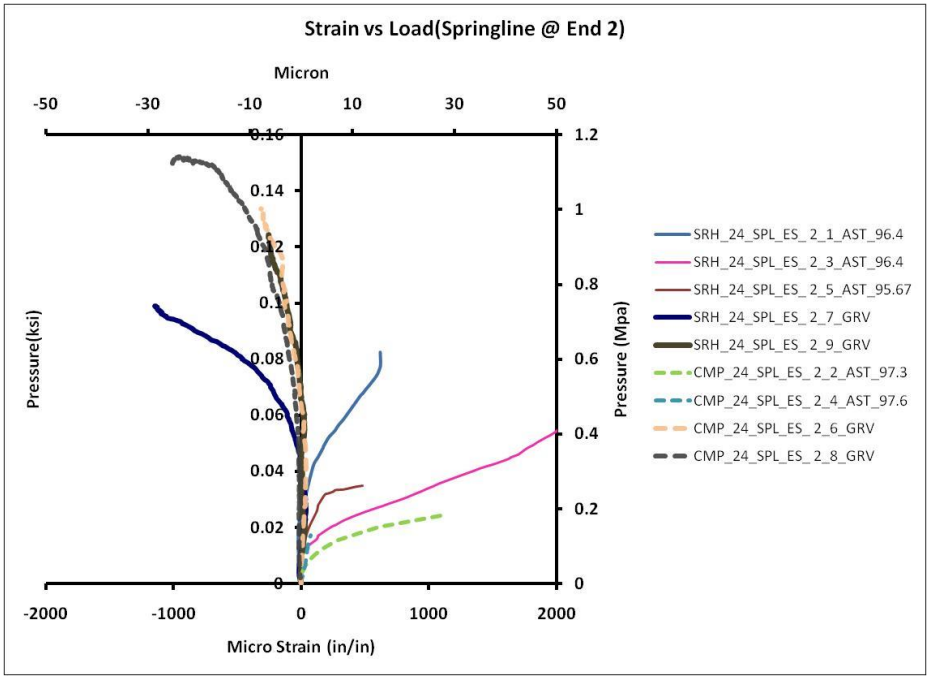

Figure A.14 Pressure vs. Strain at the Springline-End Section of the 24 in. Pipe Position 2.

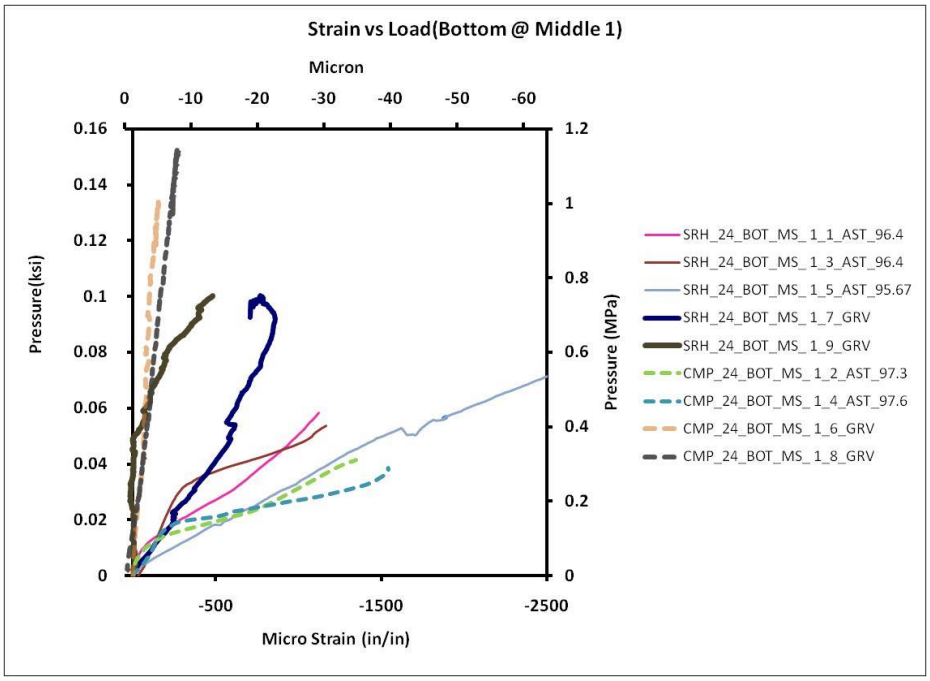

Figure A.15 Pressure vs. Strain at the Bottom-Middle of the 24 in. Pipe Position 1.

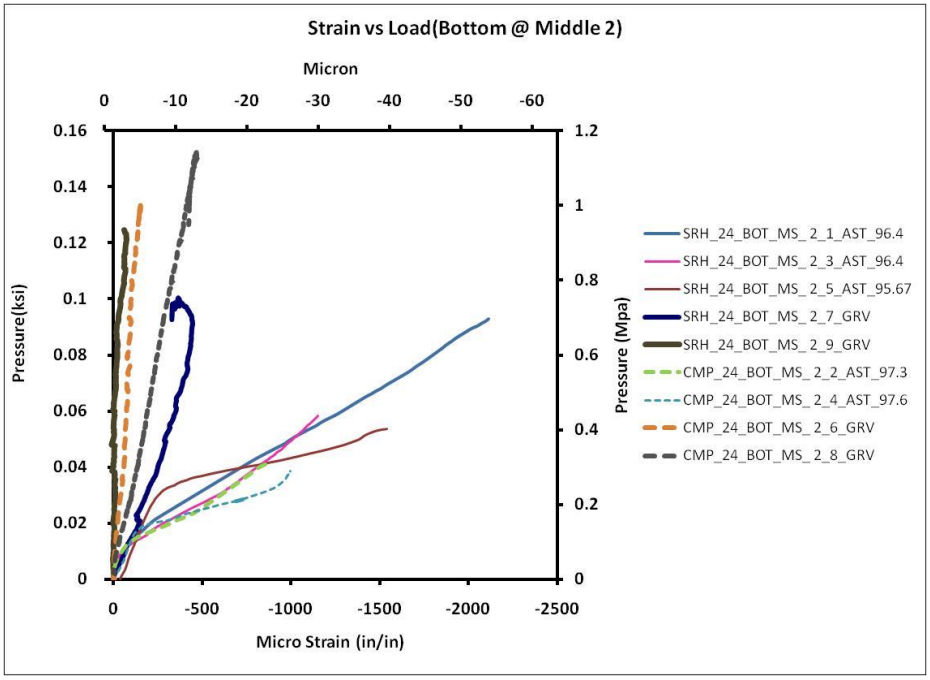

Figure A.16 Pressure vs. Strain at the Bottom-Middle Section of the 24 in. Pipe Position 2.

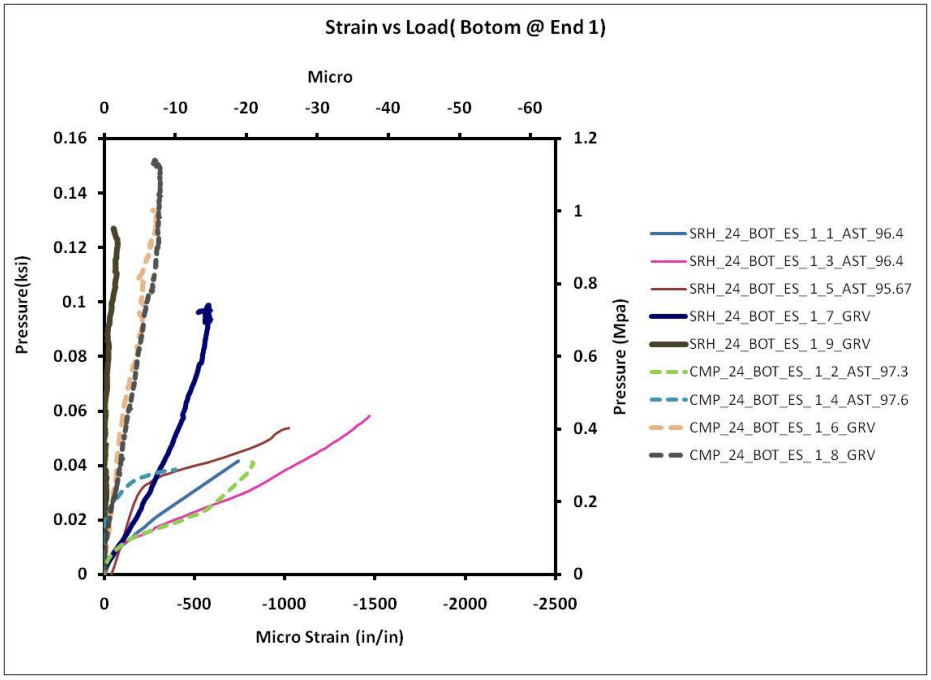

Figure A.17 Pressure vs. Strain at the Bottom-End Section of the 24 in. Pipe Position 1.

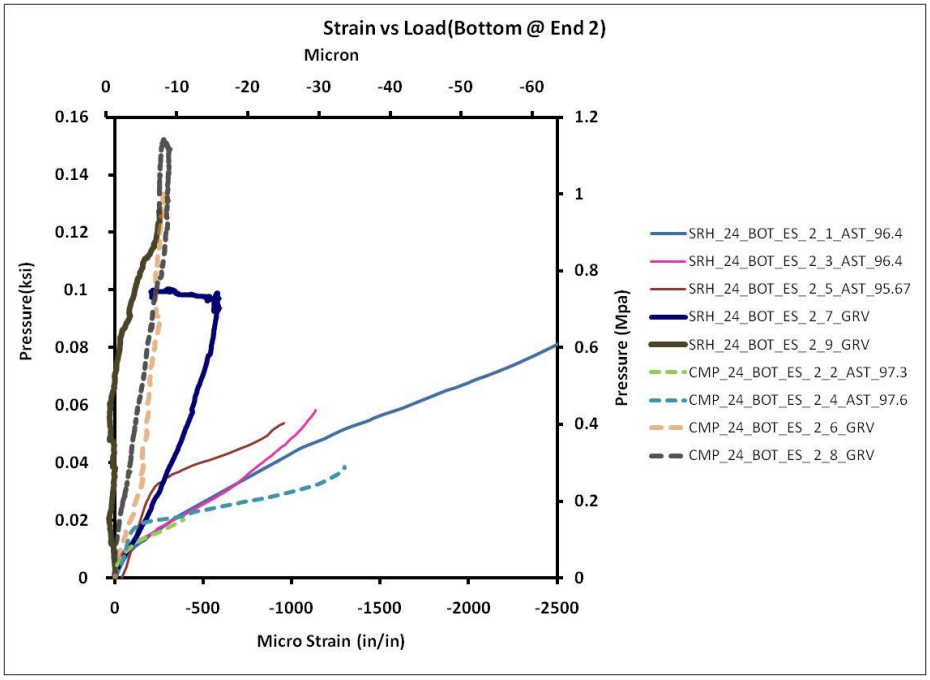

Figure A.18 Pressure vs. Strain at the Bottom-End Section of the 24 in. Pipe Position 2.

A Results of 36 in. Pipe Diameter

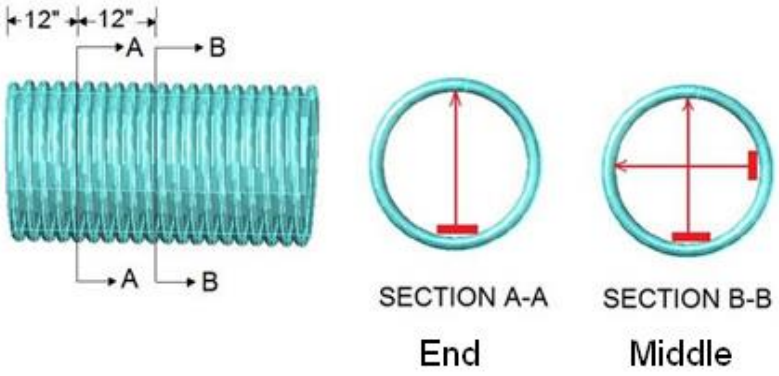

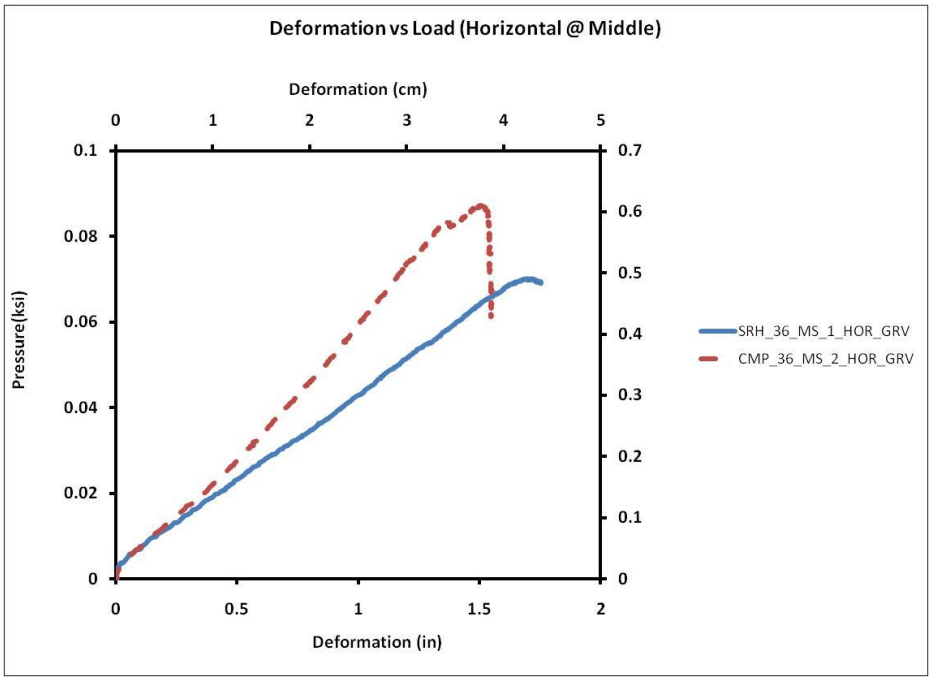

Figure A.19 Pressure vs. Horizontal Deformation at the Middle Section of the 36 in. Pipe.

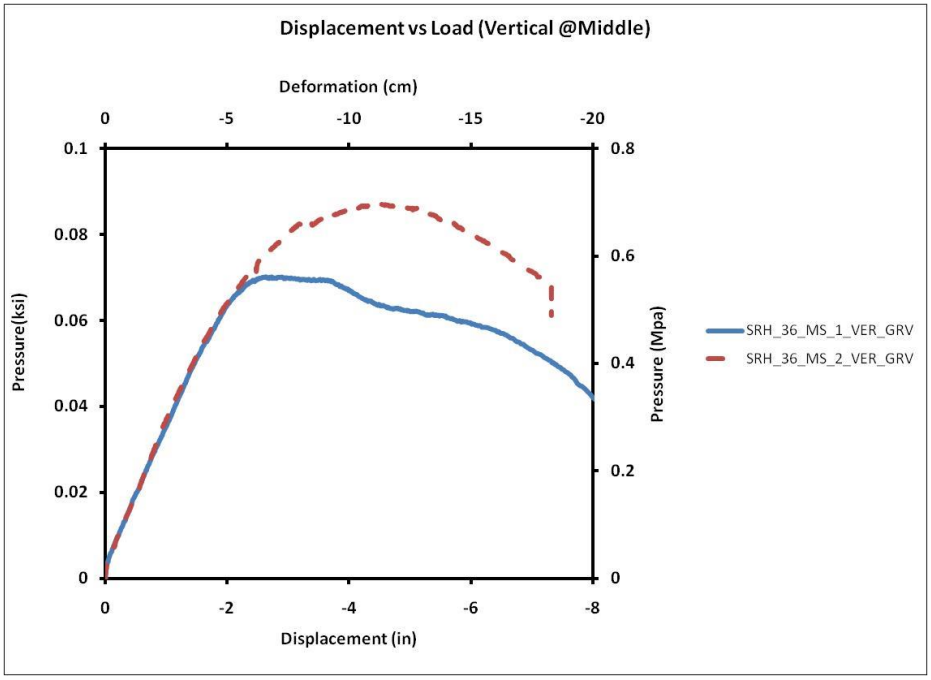

Figure A.20 Pressure vs. Vertical Deformation at the Middle Section of the 36 in. Pipe.

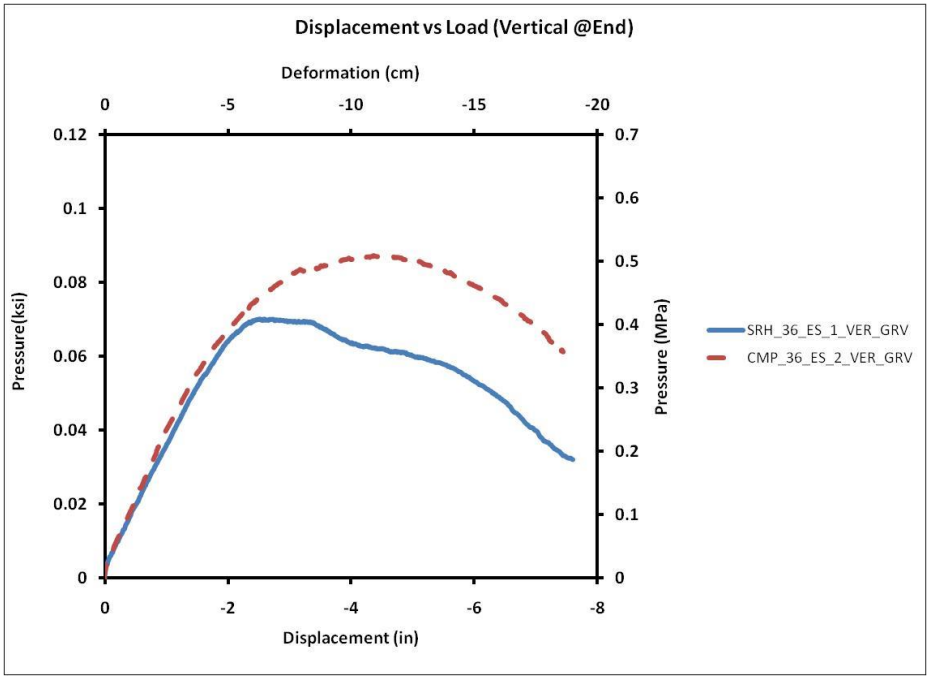

Figure A.21 Pressure vs. Vertical Deformation at the End Section of the 36 in. Pipe.

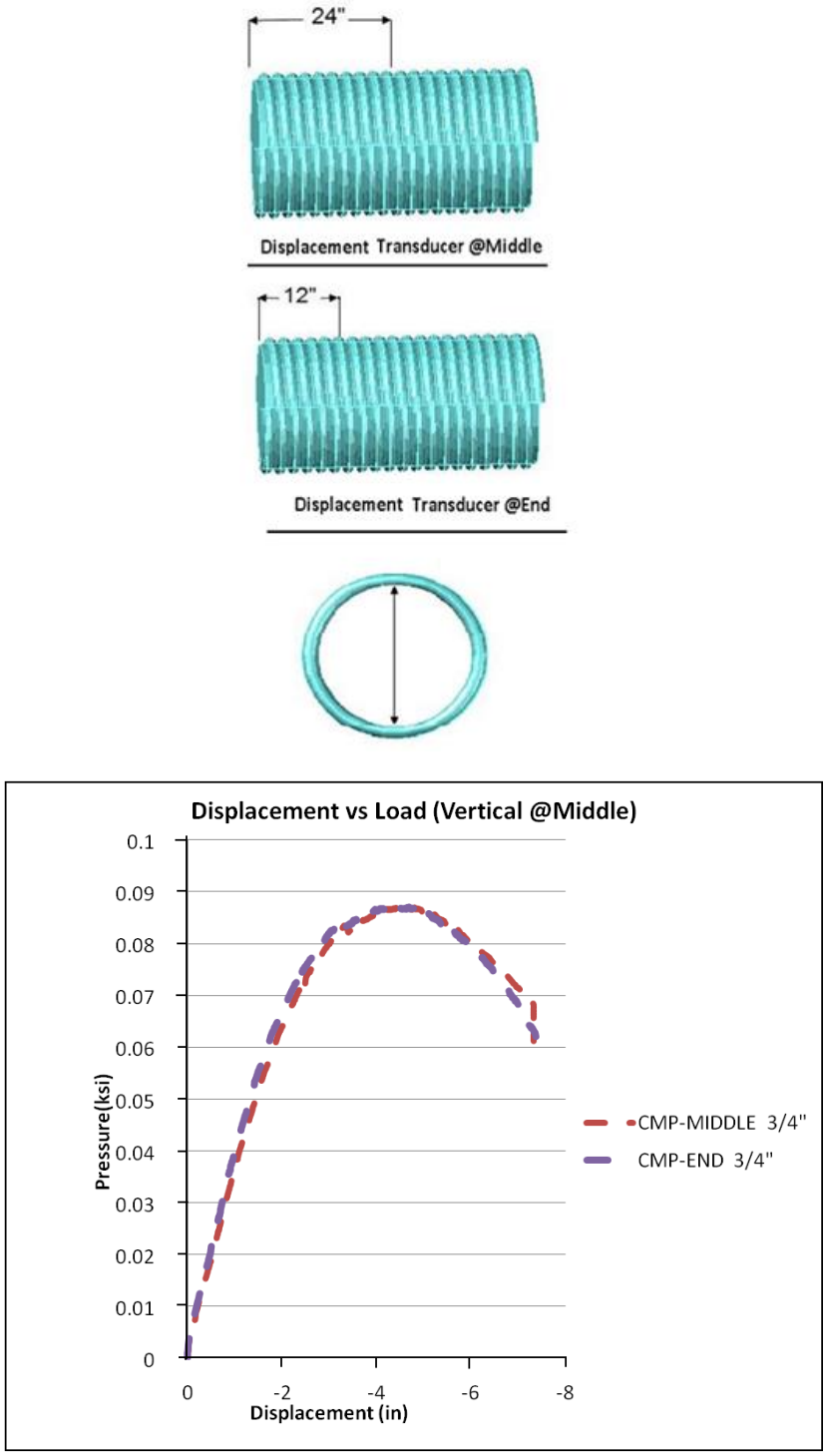

Figure A.22 Comparison of Pressure vs. Vertical Deformation at the Middle and End Sections of the 36 in. Pipe.

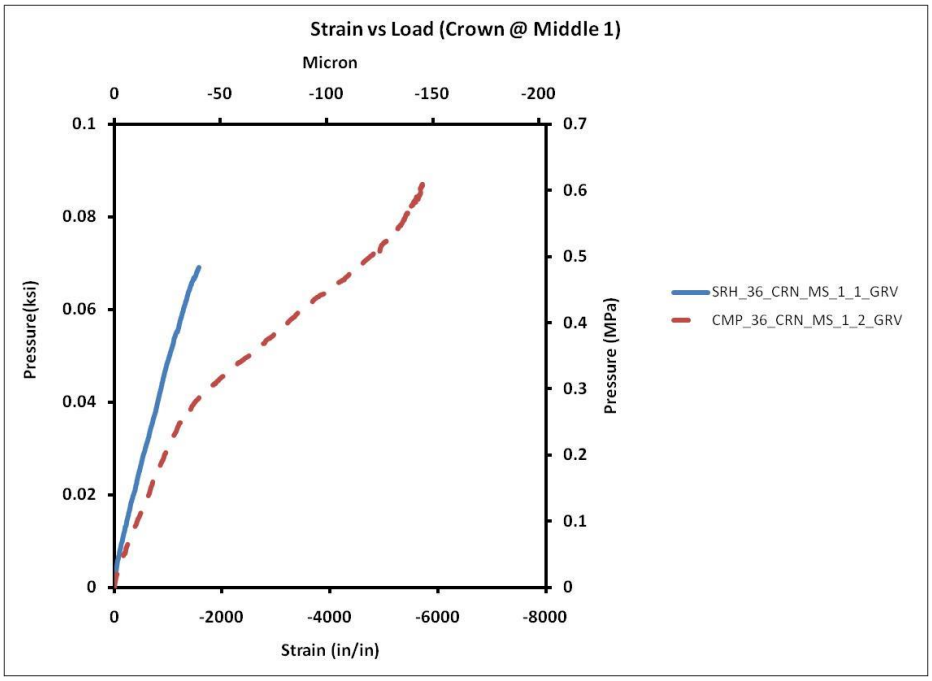

Figure A.23 Pressure vs. Strain at the Crown-Middle Section of the 36 in. Pipe Position 1.

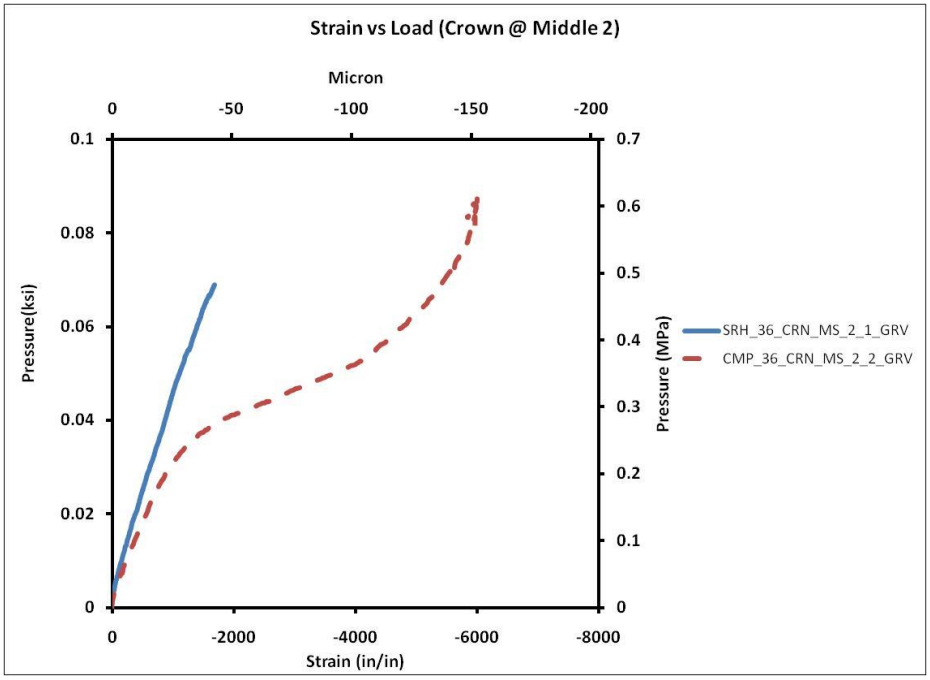

Figure A.24 Pressure vs. Strain at the Crown-Middle Section of the 36 in. Pipe Position 2.

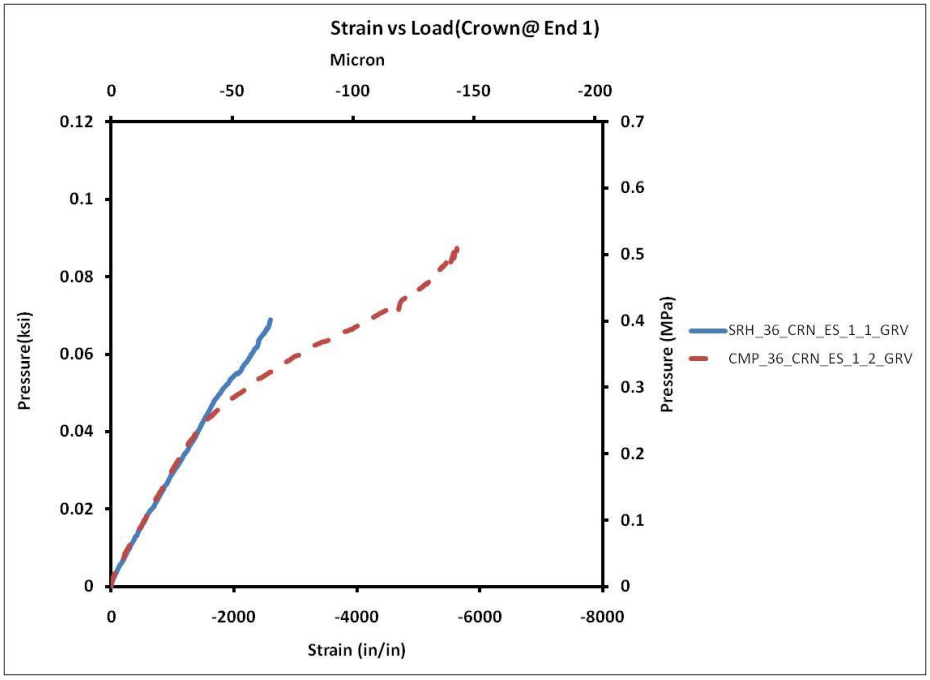

Figure A.25 Pressure vs. Strain at the Crown-End Section of the 36 in. Pipe Position 1.

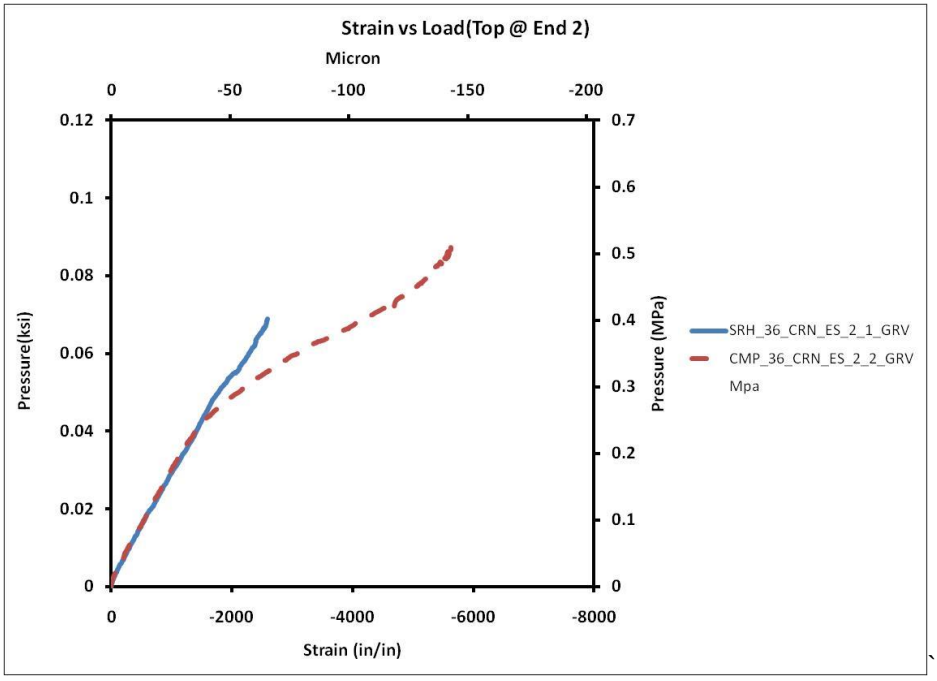

Figure A.26 Pressure vs. Strain at the Crown-End Section of the 36 in. Pipe Position 2.

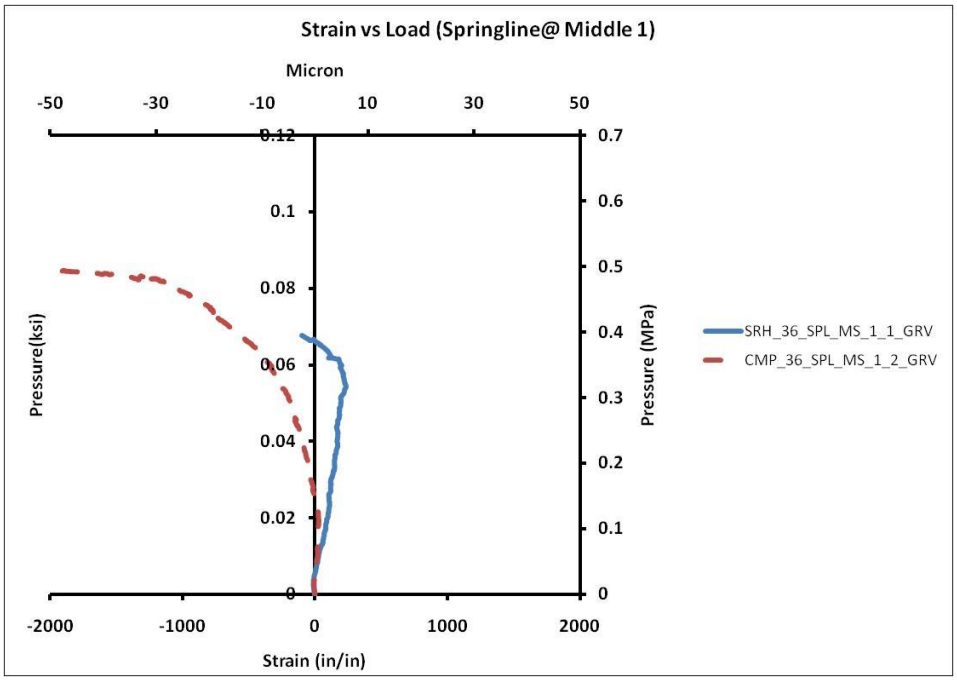

Figure A.27 Pressure vs. Strain at the Springline-Middle Section of the 36 in. Pipe Position 1.

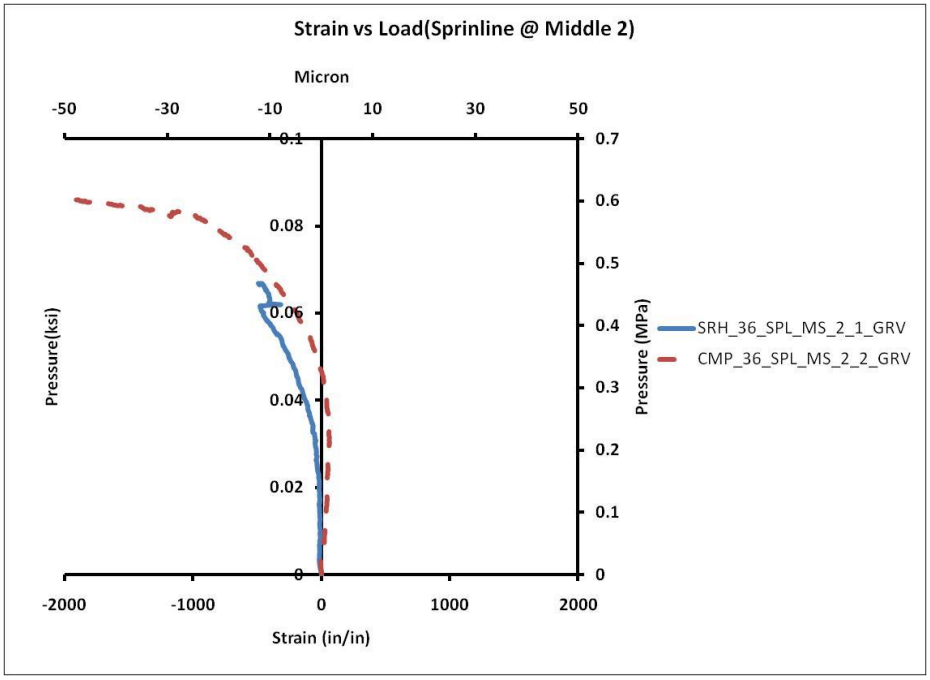

Figure A.28 Pressure vs. Strain at the Springline-Middle Section of the 36 in. Pipe Position 2.

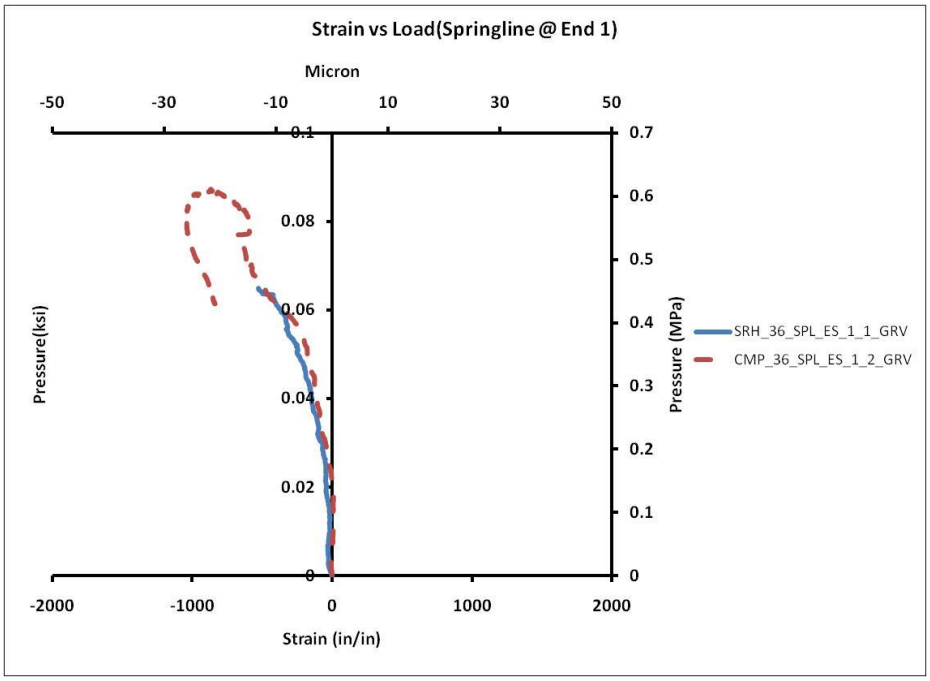

Figure A.29 Pressure vs. Strain at the Springline-End Section of the 36 in. Pipe Position 1.

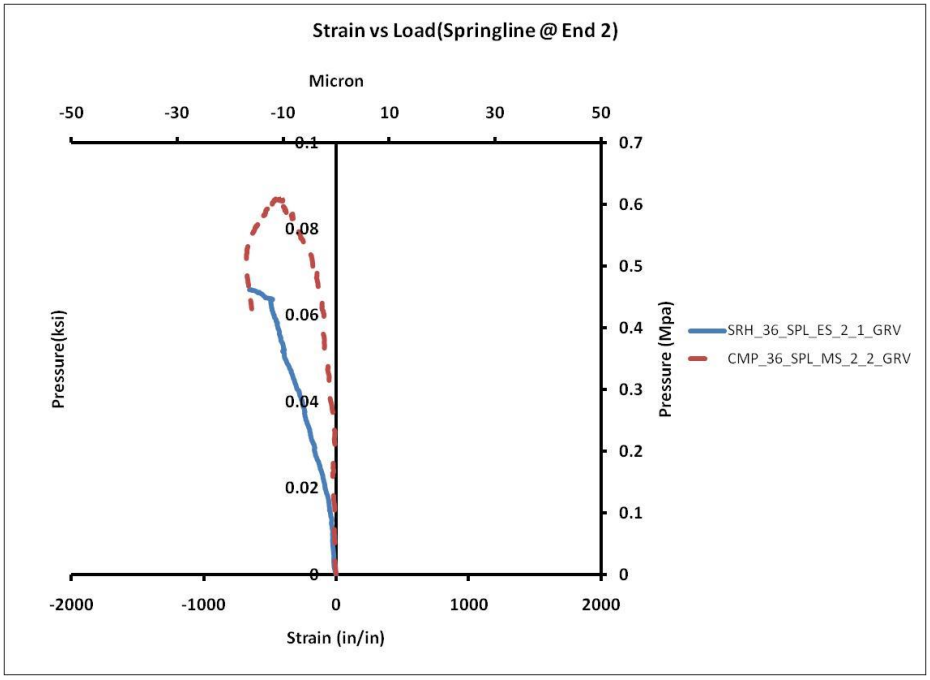

Figure A.30 Pressure vs. Strain at the Springline-End Section of the 36 in. Pipe Position 2.

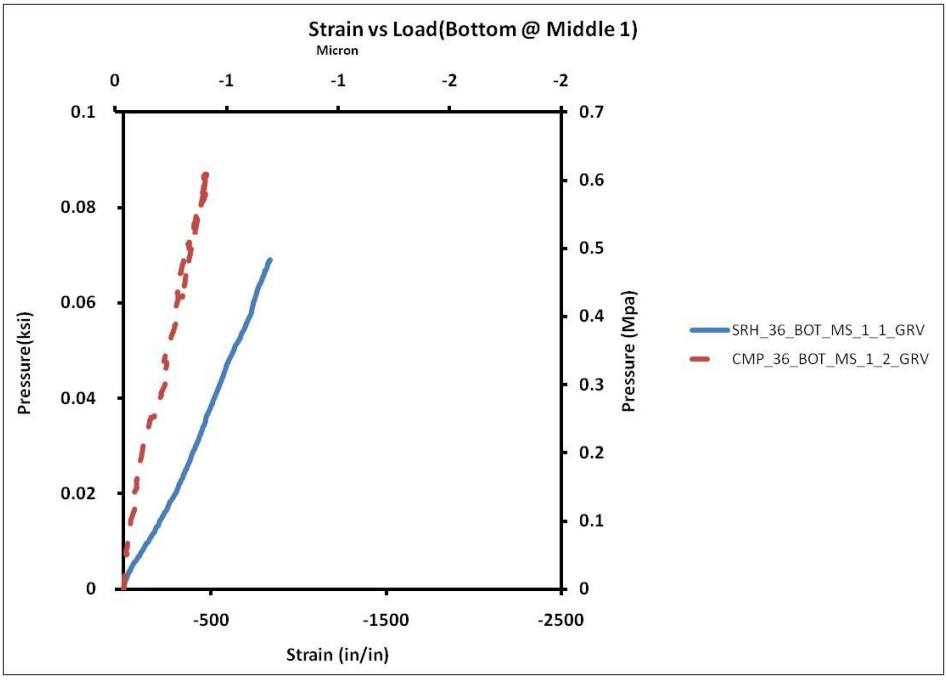

Figure A.31 Pressure vs. Strain at the Bottom-Middle Section of the 36 in. Pipe Position 1.

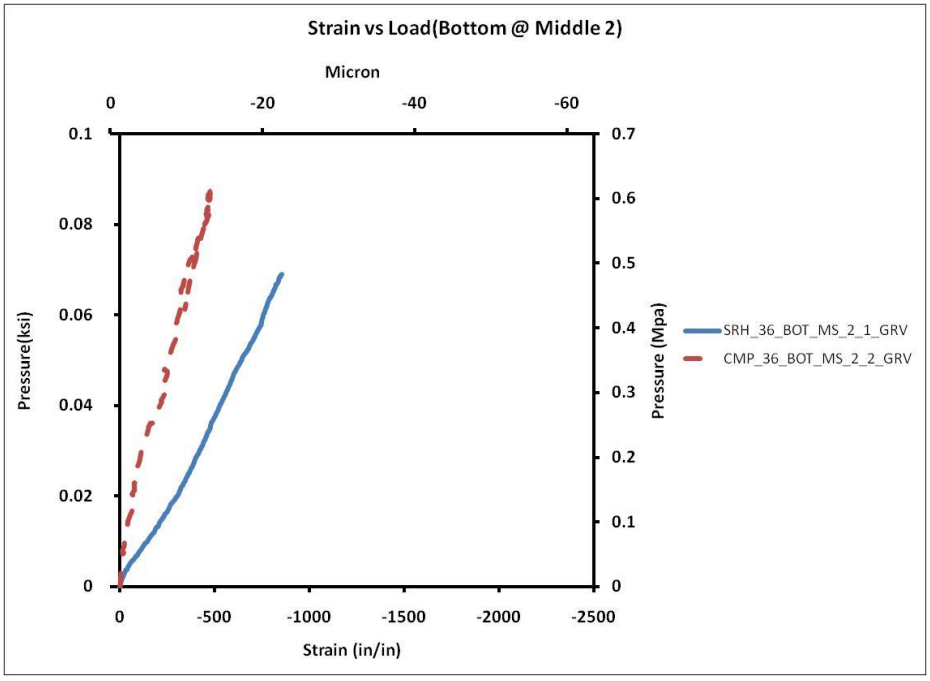

Figure A.32 Pressure vs. Strain at the Bottom-Middle Section of the 36 in. Pipe Position 2.

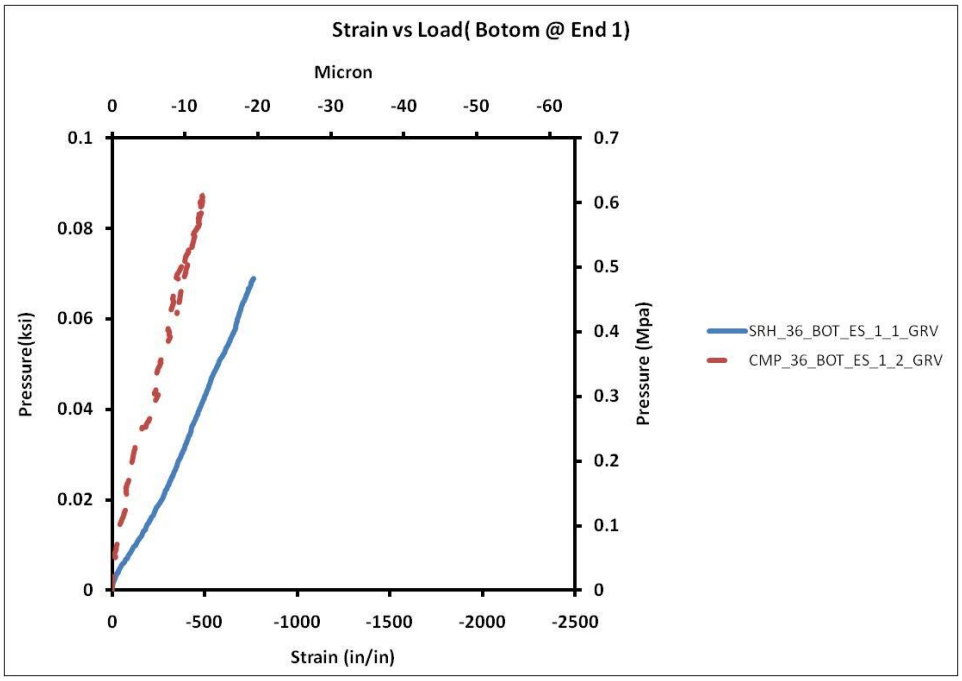

Figure A.33 Pressure vs. Strain at the Bottom-End Section of the 36 in. Pipe Position 1.

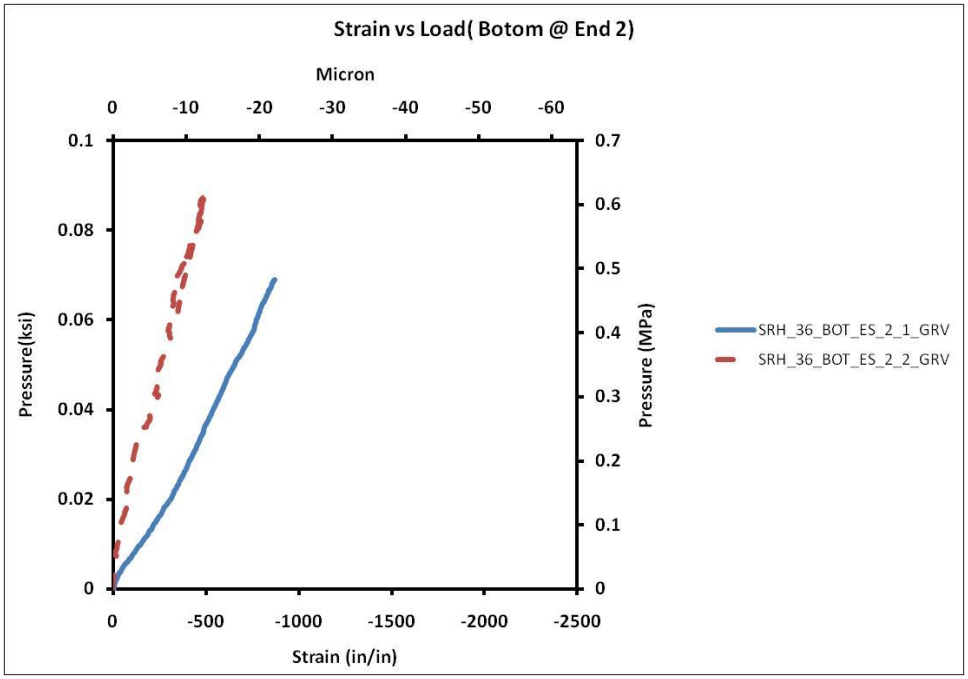

Figure A.34 Pressure vs. Strain at the Bottom-End Section of the 36 in. Pipe Position 2.

A.3 Results of 48 in. Pipe Diameter

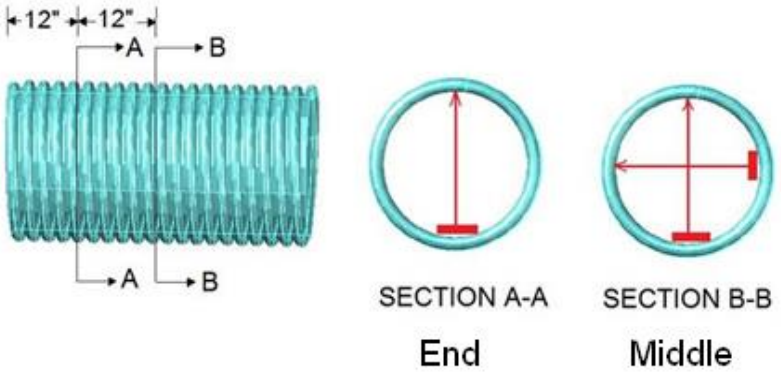

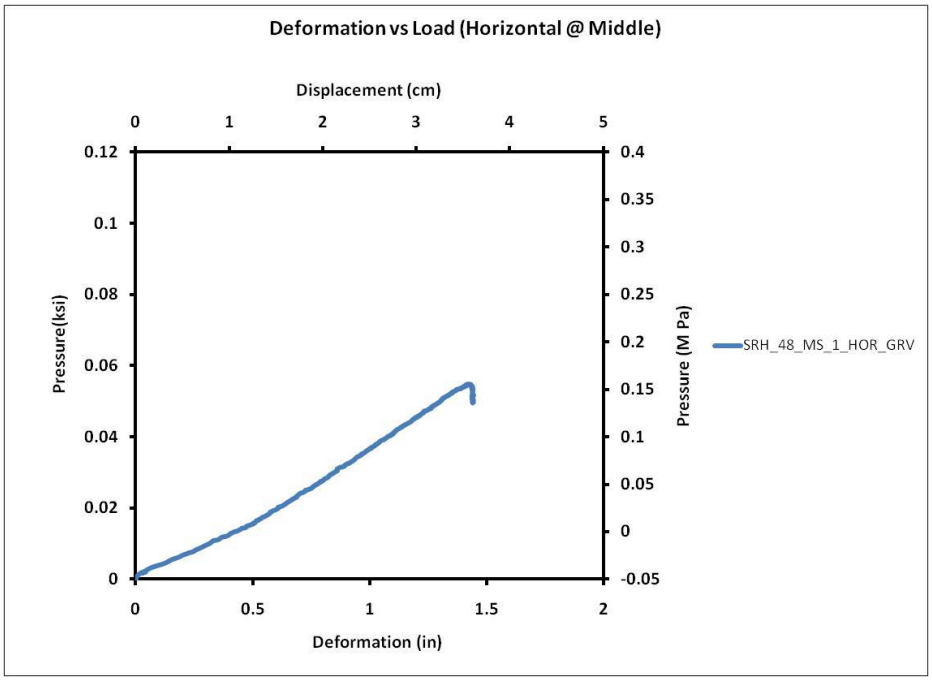

Figure A.35 Pressure vs. Horizontal Deformation at the Middle Section of the 48 in. Pipe.

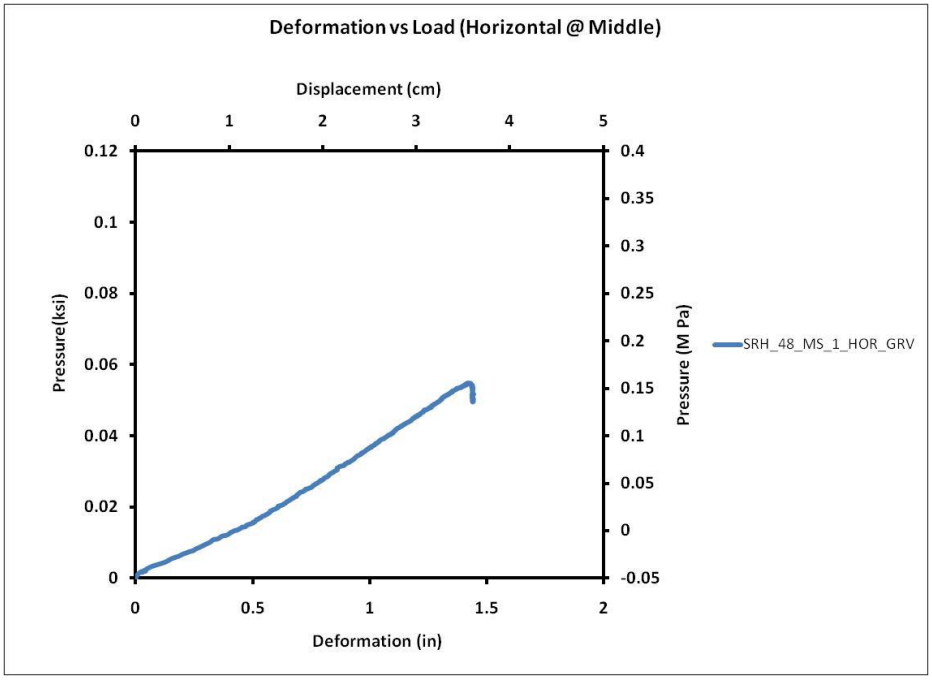

Figure A.36 Pressure vs. Vertical Deformation at the Middle Section of the 48 in. Pipe.

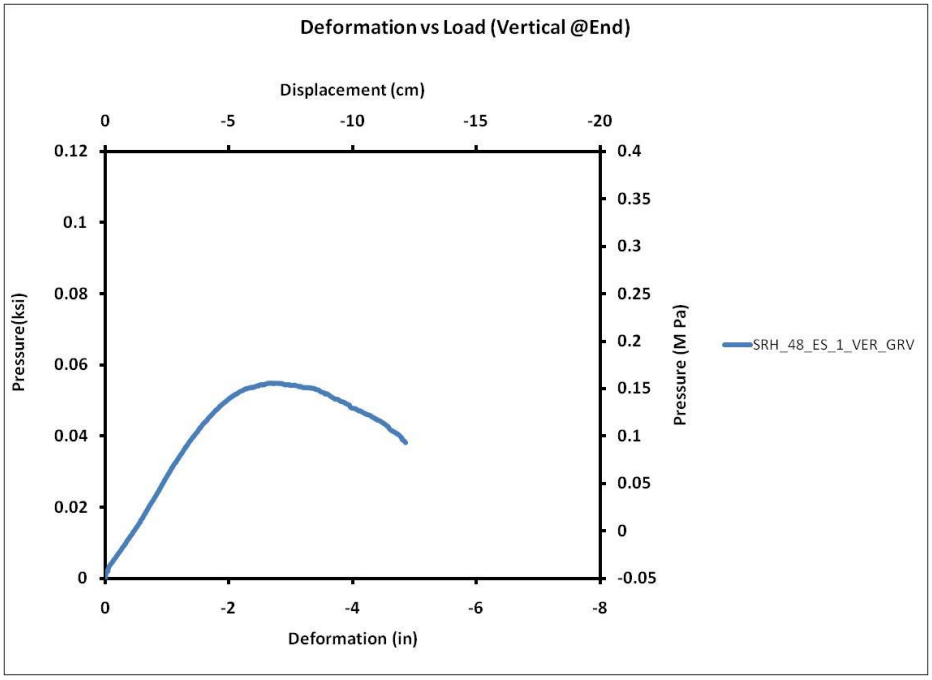

Figure A.37 Pressure vs. Vertical Deformation at the End Section of the 48 in. Pipe.

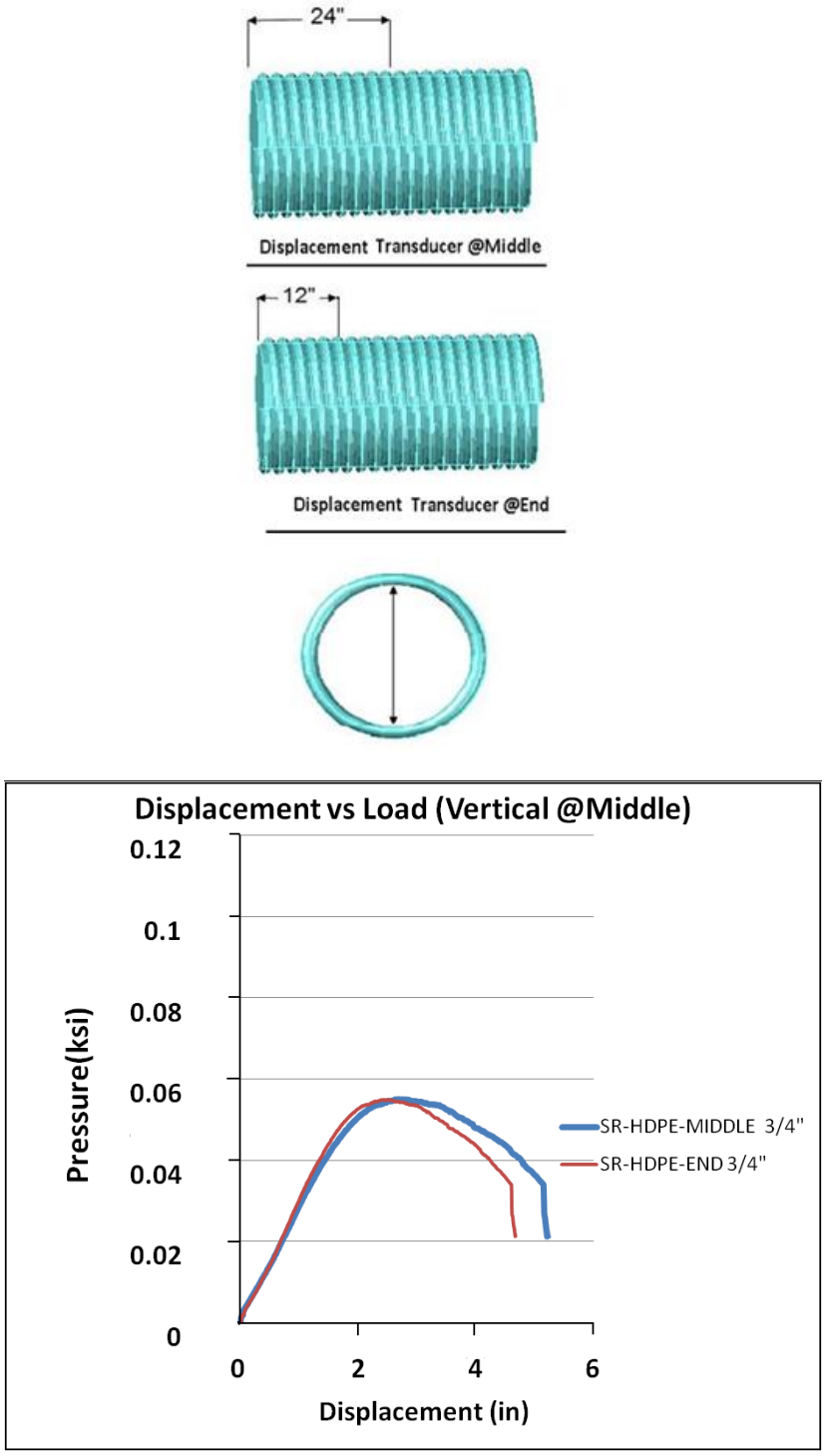

Figure A.38 Pressure vs. Vertical Deformation at the Middle Section of the Pipe.

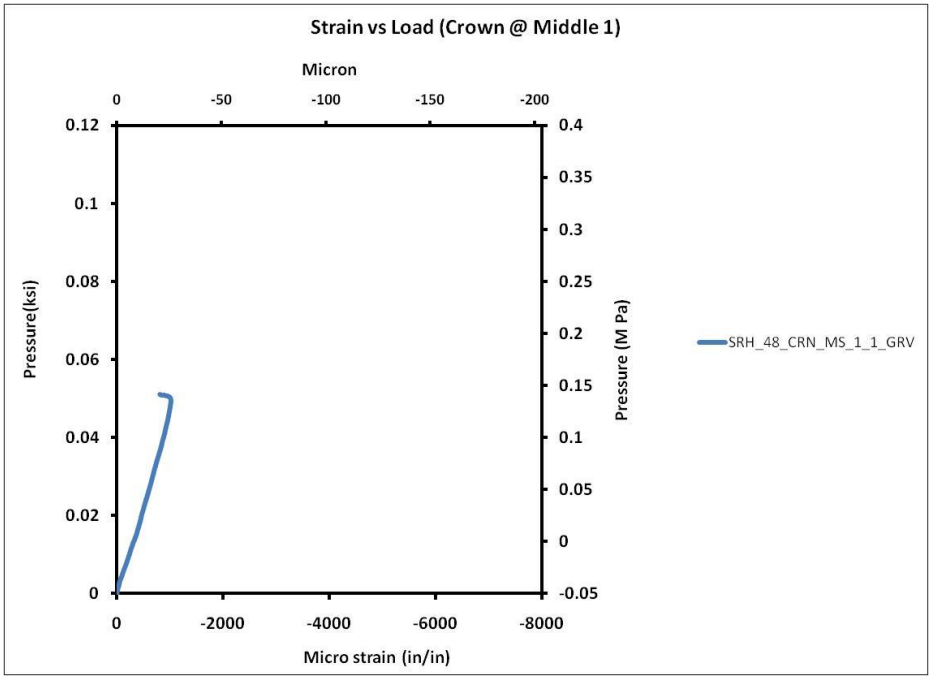

Figure A.39 Pressure vs. Vertical Deformation at the Middle Section of the Pipe.

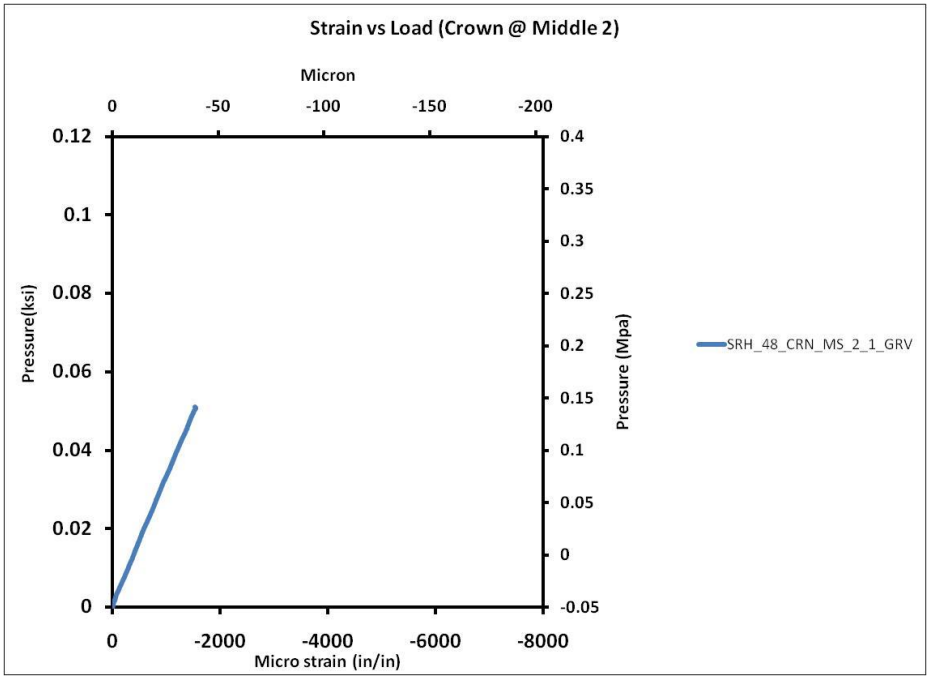

Figure A.40 Pressure vs. Vertical Deformation at the Middle Section of the Pipe.

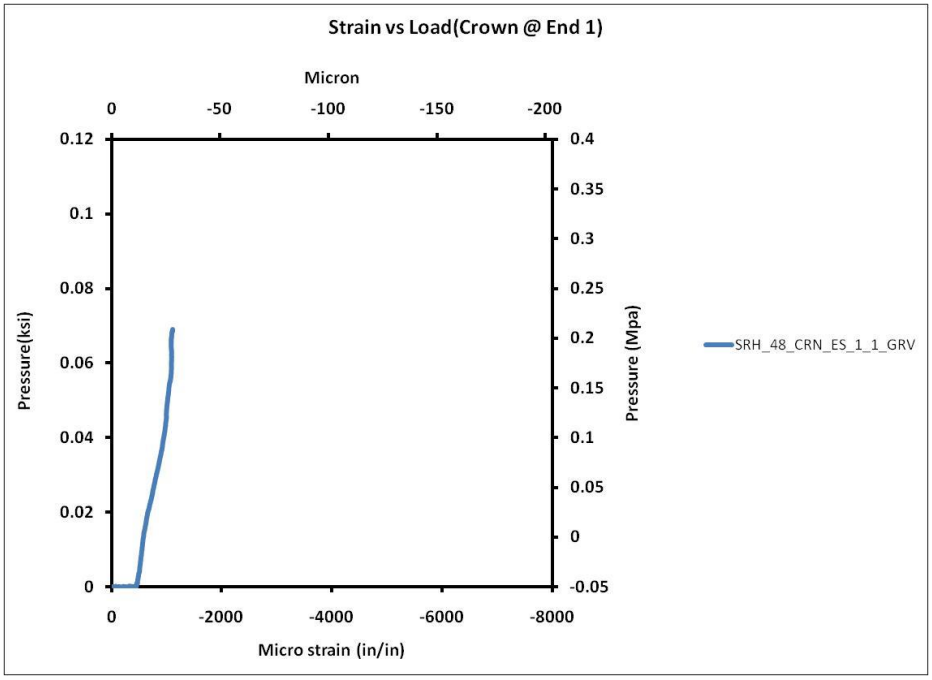

Figure A.41 Pressure vs. Vertical Deformation at the Middle Section of the Pipe.

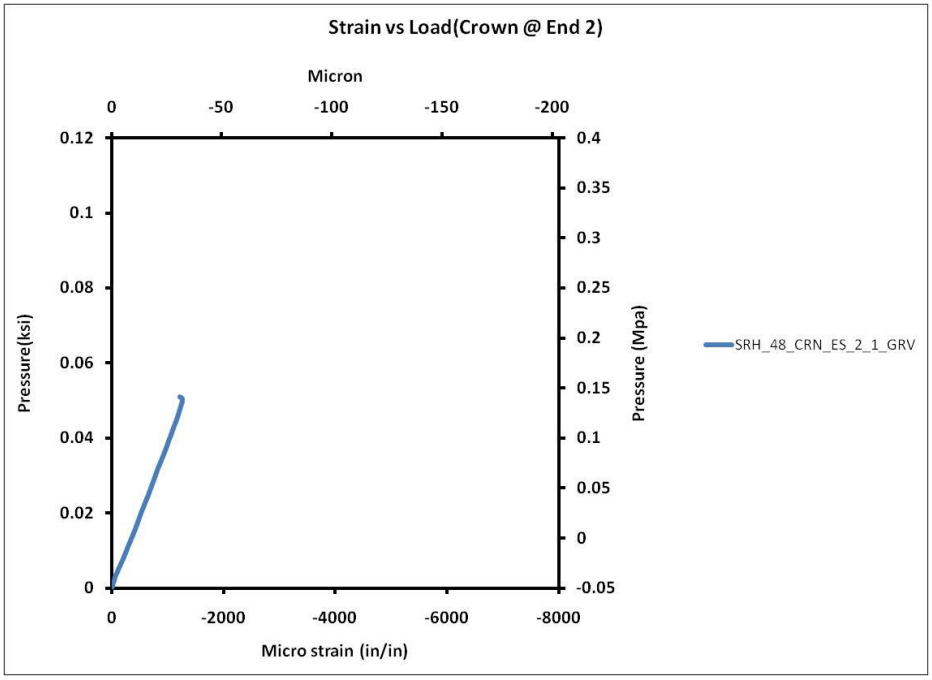

Figure A.42 Pressure vs. Vertical Deformation at the Middle Section of the Pipe.

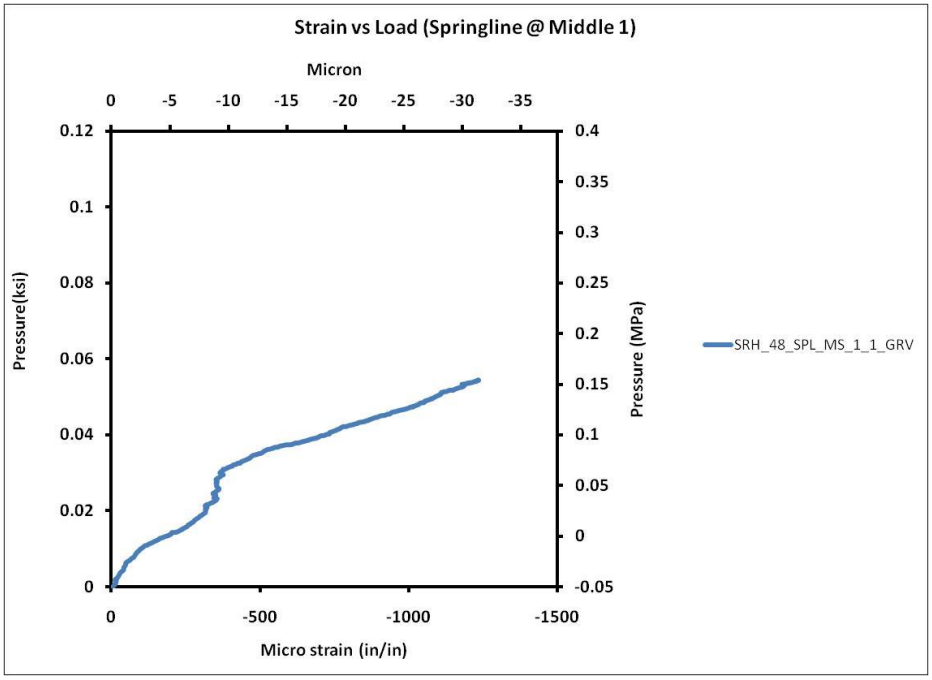

Figure A.43 Pressure vs. Vertical Deformation at the Middle Section of the Pipe.

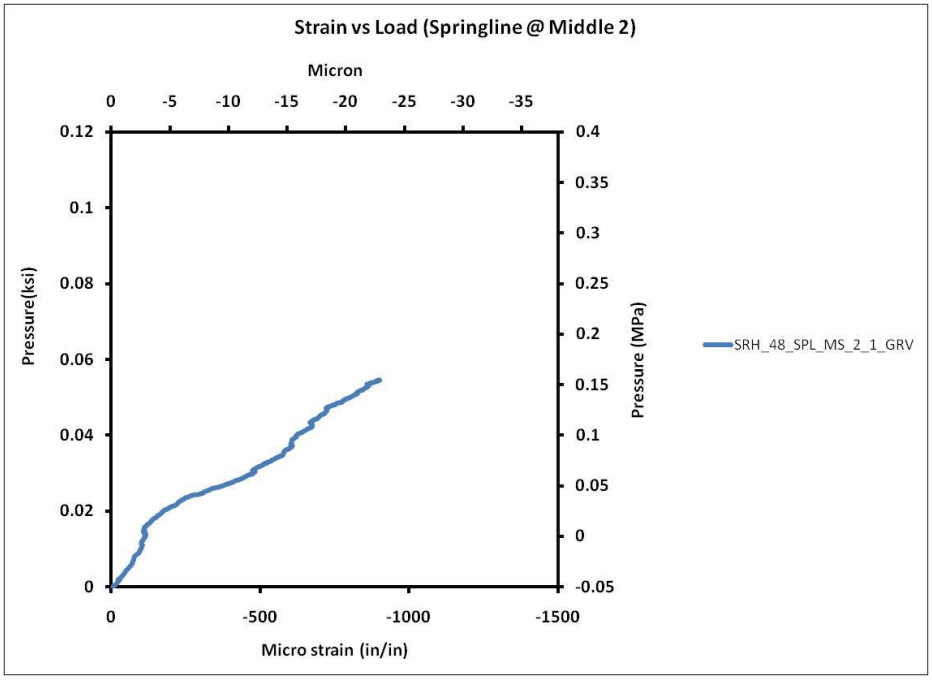

Figure A.44 Pressure vs. Vertical Deformation at the Middle Section of the Pipe.

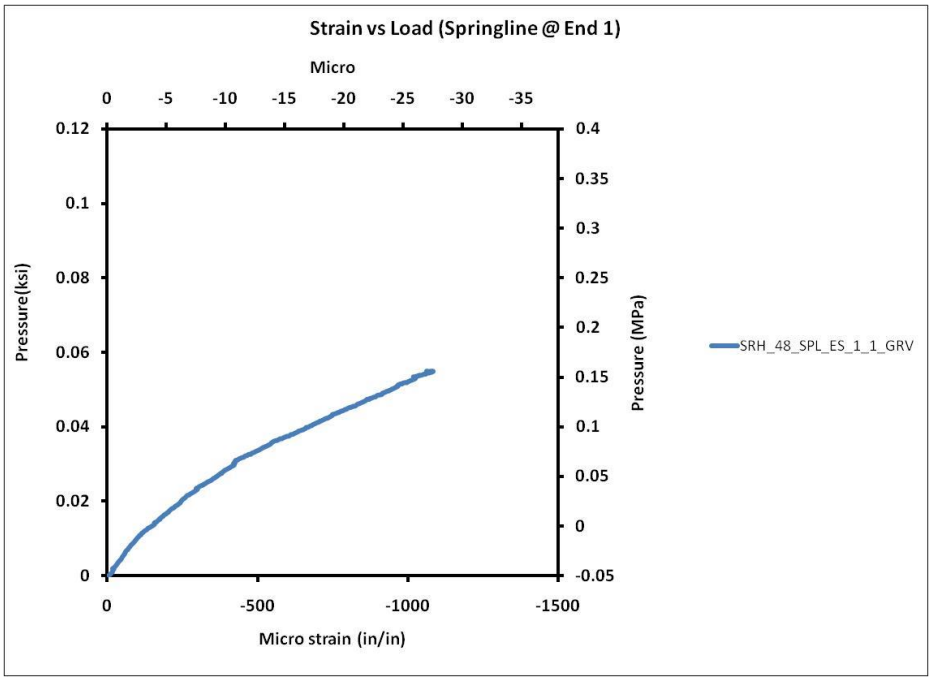

Figure A.45 Pressure vs. Vertical Deformation at the Middle Section of the Pipe.

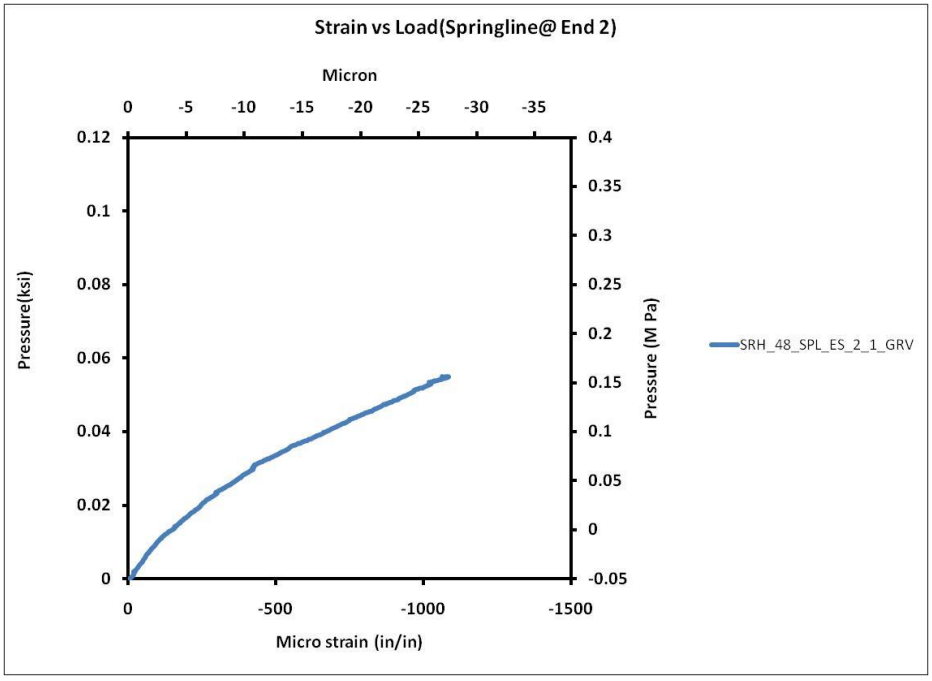

Figure A.46 Pressure vs. Vertical Deformation at the Middle Section of the Pipe.

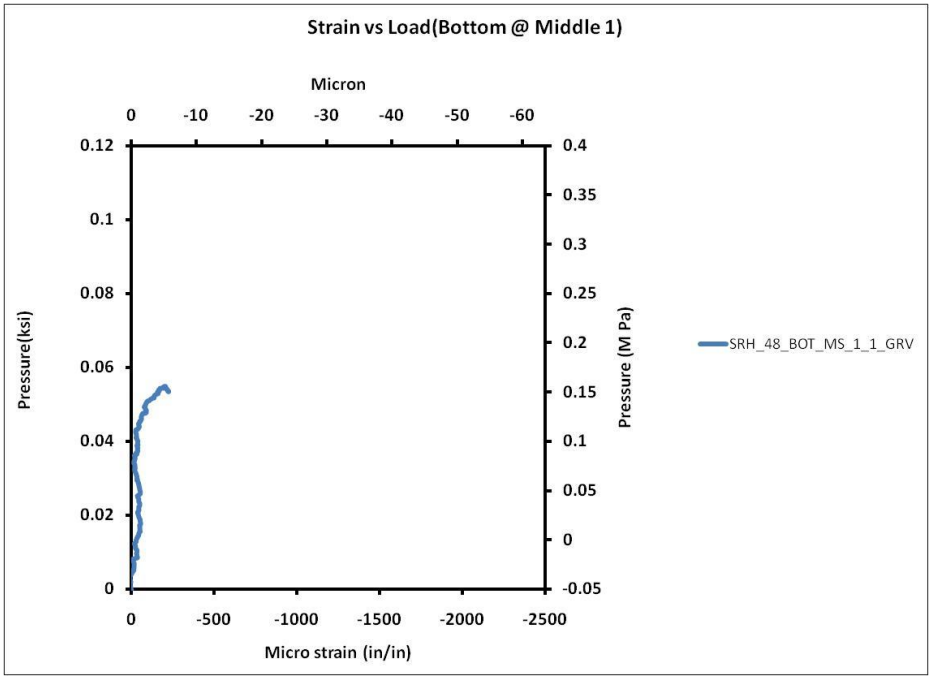

Figure A.47 Pressure vs. Vertical Deformation at the Middle Section of the Pipe.

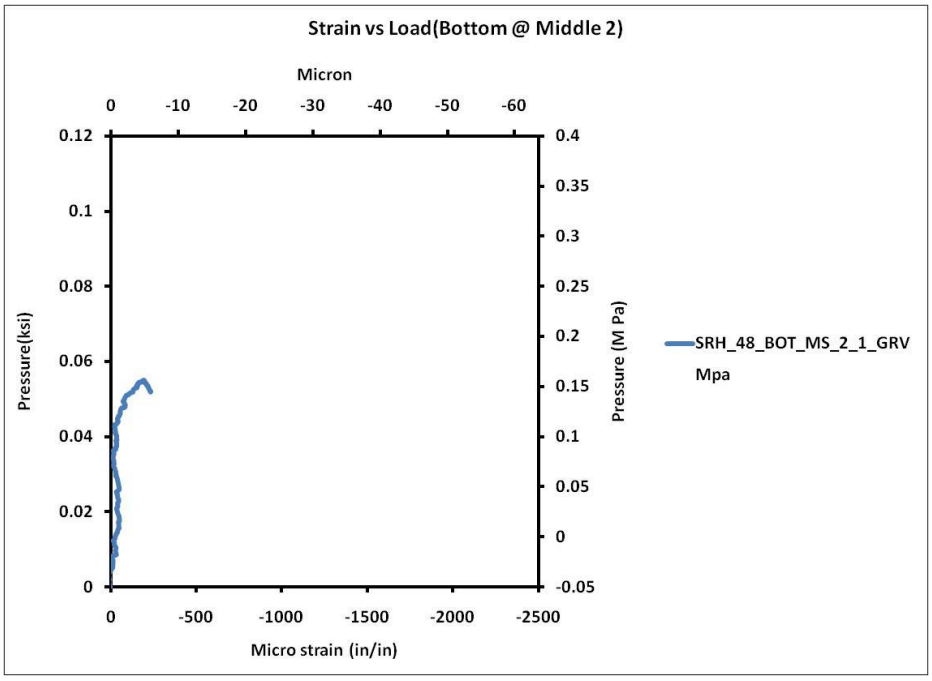

Figure A.48 Pressure vs. Vertical Deformation at the Middle Section of the Pipe.

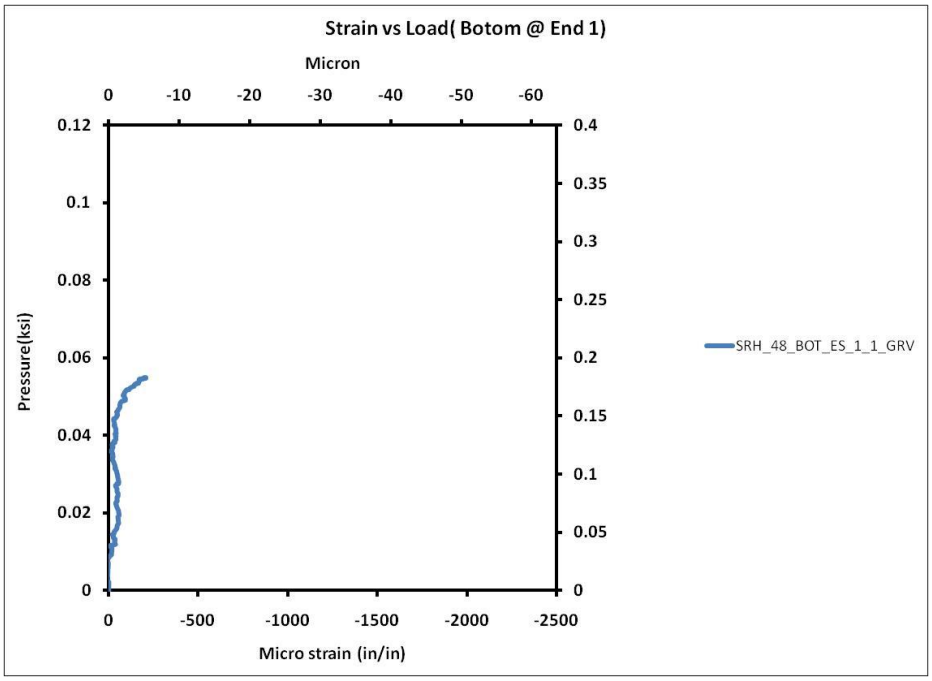

Figure A.49 Pressure vs. Vertical Deformation at the Middle Section of the Pipe.

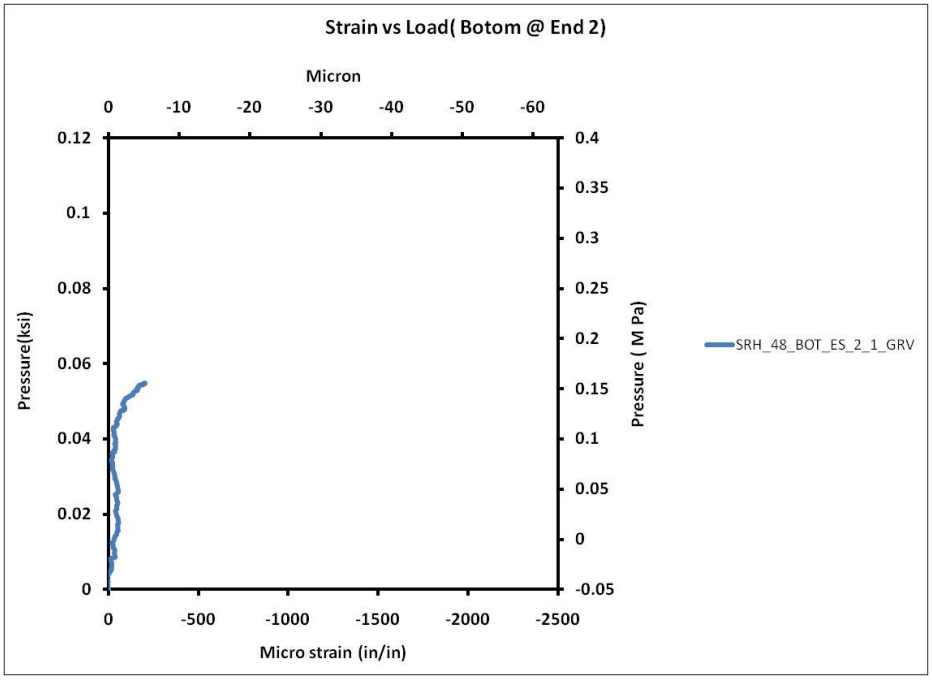

Figure A.50 Pressure vs. Vertical Deformation at the Middle Section of the Pipe.

APPENDIX B

EXPERIMENTAL PIPE COMPACTION RESULTS

SAM ENGINEERING & TESTING, L.P.

Geotechnical
Materials Testing — SE&T — Failure Investigation
Environmental

Serving The Geo-Industry Since 1974
1115 Luke Street, Suite 100
Irving, Texas 75061
Phone: (972) 790-1910 • FAX: (972) 790-0967

IN-PLACE DENSITY OF SOIL

CLIENT: Hanson Pipe & Precast
860 Airport Frwy., Ste: 300
Hurst, TX 76054

REPORT DATE: 5/17/10 **TEST DATE:** 5/14/10

TEST METHOD: ASTMD-2922 & 3017

PROJECT: Research Pro. # ACPA-SRHDPE Project
Deformation Property
Pipe Bedding Materials
Under Hanson Concrete Pipe

***ASTM D698A - See Proctor Report for Details**

Minimum Required Compaction = 95% & MC = 4-10%

PROJECT # 108E/TX6K10

REPORT #: 4 **PAGE 1 OF 1**

ATTN: Professor Joe Lundy

SE&T TECHNICIAN: Adel Alhemidawi

TEST AREA	FIELD RESULTS				LAB RESULTS *					
LOCATION	LIFT #	DEPTH FEET	DENSITY PCF	MC %	MAT #	MAX DEN PCF	OPT MC %	RANGE MC	COMP %	PASS/ FAIL
Box #2										
NEC of 6'x6'x6' covering layer	FG	1	107.6	9.3	1	112	8	4-10	96.0	P
Center of 6'x6'x6' covering layer	FG	1	110.3	8.8	1	112	8	4-10	98.4	P
SWC of 6'x6'x6' covering layer	FG	1	106.9	9.4	1	112	8	4-10	95.4	P

Note: FG = Upper 1' of 2' of the covered sand layer above the 2' diameter flexible plastic pipe.

All densities meet the minimum required values unless otherwise noted. It has been a pleasure to serve you on this project and we trust that this report is satisfactory.

Very Truly Yours,
SAM Engineering & Testing, L.P.

Sadik (SAM) Al-Musawe, M.Sc., Ph.D., P.E. F ASCE
Civil & Environmental Engineer
Texas Registration Number: 61893
Texas Professional Firm Registration No: F-001587

G:/2010/108e/tx6k10/Density/DEN4

SAM ENGINEERING & TESTING, L.P.

Serving The Geo-Industry Since 1974
1115 Luke Street, Suite 100
Irving, Texas 75061
Phone: (972) 790-1910 • FAX: (972) 790-0967

Geotechnical
Materials Testing — SE&T — Failure Investigation
Environmental

IN-PLACE DENSITY OF SOIL

CLIENT: Hanson Pipe & Precast
860 Airport Frwy., Ste: 300
Hurst, TX 76054

REPORT DATE: 5/17/10 **TEST DATE:** 4/26/10

TEST METHOD: ASTMD-2922 & 3017

PROJECT: Research Pro. # ACPA-SRHDPE Project
Deformation Property
Pipe Bedding Materials
Under Hanson Concrete Pipe

***ASTM D698A - See Proctor Report for Details**

Minimum Required Compaction = 95% & MC = 4-10%

PROJECT # 108E/TX6K10

REPORT #: 2 **PAGE 1 OF 1**

ATTN: Professor Joe Lundy

SE&T TECHNICIAN: Adel Alhemidawi

TEST AREA		FIELD RESULTS			LAB RESULTS *					
LOCATION	LIFT #	DEPTH FEET	DENSITY PCF	MC %	MAT #	MAX DEN PCF	OPT MC %	RANGE MC	COMP %	PASS/ FAIL
*NEC of the 6'x6'x6' box with sand bedding layer	SG*	1*	104.7	4.7	1	112	8	4-10	93.4	F*
*Center of the 6'x6'x6' box with sand bedding layer	SG*	1*	107.8	3.9	1	112	8	4-10	96.2	F*
*SWC of the 6'x6'x6' box with sand bedding layer	SG*	1*	103.8	5.0	1	112	8	4-10	92.6	F*

Notes: (1). The above 3 Field Density Tests (FDT) were performed on the upper 1' of the 2' thick sand bedding layer placed under the 2' diameter flexible plastic pipe.

(2).* These FDT's failed due to low compaction.

(3). SG = Subgrade = 1' below the 2' diameter flexible plastic pipe.

All densities meet the minimum required values unless otherwise noted. It has been a pleasure to serve you on this project and we trust that this report is satisfactory.

Very Truly Yours,
SAM Engineering & Testing, L.P.

Sadik (SAM) Al-Musawe, M.Sc., Ph.D., P.E. F ASCE
Civil & Environmental Engineer
Texas Registration Number: 61893
Texas Professional Firm Registration No: F-001587

STATE OF TEXAS
SADIK JAFFER AL-MUSAWE
61893
REGISTERED PROFESSIONAL ENGINEER

G:/2010/108e/tx6k10/Density/DEN2

SAM ENGINEERING & TESTING, L.P.

Serving The Geo-Industry Since 1974
1115 Luke Street, Suite 100
Irving, Texas 75061
Phone: (972) 790-1910 • FAX: (972) 790-0967

Geotechnical
Materials Testing — SE&T — Failure Investigation
Environmental

IN-PLACE DENSITY OF SOIL

CLIENT: Hanson Pipe & Precast
860 Airport Frwy., Ste: 300
Hurst, TX 76054

REPORT DATE: 5/17/10 **TEST DATE:** 4/26/10

TEST METHOD: ASTMD-2922 & 3017

PROJECT: Research Pro. # ACPA-SRHDPE Project Deformation Property
Pipe Bedding Materials
Under Hanson Concrete Pipe

***ASTM D698A - See Proctor Report for Details**

Minimum Required Compaction = 95% & MC = 4-10%

PROJECT # 108E/TX6K10 **REPORT #: 3** **PAGE 1 OF 1**

ATTN: Professor Joe Lundy **SE&T TECHNICIAN:** Adel Alhemidawi

TEST AREA		FIELD RESULTS			LAB RESULTS *					
LOCATION	LIFT #	DEPTH FEET	DENSITY PCF	MC %	MAT #	MAX DEN PCF	OPT MC %	RANGE MC	COMP %	PASS/ FAIL
Box #1										
NWC of 6'x6'x6' bedding layer	SG	1	106.8	8.3	1	112	8	4-10	95.3	P
Center of 6'x6'x6' bedding layer	SG	1	107.3	8.2	1	112	8	4-10	95.8	P
SEC of 6'x6'x6' bedding layer	SG	1	106.9	8.4	1	112	8	4-10	95.4	P
Box #1										
NEC of 6'x6'x6' covering layer	FG	1	109.5	8.7	1	112	8	4-10	97.7	P
Center of 6'x6'x6' covering layer	FG	1	109.4	8.8	1	112	8	4-10	97.6	P
SWC of 6'x6'x6' covering layer	FG	1	108.3	8.4	1	112	8	4-10	96.6	P
Box #2										
NEC of 6'x6'x6' bedding layer	SG	1	109.5	8.6	1	112	8	4-10	97.7	P
Center of 6'x6'x6' bedding layer	SG	1	110.3	8.5	1	112	8	4-10	98.4	P
SWC of 6'x6'x6' bedding layer	SG	1	109.7	8.5	1	112	8	4-10	97.9	P

Note: (1). SG = 1' below the 2' diameter flexible plastic pipe.
(2). FG = Upper 1' of 2' of the covered sand layer above the 2' diameter flexible plastic pipe.

All densities meet the minimum required values unless otherwise noted. It has been a pleasure to serve you on this project and we trust that this report is satisfactory.

Very Truly Yours,
SAM Engineering & Testing, L.P.

Sadik (SAM) Al-Musawe, M.Sc., Ph.D., P.E. F ASCE
Civil & Environmental Engineer
Texas Registration Number: 61893
Texas Professional Firm Registration No: F-001587

STATE OF TEXAS
SADIK JAFFER AL-MUSAWE
61893
REGISTERED
PROFESSIONAL ENGINEER

G:/2010/108e/tx6k10/Density/DEN3

SAM ENGINEERING & TESTING, L.P.

Serving The Geo-Industry Since 1974
1115 Luke Street, Suite 100
Irving, Texas 75061
Phone: (972) 790-1910 • FAX: (972) 790-0967

Geotechnical
Materials Testing — SE&T — Failure Investigation
Environmental

LABORATORY PROCTOR SHEET

REPORT DATE: 5/17/10

TEST DATE: 4/26 & 27/10
DATE SAMPLED: 4/26/10

CLIENT: Hanson Pipe & Precast
860 Airport Frwy., Ste: 300
Hurst, TX 76054

TEST METHOD: ASTM D-2922-3017 FDT
COMPACTION: ASTM D-698A
ATTERBERG LIMITS: ASTM D-4318
% FINE (-200): ASTM D-1140
REQD. MIN. % COMPACTION: 95%
REQ. MOISTURE RANGE: 4-10%

PROJECT: Research Project # ACPA-SRHDPE Project
Deformation Property
Pipe Bedding Materials
Under Hanson Concrete Pipe

MATERIAL #1: 4-10

ATTN: Professor Joe Lundy

SE&T TECHNICIAN: Mathew Varughese & Dusty McClendon

PROJECT NO.: 108E/TX6K10 **REPORT NO.** 1 **PAGE 1 OF 1**

MATERIAL #	DESCRIPTION	Maximum Density pcf	Optimum MC %
1*	Reddish & yellowish brown silty fine **SAND** with trace/some medium/coarse sand Atterberg Limits (ASTM D-4318): LL = 12, PI = NP (Non-Plastic) % Fine/-200 (ASTM D-1140) 45% Silts & Clays	112	8

Note: * Reported by the client as manufactured sand.

It has been a pleasure to serve you on this project & we trust that this report is satisfactory.

Very Truly Yours,
SAM Engineering & Testing, L.P.

Sadik (SAM) Al-Musawe, M.Sc., Ph.D., P.E., F. ASCE
Civil & Environmental Engineer
Texas Registration Number: 61893
Texas Professional Registration No: F-001587

Pro

SAM ENGINEERING & TESTING, L.P.

Serving The Geo-Industry Since 1974
1115 Luke Street, Suite 100
Irving, Texas 75061
Phone: (972) 790-1910 • FAX: (972) 790-0967

Geotechnical
Materials Testing — SE&T — Failure Investigation
Environmental

IN-PLACE DENSITY OF SOIL

CLIENT: Hanson Pipe & Precast
860 Airport Frwy., Ste: 300
Hurst, TX 76054

REPORT DATE: 7/6/10 **TEST DATE:** 7/2/10

TEST METHOD: ASTMD-2922 & 3017

PROJECT: Research Pro. # ACPA-SRHDPE Project
Deformation Property
Pipe Bedding Materials
Under Hanson Concrete Pipe

***ASTM D698A - See Proctor Report for Details**

Minimum Required Compaction = 95% & MC = 4-10%

PROJECT # 108E/TX6K10

REPORT #: 7 **PAGE 1 OF 1**

ATTN: Professor Joe Lundy

SE&T TECHNICIAN: Jude Brignac

TEST AREA		FIELD RESULTS			LAB RESULTS *					
LOCATION	LIFT #	DEPTH FEET	DENSITY PCF	MC %	MAT #	MAX DEN PCF	OPT MC %	RANGE MC	COMP %	PASS/ FAIL
Box #2										
Final Layer - Northwest	FG	1	108	6	1	112	8	4-10	96	P
Final Layer - Center	FG	1	107	9	1	112	8	4-10	95	P
Final Layer - Southeast	FG	1	108	9	1	112	8	4-10	96	P

Note: FG = Upper 1' of 2' of the covered sand layer above the 2' diameter flexible plastic pipe.

All densities meet the minimum required values unless otherwise noted. It has been a pleasure to serve you on this project and we trust that this report is satisfactory.

Very Truly Yours,
SAM Engineering & Testing, L.P.

Mike Saint, Lab Manager & Vice President

Texas Professional Firm Registration No: F-001587

G:/2010/108e/tx6k10/Density/DEN7

REFERENCES

American Association of State Highway and Transportation Officials. AASHT Bridge Design Specification Washington, DC, 2005.

American Concrete Pipe Association (ACPA). *Steel Reinforced High Density Polyethylene Pipe*, 2009

American Society for Testing and Materials Standards. Philadelphia, PA, 2008.

Farshad, M. *Plastic pipe systems: Failure investigation and diagnosis Elsevier Science*, New York, 2006

David J. Keatley. *Three-Dimensional Nonlinear Analysis of Deeply-Buried Corrugated Annular HDPE Pipe with Changes in Its Profile-Wall,* 2009

Gabriel, Lester H., and Orin Bennett. The Complete Corrugated Polyethylene Pipe Design Manual and Installation Guide. Plastic Pipe Institute. n.p. 2003.

P. Krishnaswamy, M. E. Tuttle, A. F. Emery, J. Ahmad. *Finite element modeling of the time-dependent behavior of nonlinear ductile polymers,* 2004

Madasamy Arockiasamy, Omar Chaallal, and Terdkiat Limpeteeprakarn, *Full-Scale Field Tests on Flexible Pipes under Live Load Application,*2006

Shad M. Sargand and Teruhisa Masada. *Performance of large-diameter honeycomb-design HDPE pipe under a highway embankmen*, 2000

Watkins, R.K., and Reeve, R.D. *Effect of heavy loads on buried corrugated polyethylene pipe.* Technical Report, dvanced Drainage Systems, Inc., Columbus, Ohio. 1982.

Ayche, Nadim. *The Effect of HDPE Pipe Profile Geometry on its StructuralPerformance*. MS Thesis. Civil Engineering Dept. Ohio University, 2005.

Sayed, G.A., Bahkt, B., & Jaeger, L.G. *Soil Steel Bridges - Desian and Construction*, New York: Mcgraw-Hill Inc. 1994

Duncan, J.M. *Behavior and Design of Long Span Metal Culverts*. ASCE,1979

Leonards, G.A., & Juang, C.H. *Predicting Performance of Buried Metal Conduits, Culverts: Analysis of Soil-Culvert Interaction and Design*. Transportation Research Record 1008, TRB, Washington, D.C. 1985.

Sharma, S., & Hardcastle, J.H *Evaluation of Culvert Deformations Using the Finite Element Method, Field performance of Structures and Non-destructive evaluation of Subsurface.* Transportation Research Record 141 5, TRB, Washington, D.C. 1993

Katona, M.G. *Analysis of Long Span Culverts by the Finite Element Method, Tolerable Movement of Bridge Foundations, Sand Drains, K-Test, Slopes, and Culverts.* Transportation Research Record 678, TRB, Washington, D.C. 1978

Katona, M.G., & Akl, A.Y. *Analysis and Behavior of Buried Culverts with Slotted Joints, Culverts: Analysis of Soil-Culvert Interaction and Design*. Transportation Research Record 1008, TRB, Washington, D.C. 1985

Chang, S.C., Espinoza, J.M., & Selig, E.T. *Computer Analysis of Newton Creek Culvert.,* ASCE 1980

Daoud S. Al-Abri and Yahia E-A. Mohamedzein.*Performance of Plastic Pipes in Dune Sand.* ASCE 2010

Teruhisa Masada and Shad M. Sargand. *Measured structural Performance of HDPE Pipe installed in CLSM-CDF.* ASCE 2004

Teruhisa Masada and Shad M. Sargand. *Peaking Deflection of Flexible Thermoplastic Pipe* ASCE 2005

McGrath, T.J., Selig, E.T., Webb M. C., and Zoladz, G. V., *Pipe Interaction with Backfill Envelope.* 1999.

Leonards, G.A., & Juang, C.H. *Predicting Performance of Buried Metal Conduits, Culverts: Analysis of Soil-Culvert Interaction and Design.* Transportation Research Record 1008, TRB, Washington, D.C. 1985.

Sharma, S., & Hardcastle, J.H. *Evaluation of Culvert Deformations Using the Finite Element Method, Field performance of Structures and Non-destructive evaluation of Subsurface*. Transportation Research Record 141 5, TRB, Washington, D.C. 1993.

Chang, S.C., Espinoza, J.M., & Selig, E.T. *Computer Analysis of Newton Creek Culvert*, ASCE 1980

Bruce H. Kjartanson, Robert A. Lohnes, F. Wayne Klaiber. *Full-Scale Field Tests on Longitudinal Uplift Response of Corrugated Metal Pipe. 2007*

Y. G. Hsuan. *Evaluation of the Stress Crack Resistance of Corrugated High Density Polyethylene Drainage Pipes.* ASCE 2005.

Madasamy Arockiasamy, Omar Chaallal, and Terdkiat Limpeteeprakarn. Full-Scale Field Tests on Flexible Pipes under Live Load Application. ASCE 2007.

Andrew Moreland. *Experimental and Numerical Investigation of a Buried Corrugated Steel Multi Plate Pipe.* Master Thesis, 200

Conard, B. E., Lohnes, R. A., Klaiber, F. W., and Wipf, T. J. *Boundary effects on response of polyethylene pipe under simulated live load.* Transportation Research Record 1624, Transportation Research Board, National Research Board, Washington, D.C. 1998

Lohnes, R. A., Wipt, T. J., Klaiber, F. W., Conard, B. E., and Ng, K. W. *Investigation of high density polyethylene pipe for highway applications*, Iowa State University, Ames, Iowa. 1997